Time-Series and Real Options Analysis of Energy Markets

Bibi Somayeh Heydari

Department of Statistical Science

University College London

A thesis submitted for the degree of

Doctor of Philosophy

August 2010

Statement of Originality

I, Bibi Somayeh Heydari, confirm that the work presented in this thesis is my own. Where information has been derived from other sources, I confirm that this has been indicated in the thesis.

Abstract

After the deregulation of electricity industries on the premise of increasing economic efficiency, market participants have been exposed to financial risks due to uncertain energy prices. Using time-series analysis and the real options approach, we focus on modelling energy prices and optimal decision-making in energy projects.

Since energy prices are highly volatile with unexpected spikes, capturing this feature in reduced-form models leads to more informed decision-making in energy investments. In this thesis, non-linear regime-switching models and models with mean-reverting stochastic volatility are compared with ordinary linear models. Our numerical examples suggest that with the aim of valuing a gas-fired power plant, non-linear models with stochastic volatility, specifically for logarithms of electricity prices, provide better out-of-sample forecasts.

Among a comprehensive scope of mitigation measures for climate change, CO_2 capture and sequestration (CCS) plays a potentially significant role in industrialised countries. Taking the perspective of a coal-fired power plant owner that may decide to invest in either full CCS or partial CCS retrofits given uncertain electricity, CO_2, and coal prices, we develop an analytical real options model that values the choice between the two technologies. Our numerical examples show that neither retrofit is optimal immediately, and the optimal stopping boundaries are highly sensitive to CO_2 price volatility.

Taking the perspective of a load-serving entity (LSE), on the other hand, we value a multiple-exercise interruptible load contract that allows the LSE to curtail electricity provision to a representative consumer multiple times for a specified duration at a defined capacity

payment given uncertain wholesale electricity price. Our numerical examples suggest that interruption is desirable at relatively high electricity prices and that uncertainty favours a delay in interrupting. Moreover, we show that a deterministic approximation captures most of the value of the interruptible load contract if the volatility is low and the exercise constraints are not too severe.

Acknowledgements

I would like to express the deepest gratitude to my primary supervisor, Dr. Afzal Siddiqui, who devoted most of his precious time and a lot of effort in direction and assistance of my thesis. The achievement of this work would have been impossible without his tremendous support. It has been my best fortune to have such a brilliant supervisor with novel, inspiring, and encouraging ideas in the area of my thesis. I would also like to thank my subsidiary supervisor, Dr. Rex Galbraith, for his review and useful comments on this thesis during the first year of my study. I am grateful to Dr. Nick Ovenden for his invaluable help with the third chapter of this thesis.

Special thanks to my scholarship sponsor, the Central Bank of Iran, which provided me the great opportunity of studying at University College London (UCL). I am also indebted to the UCL Graduate School for the Student Conference Fund to present my work at the 2008 International Association for Energy Economics (IAEE) International Conference and the 2010 FIBE Conference. I am also appreciative to the Department of Statistical Science for providing a great environment to study as well as for its teaching opportunity, which gave me a valuable experience.

I am grateful to Dr. Richard Chandler, Professor Stein-Erik Fleten, and João Jesus for their helpful comments. I also acknowledge the attendees of the IAEE International Conference (Istanbul, Turkey), the 2009 CMS Conference (Geneva, Switzerland), the 2010 FIBE Conference (Bergen, Norway), ELDEV Winter Workshop (Trondheim, Norway), and the 2010 ENERDAY Conference (Dresden, Germany) for their valuable feedback. In particular, I am thankful to lead

discussant, Professor Petter Bjerksund, from the FIBE Conference. This thesis has also benefited from the comments received from seminar participants at RWTH Aachen, the Center for Energy and Environmental Policy Research at the Beijing Institute of Technology, the Central Research Institute of Electric Power Industry in Tokyo, Japan, the Institute for Advanced Studies in Glasgow, UK, and the UCL Energy Institute. I am also indebted to the APX Group for providing access to their data. Thanks and extreme appreciation to Dr. Alexandros Beskos and Professor Derek Bunn, whose feedback has greatly improved my thesis.

I would like to thank all my friends at the UCL as well as the amiable staff of the Department of Statistical Science for their friendship, support, and help.

Finally, I would like to show the greatest gratitude to my family, none of my accomplishments would have been done without their support. My extreme appreciation is given to my husband, Alireza, who has been supportive, helpful, and inspiring even during the most difficult times. I am profoundly indebted to my parents who have always encouraged me to pursue my study and taught me how to deal with difficulties in my life.

Contents

List of Acronyms

ADF	Augmented Dickey-Fuller
CCS	Carbon capture and sequestration
CDF	Cumulative distribution function
CO_2	Carbon dioxide
ERMSE	Expected root-mean-square error
FCCS	Full carbon capture and sequestration
GBM	Geometric Brownian motion
GMR	Geometric mean reverting
IL	Interruptible load
IPE	International Petroleum Exchange
LSE	Load-serving entity
MR	Mean reversion for both logarithms of electricity and gas prices
MRRS	Mean reversion with Markov regime switching for the logarithm of the electricity price and simple linear mean reversion for the logarithm of the gas price
MRS	Markov regime-switching
MRSV1	Mean reversion with stochastic volatility for the logarithm of the electricity price and deterministic volatility for the logarithm of the gas price
MRSV2	Mean reversion with stochastic volatility for both logarithms of electricity and gas prices
NPV	Net present value
NETA	New Electricity Trading Arrangement
OCM	On-the-day Commodity Market
PC	Pulverised coal
PCCS	Partial carbon capture and sequestration
PDF	Probability density function
REC	Regional Electricity Companies
RMSE	Root-mean-square error
RPD	Reference price data
UKAPX	UK Automated Power Exchange
UKPX	UK Power Exchange

List of Figures

List of Tables

Chapter 1

Introduction

Until the 1990s, electricity industries had been vertically integrated[1] worldwide, where regulators fixed prices as a function of generation, transmission, and distribution costs. Due to little uncertainty in prices, investors could, therefore, make decisions by applying standard deterministic valuation tools such as discounted cash flow analysis. In recent years, electricity industries in many countries have been deregulated with the aim of introducing competition in generation and retail activities. Wilson (2002) and Wolak (1999) provide a comprehensive survey of reformed electricity markets in developed countries. Wilson (2002) claims that vertically integrated structures are most desirable when there is strong competition, and optimisation to meet system constraints is preferable to participants' flexibility to optimise their own operations. On the other hand, the deregulated approach works better when incentives for cost minimisation and good scheduling decisions by participants are preferable to coordination in electricity markets. Wolak (1999) shows that market structures and market rules can have an important impact on behaviour of market prices.

This change from a regulated monopoly to private ownership of generation and market liberalisation may result in lower prices and more efficient use of resources. However, prices, which are now to be determined by the interaction of supply and demand, have become highly volatile with unexpected spikes. These sudden spikes may be explained as a response to temperature, supply, or

[1]The electricity industry had been a naturally regulated monopoly with a guaranteed rate of return in exchange for an obligation to serve.

transmission shocks. Accounting for uncertainty in energy prices and modelling market-based decision-making is, thus, crucial under the deregulated paradigm. Indeed, ignoring such aspects of deregulated markets is likely to result in mis-valuation of energy projects.

1.1 Modelling Electricity and Gas Prices

Although there are many papers on modelling energy prices, there is limited information about modelling electricity and natural gas spot prices distinctly, i.e., taking into account their correlation together with either unexpected spikes or stochastic volatility. This is important because both electricity and natural gas prices exhibit such features. In addition, natural gas tends to be the price-setting fuel in many markets, such as in the UK.

Schwartz & Smith (2000) has developed a two-factor model for commodity prices where the short-term derivatives are modelled with a mean-reverting process and the equilibrium to which prices revert evolves according to a Brownian motion process; however, it considers neither the existence of correlation between commodity prices, such as electricity and gas, nor the presence of high-frequency spikes. Using a similar two-factor analysis, Näsäkkälä & Fleten (2005) models the spark spread, defined as the difference between the price of electricity and the cost of gas required for the generation of electricity, directly. It may lose some information about the spark spread's uncertainty structure compared to models with separate electricity and gas price processes. Cortazar & Schwartz (1994), Laughton & Jacoby (1993), and Smith & McCardle (1998) argue that mean-reverting price processes, instead of geometric Brownian motion (GBM) process models, are more appropriate for commodities. On the other hand, Pindyck (1999) analyses the long-run evolution of energy prices, such as oil, coal, and natural gas, and suggests that although the long-run energy prices are mean reverting, since their rate of mean reversion is low, the use of GBM models is unlikely to lead to large errors in optimal investment rules.

Kosater & Mosler (2006) has successfully applied non-linear autoregressive Markov regime-switching models in the spirit of Hamilton (1989). Its forecast study suggests that it is beneficial to apply the non-linear model, at least for

long-term forecasting. The idea behind this approach is to model the spikes as a separate regime. Karakatsani & Bunn (2008) also uses a regime-switching model in order to discover the response of agents and, thus, alterations in prices during temporary market irregularities. Maribu *et al.* (2007) applies mean-reverting models for both electricity and gas by considering two variants for electricity: one with constant volatility and one with stochastic volatility. However, it does not allow for the possible stochastic volatility of gas prices simultaneously.

In energy markets, a wide range of bottom-up models that include supply/demand fundamentals is also available (see, e.g., Fleten & Lemming (2003); Kumbaroğlu & Madlener (2003); Martinsen *et al.* (2003)). While these models may be used more by practitioners, financial models require access only to market prices, which are more readily available than bottom-up data. Such accessibility makes financial models desirable from this perspective. Furthermore, neural networks have also been employed with some success in forecasting energy prices (see, e.g., Azadeh *et al.* (2008); Connor (1996); Rodriguez & Anders (2004); Szkuta *et al.* (1999)).

In this thesis, due to spikes and stochastic volatility in energy prices, we propose non-linear regime-switching models and models with mean-reverting stochastic volatility. For the former objective, we extend the model described in Kosater & Mosler (2006) and Karakatsani & Bunn (2008) to a multivariate model with two regimes for the logarithms of correlated electricity and gas spot prices. For the latter one, the work by Maribu *et al.* (2007) is extended such that the possibility of stochastic volatility for both the logarithm of electricity price and the logarithm of gas price is investigated. The innovation of this part of our study is that the cross-variogram is used to estimate the unobservable parameters of the stochastic volatilities. Finally,we examine the implications of modelling assumptions on investment decisions. In particular, we take the perspective of an investor in a UK gas-fired power plant by modelling the logarithms of electricity and gas prices distinctly via both linear and non-linear multivariate models. We are then able to assess the out-of-sample forecasting performance of such models by valuing a gas-fired power plant with and without daily operational flexibility using data from 2001 to 2006.

1.2 Investment Decision-Making in Energy Markets

As another result of the deregulation of electricity industries on the premise of increasing economic efficiency, market participants, such as generators, retailers, and marketers, have been exposed to uncertain electricity, fuel, and CO_2 prices. In order to make optimal investment and operational decisions, participants may find it beneficial to take the real options approach (Dixit & Pindyck (1994)). In addition to facilitating optimal timing of decisions, it also permits the analysis of mutually exclusive projects, e.g., in terms of technology choice, and sequential nested projects, e.g., lagged decisions that arise frequently in the energy sector and are not easily addressed by traditional approaches.

1.2.1 Carbon Capture and Sequestration (CCS) Technology

Since the 1970s, as global greenhouse gas (GHG) emissions have increased significantly due to human activities, so have temperatures. Global average sea levels have been rising, global average air and ocean temperatures have been increasing, and wind patterns as well as snow, ice, and frozen ground have been changing (IPCC (2005)). Carbon dioxide (CO_2) is referred to as the most critical anthropogenic GHG, annual emissions of which grew by about 80% between 1970 and 2004 (IPCC (2007)) mainly due to fossil-fuel combustion and deforestation. Continuing CO_2 emissions at or above current rates would result in further warming and more changes to the global climate during the 21st century.

Serious consideration is currently being given by industrialised countries to reducing their CO_2 emissions. These countries, known as Annex 1 (forty countries and separately the European Union), joined the 1997 Kyoto Protocol and have agreed to reduce their CO_2 emissions to an average of 5% below 1990 levels during the period 2008-2012. In order to implement its commitments, the European Union introduced a CO_2 Emission Trading Scheme (EU ETS) that allocates CO_2 emission permits to its facilities in the power sector, iron and steel manufacturing, and other heavy industries. Such facilities may emit CO_2 annually up to their

allowance limits, and any additional emission requires purchase of surplus permits from counterparties. Thus, the negative externality of CO_2 emissions may be reflected in the cost of purchasing additional permits.

A wide range of mitigation options is now available or proposed to be available by 2030. These options include better end-use efficiency improvements, conversion to less carbon-intensive fuels (e.g., switching from coal to gas), nuclear power, renewable energy sources (such as hydropower, wind, and solar), and CO_2 capture and sequestration (CCS) technology. However, since primary energy use will continue to rely on fossil fuels in the near term, CCS technology could play a key intermediate role in alleviating climate change. Moreover, CCS is more likely to reduce overall mitigation costs and allow additional flexibility in attaining GHG emission reduction (IPCC (2005)). Nevertheless, according to Hildebrand & Herzog (2008), capturing almost all emissions, or full capture, is a policy that is less likely to progress either new coal-fired plants or CCS technology in the near term. The implementation of full capture at a coal-fired power plant has a critical effect on plant technology, operation, and economics. On the other hand, partial capture of the emissions could be a very good replacement at the first step. In effect, it could provide plant owners with additional flexibility in offsetting emissions costs without the burdensome capital investment or efficiency loss associated with full CCS.

This thesis considers the perspective of a coal-fired power plant owner that must decide how to mitigate its CO_2 emissions by investing in either partial (PCCS) or full (FCCS) CCS technology. The former may correspond to either retrofitting only some of the generators in a power plant or capturing some of the CO_2 emissions. We assume that the power plant is operating at its rated capacity in a CO_2-constrained environment that requires the purchase of permits for any CO_2 emissions. Given uncertainty in electricity, coal, and CO_2 prices, following the standard smooth-fit techniques developed by Dixit & Pindyck (1994), we value each mutually exclusive mitigation option via the real options approach and determine when to adopt it assuming discretion over timing and technology choice. We use an approach that is similar to the one described in Décamps *et al.* (2006), which extends the analysis of Dixit (1993) by providing some con-

ditions under which the optimal investment region is dichotomous under price uncertainty.

Herbelot (1992) also applies option valuation techniques in a similar study, but it analyses the investment situation of a coal-fired power plant that has to reduce its sulfur emissions by either switching to lower-sulfur coal or investing in an emission control system. The two stochastic variables in this study (allowance price and coal price premium[2]) follow correlated geometric Brownian motion (GBM) processes. It develops a discrete-time binomial model to evaluate numerically the investment opportunity. Pindyck (2002) proposes a continuous-time model of environmental policy adoption that takes into account uncertainty over both environmental change and the social costs of environmental damage. The analytical solution to this problem is formalised in Adkins & Paxson (2010), which examines an asset depending on both uncertain revenues and operation costs that has a renewal opportunity. It provides a stochastic two-factor real options model that is solved analytically. While Wickart & Madlener (2007) also uses the real options approach to consider a two-factor model, i.e., the mutually exclusive investment choice between combined heat-and-power production and a conventional heat-only generation system, it accounts for uncertainty in one variable at a time. Abadie & Chamarro (2008a), on the other hand, assumes two sources of risk, viz., the price of emissions allowance and the price of electricity, and evaluates the option to install a CCS unit in a coal-fired power plant via a lattice-based approach. It models the electricity and CO_2 emissions permit prices as evolving according to correlated geometric mean-reverting (GMR) and GBM processes, respectively, and obtains the allowance price thresholds above which it is optimal to invest in CCS immediately. The results indicate that current permit prices do not lead to an immediate adoption of this technology. Similarly, Abadie & Chamarro (2008b), applying binomial lattices, studies the choice between investing either in a natural gas combined cycle power plant or in an integrated gasification combined cycle power plant.

In this thesis, we analyse the incentives for CCS retrofits and expand the real options theory for mutually exclusive investment under uncertainty to the case with two risk factors. We examine two situations:

[2]The difference between low-sulfur and high-sulfur coal prices.

- Individual investment options, when investing in FCCS and PCCS technologies are analysed independently.

- Mutually exclusive options, when the decision to invest in either FCCS or PCCS technology is explored.

Having more than one stochastic variable and following the same procedure as in Adkins & Paxson (2010), we evaluate the individual investment options analytically. Moreover, we calculate an optimal stopping boundary for the CO_2 permit price, depending on the fuel price, above which it is optimal to invest in FCCS/PCCS technology immediately. Our results suggest that at current CO_2 and coal prices, adopting the emission-reduction policy is not optimal, although both technologies (FCCS and PCCS) are in-the-money. This general conclusion is thoroughly consistent with previous studies, such as Abadie & Chamarro (2008a). However, as a result of applying different approaches and using different stochastic models for prices, the CO_2 thresholds may, unsurprisingly, differ in comparable studies.

Evaluating the mutually exclusive options, we generalise the theory proposed by Décamps *et al.* (2006) into a two-dimensional space. We introduce an indifference region around the intersection of the NPVs of the projects, over which it is optimal to wait before investing in either technology. As the FCCS technology produces higher cash flows than the PCCS one along with a significantly larger sunk capital cost, the optimal investment region may become dichotomous. After evaluating each project separately, we have two different option values and, correspondingly, two optimal stopping boundaries: $C^{*(pccs)}(F)$ and $C^{*(fccs)}(F)$. If the CO_2 price is less than $C^{*(pccs)}(F)$, then the plant owner waits until the CO_2 price reaches this value via either an increase in the CO_2 price or a decrease in the fuel price. However, for high values of CO_2, around the indifference curve, the solution to the separate valuation is no longer optimal. Over this region, there are two critical thresholds, $C^*_L(F)$ and $C^*_U(F)$ $(C^*_L(F) < C^*_U(F))$. When the current CO_2 price is included in $[C^{*(pccs)}(F), C^*_L(F)]$, it is optimal to invest immediately in PCCS technology, while for those values greater than $C^*_U(F)$, it is optimal to invest immediately in FCCS. For values in $[C^*_L(F), C^*_U(F)]$, however,

it is optimal to wait. Since there is no analytical solution to valuing the mutually exclusive option to retrofit, we propose an algorithm in order to solve this two-factor real options problem numerically. After valuing the mutually exclusive options, we show that without considering the waiting opportunity over the indifference region, the plant owner may lose a modest amount of money by investing immediately. We then explore how these variables, viz., the CO_2 emission allowance and coal prices, may interact in affecting the time of adoption. Finally, we focus on the effects of price volatility on such mutually exclusive mitigation options.

1.2.2 Multiple-Exercise Interruptible Load Contract

Under deregulation, although forward and spot markets have been used by suppliers in making investment and operational decisions, demand response, the lack of which creates risk exposure for load-serving entities (LSEs), has been conspicuously absent in most regions. Demand response programmes significantly decrease the costs of managing risk and improve the overall supply reliability (PG&E (2008a)), which is beneficial for both consumers and LSEs. Incentive-based demand response programmes, such as interruptible load (IL) contracts provided by LSEs, give consumers load reduction incentives in order to encourage their participation.

In this thesis, we take the perspective of an LSE that has its representative consumer on an IL contract with multiple interruption opportunities. The LSE must decide when to exercise each interruption opportunity given uncertainty in the electricity price. Once each interruption is exercised, it continues for a specified duration of time, and the next interruption becomes available at least one day after the end of the current curtailment, i.e., a problem of making sequential nested decisions with lags. Although there is a huge literature in the area of making sequential decisions, there is little information on problems with lags that depend on prices with structural stochastic processes. For example, Baldwin (1982) considers sequential investments in which the opportunities arrive one at a time with no time to complete. Similarly, Dixit & Pindyck (1994) analyses a two-stage investment where each stage takes no time, and Majd & Pindyck (1987)

values a sequential investment where each unit of investment buys an option on the next unit.

Nevertheless, Bar-Ilan & Strange (1998) examines a model of two-stage sequential investment where each stage takes time to complete, i.e., there are lags. Gollier *et al.* (2005), on the other hand, not only assumes a construction lag time between each two stages, but also examines a multiple sequential investment with a power plant consisting of four modules, where each module is available only after the construction of the previous one.

In analysing IL contracts, Kamat & Oren (2001) considers a simple form of an IL contract consisting of only two interruption opportunities, while Baldick *et al.* (2006) allows for the possibility of multiple interruptions. In particular, Kamat & Oren (2001) focuses on the pricing of a bundle of a simple forward contract with a two-exercise IL contract, where electricity prices are modelled with three different single-factor stochastic processes: a geometric Brownian motion (GBM) process, a mean-reverting model, and a mean-reverting model with jumps. It shows that under realistic price models, such contracts alleviate peak demand and energy shortages. On the other hand, Baldick *et al.* (2006) considers the impact of interruption on the spot price of electricity by constructing a structural model using data from Texas in which the spot price of electricity is determined by the interaction of supply and demand. It shows that when the supply is inadequate, such that the retailer has to resort to the electricity spot market, the IL contract becomes quite valuable. Nonetheless, as the number of power plants or competing retailers increases, the value of the IL contract decreases, and interruptions are exercised at higher expected loads.

In contrast to the structural modelling in Baldick *et al.* (2006), here, we assume that the electricity spot price follows a GBM process as in Bar-Ilan & Strange (1998) and Gollier *et al.* (2005), which solve sequential nested decision-making problems with lags, and in Oren (2001), which derives the value of a financial instrument referred to as a double-call option. In this thesis, we extend the approach described in Bar-Ilan & Strange (1998) and Gollier *et al.* (2005) by providing a quasi-analytical solution to multiple sequential investment problems with lags. Bar-Ilan & Strange (1998) analyses a project that involves two stages with the possibility of abandonment and suspension after the end of the first stage.

Although an analytical solution to the problem is provided, it is not easily possible to generalise it to a multiple sequential investment. On the other hand, Gollier *et al.* (2005) considers a multiple sequential investment with lags, however, it does not solve the problem analytically. In a general sense, the methodology of solving multiple sequential investment with lags is similar to that of swing options, but, there is little information on either sequential or swing options that is analytical. Deng & Xia (2006) and Jaillet *et al.* (2004), e.g., use numerical methods to solve problems concerning swing options. Taking the perspective of a tolling contract[3] holder, Deng & Xia (2006) proposes a real options approach that values the tolling contract by maximising the total payoff associated with all exercise tolling options given that no more than N options can be exercised during the life of the contract. It uses dynamic programming and value function approximation by Monte Carlo based least-squares regression to solve the valuation problem. Similarly, Jaillet *et al.* (2004) implements numerical scheme for pricing swing options, which permit their holders the right to receive greater or smaller amounts of energy subject to both daily and periodic limits, from the point of view of a profit-maximising agent.

In this thesis, a formal methodology for solving a sequential nested decision-making problem with lags under uncertainty is provided. The methodology is then applied to value multiple-exercise IL contracts in order to obtain policy insights. Although there is an analytical solution to the single-exercise IL contract, the solution to the multiple-exercise IL contract is expressed in a recursive form that can be solved numerically starting from the last interruption and working backwards. We also compare our solution to a deterministic approximate IL contract valuation. Our numerical examples reveal that this approximation captures most of the value of an IL contract when the electricity price volatility is low and the interruption lag is not large.

[3] A tolling contract signed between a buyer and a power plant owner gives the buyer the right to either operate the power plant or take the output electricity subject to certain constraints during pre-specified time periods for an upfront premium.

1.3 Structure of the Thesis

The remainder of this thesis is organised as follows. Chapter 2 proposes four linear stochastic models frequently used in energy markets to model the logarithms of electricity and gas spot prices for the purposes of valuing a gas-fired power plant. Next, due to spikes and stochastic volatility in energy spot prices, Markov regime-switching approaches and a mean-reverting stochastic volatility model are posited to improve upon these simple linear models. Finally, the performances of these models are compared using UK electricity and natural gas daily spot prices for valuing both flexible and inflexible power plants. Chapter 3 takes the perspective of a coal-fired power plant owner in order to develop a real options model that values the choice between two emissions-reduction technologies. Specifically, the plant owner may decide to invest in either full or partial carbon capture sequestration retrofits given electricity, CO_2, and coal prices, which follow correlated stochastic processes. The optimal stopping boundaries are also calculated for both individual and mutually exclusive options. Chapter 4 develops a real options analysis of multiple-exercise interruptible load contracts from the viewpoint of an LSE that provides electricity to consumers at a fixed tariff while procuring this electricity at a stochastic wholesale price. It is assumed that the consumer is on a multiple-exercise interruptible load contract that allows the LSE to interrupt electricity provision a fixed number of times for specified durations at defined capacity payments. By solving recursive equations starting from the last interruption, we obtain the value of the contract and optimal interruption price thresholds as well as their deterministic approximation. Chapter 5 concludes with a discussion about the findings and limitations of the current approaches. Future research recommendations in these areas are also provided.

Chapter 2

Valuing a Gas-Fired Power Plant: a Comparison of Ordinary Linear Models, Regime-Switching Approaches, and Models with Stochastic Volatility

Energy prices are often highly volatile with unexpected spikes. Capturing these sudden spikes may lead to more informed decision-making in energy investments, such as valuing gas-fired power plants, than ignoring them. In this chapter, non-linear regime-switching models and models with mean-reverting stochastic volatility are compared with ordinary linear models. The study is performed using UK electricity and natural gas daily spot prices and suggests that with the aim of valuing a gas-fired power plant with and without operational flexibility, non-linear models with stochastic volatility, specifically for logarithms of electricity prices, provide better out-of-sample forecasts than both linear models and regime-switching models.

2.1 Market Structure, Data, and Descriptive Statistics

In the pre-privatisation electricity industry in Britain, prior to 1990, the Central Electricity Generating Board had a dominant role. It sold electricity to twelve government-owned Area Boards, which distributed and supplied the electricity to consumers in their regional districts. After privatisation on 1 April 1990, these Area Boards were left unchanged and converted to twelve Regional Electricity Companies (REC). Large industrials with peak demand greater than 1 MW were then able to choose their suppliers from any of these twelve RECs as well as from National Power or PowerGen directly. This peak demand level was reduced to 100 kW in 1994, and it was removed in 1998 when even residential customers were given the option of choosing their supplier from any of the twelve RECs. Several studies have provided important insights on this restructuring (see, e.g., Bolle (1992); Green (1996); Green & Newbery (1992); Klemperer & Meyer (1989); Wolak (1999)). After successful performance of this restructuring when the generators bid into an Electricity Pool[1], in 1997, the Power Pool was judged by the regulator and government to have failed and was replaced by the New Electricity Trading Arrangements (NETA) on 27 March 2001. The outcomes achieved under NETA over its first year of operation include: a) significant increase in the liquidity[2] and improvement in the transparency of the wholesale markets, b) facilitation of a decrease in wholesale and retail prices, and c) considerable development in the performance of the balancing market (see Hesmondhalgh (2003)). Prices in this balancing market with full competition have been highly volatile, although a number of rule changes have been agreed to reduce this volatility. Three power exchanges were established for trading: the UK Power Exchange (UKPX), the UK Automated Power Exchange (UK APX)[3], and the International Petroleum

[1] In order to keep generation in balance with demand, a special spot market known as the Pool was created, and all major generators and suppliers were required to, respectively, sell to and buy from the Pool at common prices.

[2] Henney *et al.* (2002) reports that the spot markets are not liquid, while the forward markets are more liquid than before.

[3] In February 2003, the APX UK was acquired by Amsterdam Power Exchange (Dutch APX), and in 2003, they merged with the UKPX into the APX Group. Finally, in December 2008, the European Energy Derivative Exchange N.V. (ENDEX N.V.) was acquired by the APX Group,

Exchange (IPE; currently IntercontinentalExchange, ICE).

A total of 2105 daily observations over six years of electricity spot prices in £/MWh$_e$ and gas spot prices in £/MWh from UK energy markets, provided by the APX Group are available and plotted in Figure 2.1.a. The sample period begins on 27 March 2001 (introduction of NETA) and ends on 31 December 2006. The electricity spot prices are daily averages of half-hour reference price data (RPD), while the gas spot prices are the weighted-average prices of all trades for the relevant gas day on the OCM (On-the-day Commodity Market)[4] platform with relative times of observations measured in years.

The data set is split into two periods (see Figure 2.1): an in-sample period[5] (from 27 March 2001 to 26 March 2004) and an out-of-sample period (from 27 March 2004 to 31 December 2006). We assume that the future prices follow the same structure as the past prices. Hence, the in-sample period is used to estimate the unknown parameters, and the out-of-sample period is used to assess the forecast of the models of interest.

With respect to the qualitative aspects of the data, some atypical fluctuations are observed in the data that are caused not only by exceptional seasons, such as freezing winters or hot summers, but also by the existence of some salient events. In particular, the critical dispute over the natural gas and transit prices between Russia and Ukraine, which started in March 2005 and culminated on 1 January 2006 when Russia cut off gas supplies passing through Ukrainian territory, affected UK energy prices (BBC (2006a, b)). The situation, however, calmed after the two countries reached an agreement in principle of restoring Russia's gas supply to Europe. Consequently, UK energy prices started returning to their historical average values (Nesterov (2009)). Moreover, the British Electricity Trading and Transmission Arrangements (BETTA), which introduced

and to complete the integration process, both companies started operating under one, unified brand name (APX-ENDEX) in June 2009 (www.apxendex.com).

[4] An on-the-day commodity market for gas has been launched as part of the new reforms to improve liquidity and increase competition in UK wholesale gas market.

[5] One may criticise that the in-sample period looks more benign and less volatile than the out-of-sample period (Figure 2.1.a). However, since the data become smoother in the logarithmic scale, Figure 2.1.b does not show a huge distinction between the in-sample and the out-of-sample data set, but if anything, it shows the robustness of the results. On the other hand, in Section 2.5.2, the in-sample period is expanded so that after forty weeks are added, it is more representative of the out-of-sample period.

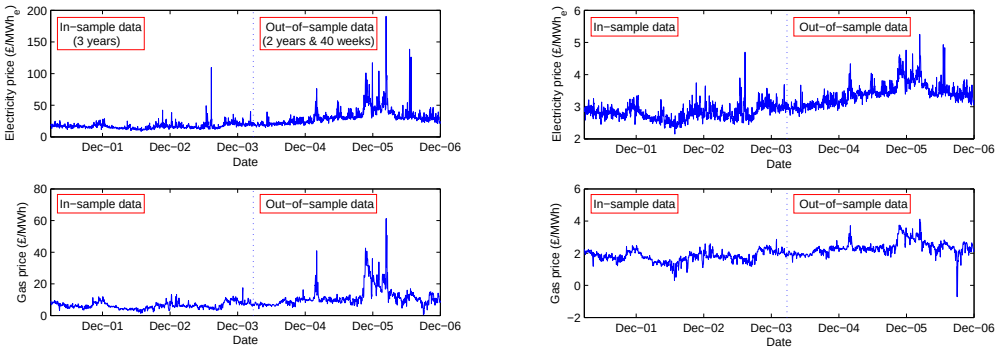

(a) Actual data

(b) Logarithms of data

Figure 2.1: UK electricity and gas spot prices, 2001-2006 (APX Group)

a single wholesale electricity market for Great Britain with a single transmission operation (National Grid) independent of generation and supply, came to force on 1 April 2005 (Treasury (2005)). In addition to the creation of BETTA, the EU ETS that started in 2005 was also a major intervention in the time series.

A summary of the descriptive statistics of electricity and gas spot prices as well as those of their natural logarithms is presented in Table 2.1. It is shown that the spot prices and their logarithms are skewed to the right (positively skewed), which clearly resulted from the upward spikes. Their positive kurtosis statistics also indicate a leptokurtic[6] distribution.

According to most of the previous articles on energy prices, such as Schwartz & Smith (2000) and Näsäkkälä & Fleten (2005), the logarithms of spot prices, $\mathbf{Y}_t$, (presented in Figure 2.1.b) are decomposed into two factors,

$$\mathbf{Y}_t = \begin{bmatrix} \log(E_t) \\ \log(G_t) \end{bmatrix} = \begin{bmatrix} X_t^E \\ X_t^G \end{bmatrix} + \begin{bmatrix} f_t^E \\ f_t^G \end{bmatrix}, \tag{2.1}$$

where E_t and G_t refer to observed electricity and gas spot prices, respectively. The first term on the right-most side is the stochastic part of log prices, and the second term is a deterministic seasonal function, which will be introduced in the next section. In Schwartz & Smith (2000) and Näsäkkälä & Fleten (2005), however,

[6] A leptokurtic distribution is described as "fat in tails" and has a more acute peak around the mean when compared to a normal one.

Table 2.1: Descriptive statistics, UK energy spot prices (£/MWh$_e$ and £/MWh) and their logarithms, 2001-2006 (APX Group)

Statistic	Electricity	ln Electricity	Gas	ln Gas
Mean	24.5397	3.1007	8.8904	2.0604
StDev	13.2800	0.4198	5.4088	0.4778
Variance	176.3580	0.1763	29.2555	0.2283
Skewness	3.3447	0.8296	3.2734	0.3699
Kurtosis	21.7419	0.8522	17.0807	1.8679
Number	2105	2105	2105	2105
Minimum	8.6030	2.1521	0.4930	-0.7073
1st Quartile	16.0570	2.7762	5.7890	1.7560
Median	20.5670	3.0237	7.6690	2.0372
3rd Quartile	29.5700	3.3868	10.1920	2.3216
Maximum	190.5490	5.2499	61.3500	4.1166

prices are assumed to follow a two-factor stochastic model with a deterministic seasonal function. These models include a short-term deviation, which reverts toward zero, and the equilibrium price level.[7] Bernard *et al.* (2008), Cartea & Williams (2008), and Aiube *et al.* (2008) also use similar models in analysing spot prices.

2.2 Seasonality

Before proposing the stochastic models for the logarithms of the energy prices, we obtain the deterministic seasonal function in Equation (2.1), using the in-sample data consisting of $n = 1095$ observations. Looking at the sample autocorrelation functions[8] of logarithms of electricity and gas prices, graphed in Figure 2.2, the

[7] Schwartz & Smith (2000), e.g., assumes that $\ln S_t = \chi_t + \xi_t + f_t$, where S_t, χ_t, ξ_t, and f_t denote, respectively, the spot price of commodity, the short-term deviation, the equilibrium price level, and the deterministic seasonal function at time t. As the forecast horizon increases, i.e., $t \to \infty$, the short-term deviation tends to zero, i.e., $\chi_t \to 0$. Therefore, long-maturity forwards are required to estimate the unobservable equilibrium price, ξ_t, and the difference between the long- and short-maturity forwards provides the information about the short-term deviations, χ_t.

[8] Sample autocorrelation functions calculate the autocorrelations of data for different lags and are commonly used in checking the randomness of data, detecting seasonality, and model identification.

existence of spikes at lags equal to seven (i.e., at lags 7, 14, 21, etc), reveals a significant weekly seasonality (particularly in electricity prices). Moreover, since the range of the in-sample data covers a three-year period, yearly seasonality is also worth considering. The time-series plot of the in-sample data, graphed in Figure 2.4.a, which shows that the data tend to increase over the winters while they decrease during the summers, also supports the presence of yearly seasonality.

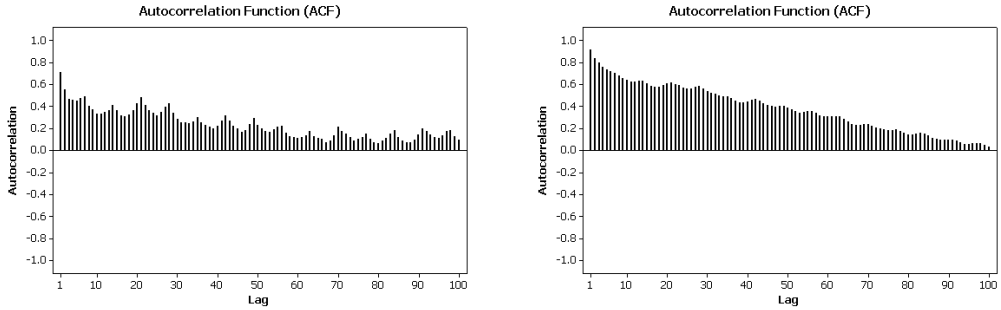

(a) Electricity (b) Gas

Figure 2.2: The sample auto-correlation functions of logarithms of electricity (a) and gas (b) before removing the seasonality

Consequently, the deterministic part of Equation (2.1) can be specified by a set of cosine and sine terms defined at the frequencies $\lambda_j = 2\pi j/s$ and $\lambda'_j = 2\pi j/s'$ as follows (see Harvey (1989) for more details):

$$\begin{aligned} f_t^{(i)} &= \sum_{j=1}^{[s/2]} \left(\gamma_{1j}^{(i)} \cos \lambda_j t + \gamma_{1j}^{*(i)} \sin \lambda_j t \right) \\ &\quad + \sum_{j=1}^{[s'/2]} \left(\gamma_{2j}^{(i)} \cos \lambda'_j t + \gamma_{2j}^{*(i)} \sin \lambda'_j t \right), \quad t = 1, 2, ..., n, \end{aligned} \tag{2.2}$$

where $i \in \{E, G\}$, the function $[a/2]$ for any $a \in \mathbb{Z}$ is defined as

$$[a/2] = \begin{cases} a/2 & \text{for } a \text{ even} \\ (a-1)/2 & \text{for } a \text{ odd} \end{cases}, \tag{2.3}$$

$s = 7$, $s' = 365$, $n = 1095$, and $\{\gamma_{1j}^{(i)}, \gamma_{1j}^{*(i)}, \gamma_{2j}^{(i)}, \gamma_{2j}^{*(i)}\}$ are the unknown coefficients that are to be estimated via applying linear regression to the data, a method similar to the one in Maribu *et al.* (2007) (estimations are provided in Appendix

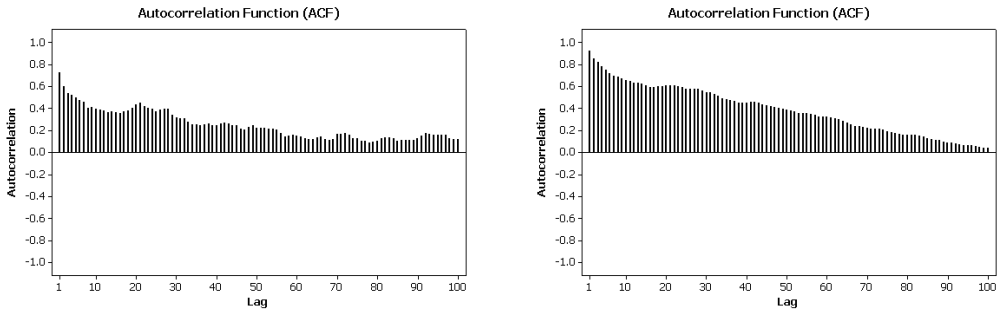

(a) Electricity (b) Gas

Figure 2.3: The sample auto-correlation functions of logarithms of electricity (a) and gas (b) after removing weekly and yearly seasonality

A. Figure 2.3 displays the sample autocorrelation function of the log prices after removing the seasonality. Clearly, no more weekly seasonality exists in these new data. Looking at Figure 2.4.b, logarithms of electricity and gas spot prices over the in-sample period after removing the seasonality, it is revealed that the yearly seasonality is also well captured because no more annual upward or downward trend is observed.

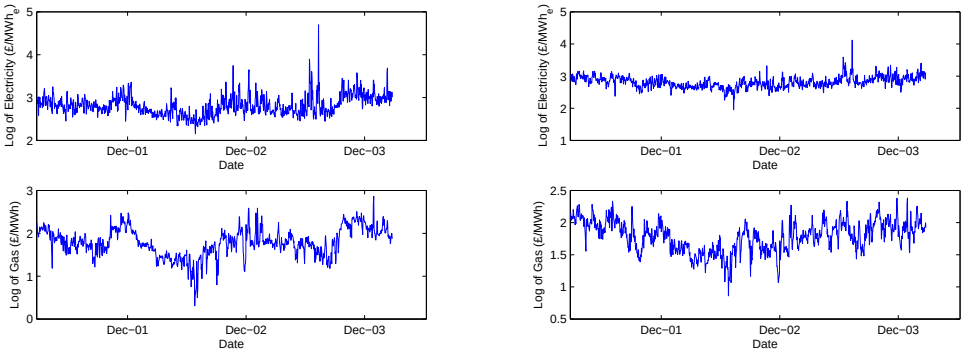

(a) Before removing the seasonality (b) After removing the seasonality

Figure 2.4: Logarithms of the UK electricity and gas spot prices (in-sample data), before (a) and after (b) removing the seasonality

2.3 Stochastic Linear Models

After capturing the seasonality, four linear stochastic models are proposed for the logarithms of prices[9]:

Model (1) Mean reversion for both electricity and gas (MR-MR)

$$dX_t^E = \kappa_E(\lambda_E - X_t^E)dt + \sigma_E dW_t^E \tag{2.4}$$

$$dX_t^G = \kappa_G(\lambda_G - X_t^G)dt + \sigma_G dW_t^G \tag{2.5}$$

where dW_t^E and dW_t^G are correlated increments of standard Brownian motion processes with $\mathbb{E}(dW_t^E dW_t^G) = \rho dt$[10].

Model (2) Arithmetic Brownian motion for electricity and mean reversion for gas (ABM-MR)

$$dX_t^E = \mu_E dt + \sigma_E dW_t^E \tag{2.6}$$

$$dX_t^G = \kappa_G(\lambda_G - X_t^G)dt + \sigma_G dW_t^G \tag{2.7}$$

Model (3) Geometric Brownian motion for both electricity and gas (GBM-GBM)

$$dX_t^E = \mu_E X_t^E dt + \sigma_E X_t^E dW_t^E \tag{2.8}$$

$$dX_t^G = \mu_G X_t^G dt + \sigma_G X_t^G dW_t^G \tag{2.9}$$

Model (4) Geometric Brownian motion for electricity and mean reversion for gas (GBM-MR)

$$dX_t^E = \mu_E X_t^E dt + \sigma_E X_t^E dW_t^E \tag{2.10}$$

$$dX_t^G = \kappa_G(\lambda_G - X_t^G)dt + \sigma_G dW_t^G \tag{2.11}$$

[9] Guthrie & Videbeck (2007) reveals that the intra-period correlation patterns of electricity prices cannot be captured by standard financial models of spot prices. Although we do not have time-dependent correlation parameters, by calculating the intra-week and intra-month correlations, no specific patterns were found in our electricity spot prices.

[10] For simplicity, we consider only instantaneous correlation between electricity and gas prices rather than lag/lead correlations.

Table 2.2: Estimation using multivariate normal regression

Parameters[a]		Model (1)	Model (2)	Model (3)	Model (4)
Electricity	σ_E	2.3761	2.5669	0.9008	0.9008
	μ_E		0.0152	0.4082	0.4082
	κ_E	106.9175			
	λ_E	2.8159			
	ρ	0.2086	0.1773	0.1542	0.1735
Gas	σ_G	1.9700	1.9675	1.1882	1.9675
	μ_G			0.6643	
	κ_G	43.6338	35.5522		35.5696
	λ_G	1.7832	1.7828		1.7828

[a]The standard errors of the estimations are reported in Appendix B

2.3.1 Estimation

Writing the discrete-time form of the processes after applying an Euler approximation based on stochastic differential Equations (2.4) to (2.11) with time steps of length $\Delta t = 1/365$, i.e., one day, we can apply multivariate normal regression to estimate the unknown parameters of the models. For example the discrete-time approximation of model (1), Equations (2.4) and (2.5), can be written as

$$\begin{bmatrix} \Delta X_t^E \\ \Delta X_t^G \end{bmatrix} = \begin{bmatrix} -\kappa_E \Delta t X_{t-1}^E \\ -\kappa_G \Delta t X_{t-1}^G \end{bmatrix} + \begin{bmatrix} \kappa_E \lambda_E \Delta t \\ \kappa_G \lambda_G \Delta t \end{bmatrix} + \mathbf{V}_t \tag{2.12}$$

where $\Delta X_t^{(.)} = X_t^{(.)} - X_{t-1}^{(.)}$, and $\mathbf{V}_t$ (2×1) is normally distributed with a mean of zero and the covariance matrix ν,

$$\nu = \begin{bmatrix} \sigma_E^2 \Delta t & \sigma_E \sigma_G \Delta t \rho \\ \sigma_E \sigma_G \Delta t \rho & \sigma_G^2 \Delta t \end{bmatrix}. \tag{2.13}$$

The in-sample data, which include observations from 27 March 2001 to 26 March 2004, are then used to estimate the unknown parameters of the four linear models. The results are reported in Table 2.2, and the models will be compared in the next subsection. The standard errors of the estimations are reported in Appendix B. In Appendix C, we show that the residuals are approximately normal with mean of zero and a roughly constant variance.

Table 2.3: RMSE of the models

	Model (1)	Model (2)	Model (3)	Model (4)
RMSE	0.1138	0.1187	0.1221	0.1187

2.3.2 Comparison

Although the data are stationary[11], i.e., a mean-reverting model is the most suitable one among the others, we are still interested in comparing both the goodness-of-fit and the out-of-sample forecasting performance of each model. The measurements used for comparison are the root-mean-square error (RMSE) for the former objective and the expected root-mean-square error (ERMSE) over the out-of-sample period for the latter one.

The RMSE value of each model is:

$$RMSE = \sqrt{\frac{1}{2n}\sum_{t=1}^{n}(\mathbf{y}_t - \hat{\mathbf{y}}_t)'(\mathbf{y}_t - \hat{\mathbf{y}}_t)} \tag{2.14}$$

where $\mathbf{y}_t$ is a vector consisting of logarithms of observed energy prices at time t, $\hat{\mathbf{y}}_t$ refers to its predicted value, and $n = 1095$ is the total number of observations over the in-sample period. The results indicate that mean reversion for both electricity and gas spot prices, model (1), with the lowest RMSE of 0.1138 is regarded as the best-fitted model (see Table 2.3).

As mentioned before, our data set is divided into two subsets: the in-sample and the out-of-sample period. After estimating the unknown parameters of models of interest using the in-sample period we calculate the r-step ahead expected values of the log prices over the out-of-sample period (from 27/03/04 to 31/12/06). In order to evaluate the forecasting performance of each model, we then find the ERMSE of the models for different values of r (from 1 to 365 days)

[11] Stationarity is confirmed by running augmented Dickey-Fuller (ADF) unit root test (see Dickey & Fuller (1979) for more details). The ADF test strongly rejects the null hypothesis of a unit root in the time series with a very small p-value of less than 0.001. The t-statistics for logarithms of electricity and gas prices are -13.5093 and -7.5401, respectively, while the critical value associated with the sample size 1095 for a significance level of 0.001 is -4.981 (Hamilton (1994)).

as follows,

$$ERMSE(r) = \sqrt{\frac{1}{2(T-r+1)} \sum_{t=n+r}^{n+T} (\mathbf{y}_t - \hat{\mathbf{y}}_{(t|t-r)})'(\mathbf{y}_t - \hat{\mathbf{y}}_{(t|t-r)})} \qquad (2.15)$$

where the vector $\mathbf{y}_t$ includes the logarithms of observed electricity and gas spot prices at time t, the vector $\hat{\mathbf{y}}_{t|t-r}$ consists of their predictions given information at time $t-r$, and T, the total number of observations over the out-of-sample period, which has the value of 1010. The results, presented in Figure 2.5, also reveal that model (1) outperforms other linear models in terms of long-term forecasting, although model (4) is better over shorter lead times. One sample path from each model, for both electricity and gas, is also graphed in Figures 2.6 and 2.7. These simulations also indicate that mean-reverting models are more appropriate for the logarithms of electricity and gas prices, although they are not powerful enough in capturing the spikes of electricity prices. Based on all these comparison methods, thus, the first model, MRMR, is picked as the best linear model and will be used when considering non-linearity in the following section.

2.4 Non-Linear Stochastic Models

In terms of the recent spikes and stochastic volatility in UK energy spot prices, Markov regime-switching approaches and a mean-reverting stochastic volatility model may be more appropriate for forecasting and valuing investments than the simple linear models of Section 2.3. Towards that end, we explore two such non-linear models in this section.

2.4.1 Markov Regime-Switching (MRS) Approaches

The idea behind modelling regime-switching commodity prices is to distinguish between two independent regimes: the stable regime and the spike regime (Hamilton (1989)). Since the regime state is not observable, we need to use Hamilton filter. The model will then be estimated applying maximum-likelihood optimisation in connection with the Hamilton filter for the unobservable regime-switching process (see Appendix D for more details). Kosater & Mosler (2006), using Ger-

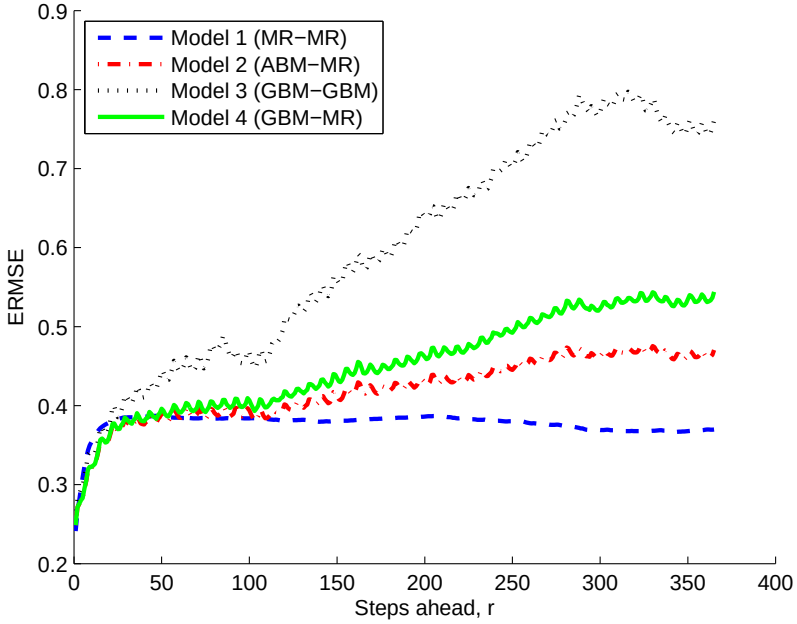

Figure 2.5: The expected root-mean-square error

man hourly electricity spot prices over four years, considers two variants for a two-regime model: one with a stable regime and a spike regime and one with a stable regime and a modified spike regime. In the latter one, it distinguishes between high spikes and low spikes as typical of very high demands over working days and very low demands over weekends and holidays. Karakatsani & Bunn (2008), analysing UK half-hourly electricity spot prices over the first year after the introduction of NETA, also suggests the presence of two, or sometimes three, regimes in the most volatile trading periods[12].

Motivated by this work on modelling electricity prices, we propose a multivariate model with two regimes for the logarithms of correlated electricity and gas spot prices. Let S_t denote the unobservable regime parameter at time t, i.e.,

$$S_t = \begin{cases} 0 & \text{stable regime} \\ 1 & \text{spike regime} \end{cases} \tag{2.16}$$

[12]In Karakatsani & Bunn (2008), each day consists of 48 trading periods, and a total number of 300 days for each period are analysed.

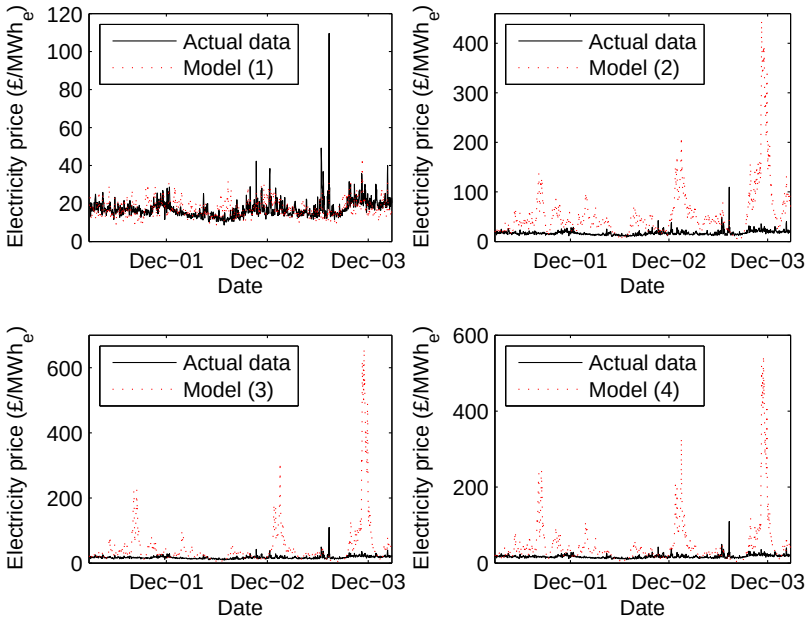

Figure 2.6: Simulation of electricity spot prices over the in-sample period

where the transition between two regimes is governed by a first-order Markov process:

$$\begin{aligned} Prob[S_t = 0|S_{t-1} = 0] &= p, \\ Prob[S_t = 1|S_{t-1} = 0] &= 1 - p, \\ Prob[S_t = 1|S_{t-1} = 1] &= q, \\ Prob[S_t = 0|S_{t-1} = 1] &= 1 - q. \end{aligned} \tag{2.17}$$

We assume that the stochastic part of the logarithms of electricity and gas spot prices in Equation (2.1) are split into two factors as follows,

$$\begin{bmatrix} X_t^E \\ X_t^G \end{bmatrix} = \begin{bmatrix} \alpha_E^{(S_t)} \\ \alpha_G^{(S_t)} \end{bmatrix} + \begin{bmatrix} Z_t^{E(S_t)} \\ Z_t^{G(S_t)} \end{bmatrix} \tag{2.18}$$

where the superscript S_t, hereafter, denotes the regime state, the first term on the right-hand side is a vector containing the long-term equilibrium levels for the log prices, and the second term consists of two correlated mean-reverting processes,

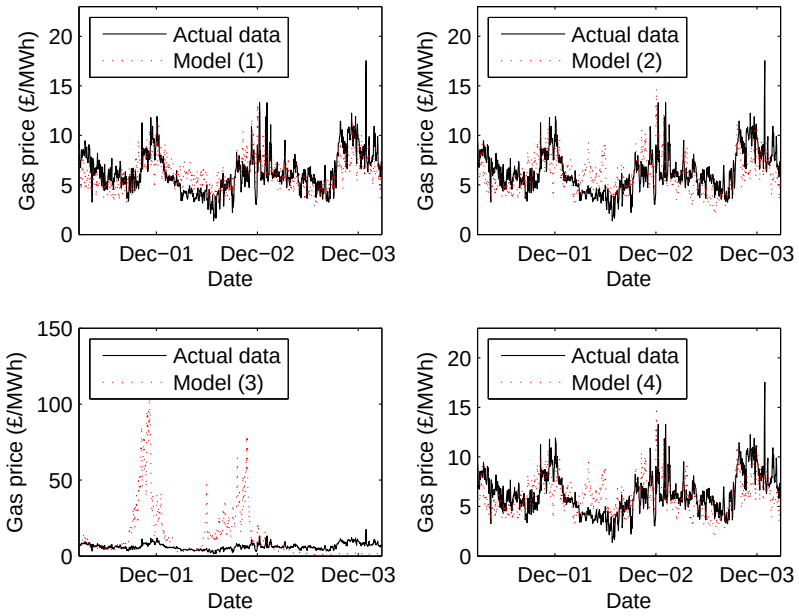

Figure 2.7: Simulation of gas spot prices over the in-sample period

following from the previous analysis on our data set,

$$\begin{bmatrix} dZ_t^{E(S_t)} \\ dZ_t^{G(S_t)} \end{bmatrix} = \begin{bmatrix} -\kappa_E^{(S_t)} Z_t^{E(S_t)} dt \\ -\kappa_G^{(S_t)} Z_t^{G(S_t)} dt \end{bmatrix} + \begin{bmatrix} \sigma_E^{(S_t)} dW_t^E \\ \sigma_G^{(S_t)} dW_t^G \end{bmatrix}, \tag{2.19}$$

where $\mathbb{E}(dW_t^E dW_t^G) = \rho dt$.[13] The discrete-time approximation of the process based on this stochastic differential equation with time steps of length $\Delta t = 1/365$ (one day) can be written as follows:

$$\begin{bmatrix} Z_t^{E(S_t)} \\ Z_t^{G(S_t)} \end{bmatrix} = \begin{bmatrix} (1 - \kappa_E^{(S_t)} \Delta t) Z_{t-1}^{E(S_{t-1})} \\ (1 - \kappa_G^{(S_t)} \Delta t) Z_{t-1}^{G(S_{t-1})} \end{bmatrix} + \begin{bmatrix} \sigma_E^{(S_t)} \Delta W_t^E \\ \sigma_G^{(S_t)} \Delta W_t^G \end{bmatrix} \tag{2.20}$$

In order to apply the Hamilton-filter algorithm, Equations (2.18) and (2.20) should now be combined into one equation,

[13] Here, for simplicity, we consider only one correlation between electricity and gas in both regimes. We could, however, consider four different correlations: correlation between the spike regime of electricity and the spike and stable regimes of gas, as well as, the correlation between the stable regime of electricity and the spike and the stable regimes of gas.

$$\begin{bmatrix} X_t^{E(S_t)} \\ X_t^{G(S_t)} \end{bmatrix} = \begin{bmatrix} \alpha_E^{(S_t)} \\ \alpha_G^{(S_t)} \end{bmatrix} + \begin{bmatrix} \phi_E^{(S_t)}(X_{t-1}^{E(S_{t-1})} - \alpha_E^{(S_{t-1})}) \\ \phi_G^{(S_t)}(X_{t-1}^{G(S_{t-1})} - \alpha_G^{(S_{t-1})}) \end{bmatrix} + \mathbf{V}_t^{(S_t)} \tag{2.21}$$

where

$$\phi_E^{(S_t)} = 1 - \kappa_E^{(S_t)}\Delta t, \tag{2.22}$$

$$\phi_G^{(S_t)} = 1 - \kappa_G^{(S_t)}\Delta t, \tag{2.23}$$

and $\mathbf{V}_t^{(S_t)}$ (2×1) given S_t, is normally distributed with mean of zero and the covariance matrix

$$\nu^{(S_t)} = \begin{bmatrix} \sigma_E^{2(S_t)}\Delta t & \sigma_E{}^{(S_t)}\sigma_G{}^{(S_t)}\Delta t\rho \\ \sigma_E{}^{(S_t)}\sigma_G{}^{(S_t)}\Delta t\rho & \sigma_G^{2(S_t)}\Delta t \end{bmatrix}. \tag{2.24}$$

In Appendix D, we show how we can estimate the unknown parameters using the Hamilton filter for this multivariate conditionally normal distribution (see Equation (2.21)).

Figure 2.4.b shows that, after removing the seasonality, no unexpected spikes are observed in the logarithms of gas spot prices over the in-sample data. Thus, we are no longer interested in capturing the spikes in gas prices. In this model, which is defined as MRRS, we assume that logarithms of gas prices follow a simple linear mean-reverting model with only one regime, while the logarithms of electricity prices are mean-reverting processes with two separate regimes, the spike regime and the stable regime.

Parameter estimates are reported in Tables 2.4 and 2.5. As we expected, the probability of remaining in the same state for the stable regime (0.9804) is very high in comparison with that value for the spike regime (0.4689), which is relatively small. Another probability reported in Table 2.4 is the initial conditional probability $\Pi_0 = Prob[S_0 = 1|\mathbf{Y}_0]$ (see Appendix D for more details) that is extremely small and indicates that the process at time zero given all available information would be almost certainly in the stable regime. The estimates of parameters of gas prices are similar to those of the mean-reverting model in the previous section; moreover, the estimates of parameters of electricity prices in stable regime are also very close to those in model (1). As we would expect, how-

Table 2.4: Estimation of probabilities

Parameter	p	q	Π_0
Estimation	0.9804	0.4689	0.0001
Stnd. error	0.0003	.0052	0.0303

Table 2.5: Estimation using Hamilton-switching-regime algorithm

		Electricity			Gas			
Parameter		α	σ	κ	α	σ	κ	ρ
Stable	Estimation	2.8117	2.0404	100.6824	1.7837	1.9716	44.1133	0.2231
	Stnd. error	0.0004	0.0018	0.2223	0.0007	0.0013	0.1465	0.0009
Spike	Estimation	2.9680	6.2511	132.8057				
	Stnd. error	0.0018	0.0317	1.7775				

ever, the volatility of the spike regime (6.25) of electricity prices is much higher than that of the stable regime (2.04), which makes it eligible to capture some spikes of the time series.

A sample path drawn from this non-linear model along with the actual data over the in-sample period is graphed in Figure 2.8. Comparing these simulations with those drawn from the linear mean-reverting model (graphed in Figures 2.6 and 2.7), it can be seen that although the regime-switching model is not able to capture the high electricity price spikes, it behaves better than the simple linear model in predicting low spikes.

2.4.2 Mean-Reverting Stochastic Volatility

In order to improve the unrealistic assumption of constant volatility in model (1), here, mean-reverting models with stochastic volatility driven by a mean-reverting process are posited. We define a mean reversion with stochastic volatility for the logarithm of the electricity price and two variants for the logarithm of the gas price: one with deterministic volatility (MRSV1) and one with stochastic volatility (MRSV2). Model MRSV1 (Equations (2.25-2.33)) is similar to the proposed model in Maribu *et al.* (2007), but, we analyse spot prices rather than forward prices.

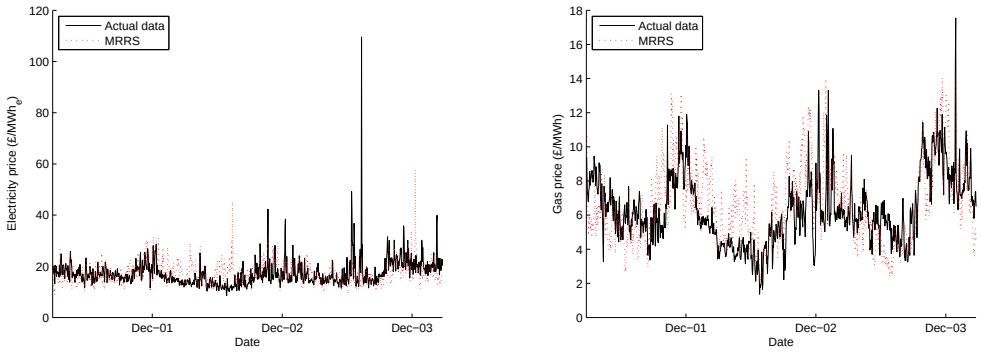

(a) Electricity (b) Gas

Figure 2.8: Simulation of electricity (a) and gas (b) spot prices over the in-sample period

In Equation (2.4), we assume that the variance, σ_E, is a function of the unobservable stochastic variable Z_t:

$$dX_t^E = \kappa_E(\lambda_E - X_t^E)dt + \sigma(Z_t^E)dW_t^E \tag{2.25}$$

where Z_t^E is another mean-reverting process independent of X_t^E:

$$dZ_t^E = -\kappa_e Z_t^E dt + \sigma_e dW_t^e \tag{2.26}$$

In this thesis, we assume that $\sigma(Z_t^E) = \gamma_E e^{Z_t^E}$ (and $\sigma(Z_t^G) = \gamma_G e^{Z_t^G}$ for model MRSV2). Notice that in model MRSV1, the natural gas price is given by the same mean-reverting process in Equation (2.5).

2.4.2.1 Estimating the Unobservable Stochastic Volatility

Since the volatility variable, Z_t^E, in Equation (2.25) is not observable, a tool from spatial statistics, the variogram, is used to estimate the unknown parameters in Equation (2.26) (Fouque *et al.* (2000)).[14]

[14] As in Chib *et al.* (2002), we can also use Markov chain Monte Carlo (MCMC) methods to estimate the unknown parameters for both unobservable and observable variables.

Variogram analysis Based on the stochastic volatility model, Equation (2.25), the normalised fluctuation of the data

$$D_t^E = \frac{\Delta X_t^E}{\sqrt{\Delta t} X_{t-1}^E} \tag{2.27}$$

can be written as

$$D_t^E = \kappa_E(\frac{\lambda_E}{X_t^E} - 1)\sqrt{\Delta t} + \frac{\sigma(Z_t^E)\Delta W_t^E}{X_{t-1}^E\sqrt{\Delta t}} \tag{2.28}$$

The first term on the right-hand side is omitted, because it is negligibly small for small values of Δt (Fouque *et al.* (2000)). The normalised fluctuation process, thus, is modelled as

$$D_n^E = \frac{\sigma(Z_n^E)\epsilon_n^E}{X_{n-1}^E} \tag{2.29}$$

where $\{\epsilon_n\}$ is a sequence of IID standard normal random variables with mean 0 and variance 1 representing $\Delta W_t^E/\sqrt{\Delta t}$. Equation (2.29) shows that the normalised increment, $D_n^{'E}$, is modelled as

$$D_n^{'E} = \frac{\Delta X_n^E}{\sqrt{\Delta t}} = D_n^E X_{n-1}^E = \sigma(Z_n^E)\epsilon_n^E \tag{2.30}$$

As suggested in Fouque *et al.* (2000), we will analyse the log absolute value of the normalised increments L_n, where

$$L_n^E = log|D_n^{'E}| = log(\sigma(Z_n)) + log|\epsilon_n^E| \tag{2.31}$$

Fouque *et al.* (2000) proves that the empirical variogram of L_n^E defined as

$$V_j^E = \frac{1}{N_j}\sum_{n=1}^{N_j}(L_{n+j}^E - L_n^E)^2, \tag{2.32}$$

where j is the lag and N_j is the total number of points, is an unbiased estimator of the semivariogram:

$$\gamma_j^E = 2c^2 + \sigma_e^2/\kappa_e(1 - e^{-j\kappa_e\Delta t}), \tag{2.33}$$

where $c^2 = Var(log|\epsilon|)$.[15] Using the in-sample data, the quantities L_n ($n = 1, 2, \ldots, 1094$) and the empirical variograms are calculated. Finally, the approximate estimations of the unknown parameters of the unobservable stochastic volatility are computed and reported in Table 2.6 (see Appendix E for more details).

If both the volatilities of logarithms of electricity and gas prices are assumed to be stochastic (MRSV2), i.e.,

$$dX_t^E = \kappa_E(\lambda_E - X_t^E)dt + \sigma(Z_t^E)dW_t^E, \tag{2.34}$$

$$dX_t^G = \kappa_G(\lambda_G - X_t^G)dt + \sigma(Z_t^G)dW_t^G, \tag{2.35}$$

where,

$$dZ_t^E = -\kappa_e Z_t^E dt + \sigma_e dW_t^e, \tag{2.36}$$

$$dZ_t^G = -\kappa_g Z_t^G dt + \sigma_g dW_t^g, \tag{2.37}$$

with $\mathbb{E}(dW_t^e dW_t^g) = \rho_{eg}dt$, then in order to take into account the available correlation between these stochastic volatilities, we propose a new model based on the empirical cross-variogram of $\{L_n^E\}$ and $\{L_n^G\}$ (defined in Chilés & Delfiner (1999)), instead of their separated empirical variograms, as follows:

$$V_j^{EG} = \frac{1}{N_j}\sum_{n=1}^{N_j}(L_{n+j}^E - L_n^E)(L_{n+j}^G - L_n^G) \tag{2.38}$$

where

$$L_n^G = log|D_n'^G| = log(\sigma(Z_n^G)) + log|\epsilon_n^G| \tag{2.39}$$

Using the same method as in Fouque *et al.* (2000), in Appendix F, we prove that this empirical cross-variogram[16] is an unbiased estimator of the semi-cross variogram:

$$\gamma_j^{EG} = \frac{\rho_{eg}\sigma_e\sigma_g}{\kappa_e\kappa_g}(2 - e^{-\kappa_e j\Delta t} - e^{-\kappa_g j\Delta t}) + 2cov(\log|\epsilon^E|, log|\epsilon^G|) \tag{2.40}$$

[15] The empirical variogram, V_j^E, is the sample mean of the semivariogram, $\gamma_j^E = \mathbb{E}(L_{n+j}^E - L_n^E)^2$.

[16] The empirical cross-variogram, V_j^{EG}, is the sample mean of the semi-cross variogram, $\gamma_j^{EG} = \mathbb{E}(L_{n+j}^E - L_n^E)(L_{n+j}^G - L_n^G)$.

The estimated parameters using the in-sample data (reported in Table 2.6) show that the stochastic volatility of the logarithm of the electricity price has a high rate of mean reversion, i.e., it is nearly four times that of the stochastic volatility of the logarithm of the gas price in model MRSV2. The positive correlation between the stochastic volatilities of electricity and gas prices indicates that any increase (decrease) in the volatility of the electricity price is associated with an increase (decrease) in the volatility of the gas price.

Table 2.6: Estimation: parameters of the unobservable stochastic volatility

Model	κ_Z^E	σ_Z^E	κ_Z^G	σ_Z^G	ρ_{eg}
MRSV1	300.0020	9.2368	-	-	-
MRSV2	297.6075	11.0237	80.8329	4.0804	0.1881

2.4.2.2 Estimating the Main Model

We can now, after estimating the stochastic volatility process, estimate the main model of the energy prices. The discrete-time approximation of the stochastic differential Equations (2.5), (2.25), and (2.26) with time steps of length Δt then can be written as

$$\mathbf{X}_t = \begin{bmatrix} (1-\kappa_E \Delta t) X_{t-1}^E \\ (1-\kappa_G \Delta t) X_{t-1}^G \end{bmatrix} + \begin{bmatrix} \kappa_E \lambda_E \Delta t \\ \kappa_G \lambda_G \Delta t \end{bmatrix} + \mathbf{V}_t(Z_t) \tag{2.41}$$

where

$$\mathbf{X}_t = \begin{bmatrix} X_t^E \\ X_t^G \end{bmatrix}, \tag{2.42}$$

$\mathbf{V}_t(Z_t)$ given Z_t is multivariate normally distributed with zero mean and the covariance matrix ν, where

$$\nu = \begin{bmatrix} \sigma_E(Z_t)^2 \Delta t & \sigma_E(Z_t)\sigma_G \Delta t \rho \\ \sigma_E(Z_t)\sigma_G \Delta t \rho & \sigma_G^2 \Delta t \end{bmatrix}. \tag{2.43}$$

It follows that $\mathbf{X}_t$ given $\{\mathbf{X}_{t-1}, Z_t\}$ is multivariate normally distributed with mean

$$\mu = \begin{bmatrix} (1-\kappa_E\Delta t)X^E_{t-1} + \kappa_E\lambda_E\Delta t \\ (1-\kappa_G\Delta t)X^G_{t-1} + \kappa_G\lambda_G\Delta t \end{bmatrix} \tag{2.44}$$

and the covariance matrix ν, indicated in Equation (2.43). The log likelihood function of this process, which can be written as follows:

$$l(\Theta, z) = \sum_{t=1}^{n} \log f(\mathbf{x}_t|\mathbf{x}_{t-1}, z_t, \Theta) \tag{2.45}$$

depends on unobservable stochastic variables Z_t. Hence, it is not possible to maximise it with respect to the unknown parameters $\Theta = \{\kappa_E,\ \lambda_E,\ \gamma_E,\ \kappa_G,\ \lambda_G,\ \sigma_G\}$ because of presence of unknown variables Z_t.

Taking $N = 10000$ sample paths $\{z_t^{(1)}, z_t^{(2)}, \ldots, z_t^{(N)}\}$ from the distribution $\{f(z_t|z_{t-1}); t = 1, \ldots, n\}$, which has been estimated before, starting with an initial value z_0, we define $\hat{\Theta}^{(j)}$ as the maximum likelihood estimator of parameter Θ corresponding to the sample path $j = 1, \cdots, N$:

$$l(\hat{\Theta}^{(j)}, z^{(j)}) = \max_{\Theta} l(\Theta, z^{(j)}), \tag{2.46}$$

Finally, the one with the highest likelihood function is defined as the quasi-maximum likelihood estimator of Θ, $\hat{\Theta}$:

$$l(\hat{\Theta}) = \max_{j=1,\cdots,N} l(\hat{\Theta}^{(j)}, z^{(j)}), \tag{2.47}$$

Estimates are reported in Table 2.7 and indicate that the parameters of the main models, such as κ_E, λ_E, κ_G, and λ_G, in both MRSV1 and MRSV2 are very close to those in the linear mean-reverting model (Table 2.2). However, the correlation between electricity and gas has decreased, specifically in model MRSV2, which is likely due to the introduction of a new correlation between their volatilities. Figures 2.9 and 2.10 display some sample paths from models MRSV1 and MRSV2 over the in-sample data set, respectively. It is observed that these models are more able to capture even very high spikes than both models MR and MRRS. Simulations drawn from model MRSV2 reveal that high spikes in electricity prices are coincident with high spikes in gas prices, while in model MRSV1 high spikes

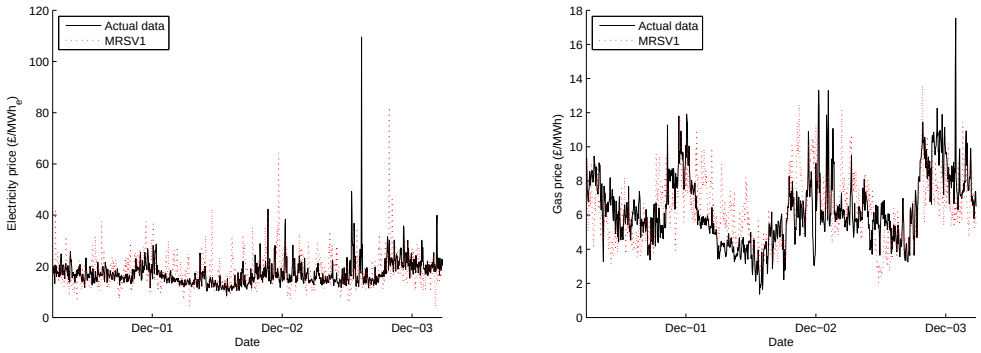

(a) Electricity (b) Gas

Figure 2.9: Simulation of electricity (a) and gas (b) spot prices over the in-sample period via model MRSV1

of electricity may occur with low or no spikes in gas prices.

Table 2.7: Estimation using mean-reverting stochastic volatility

Parameters		MRSV1		MRSV2	
		Estimate	Stnd. Error	Estimate	Stnd. Error
Electricity	κ_E	108.9525	0.1460	121.5248	0.1452
	λ_E	2.8320	0.0002	2.8015	0.0002
	γ_E	2.5813	0.0012	3.3313	0.0015
	E_0	3.1375	0.0116	3.1685	0.0016
	ρ	0.1883	0.0007	0.1906	0.0006
Gas	σ_G	1.9687	0.0009		
	κ_G	40.0335	0.1095	43.5456	0.1034
	λ_G	1.7860	0.0006	1.7827	0.0006
	γ_G			2.0859	0.0011
	G_0	2.2013	0.0025	2.2024	0.0049

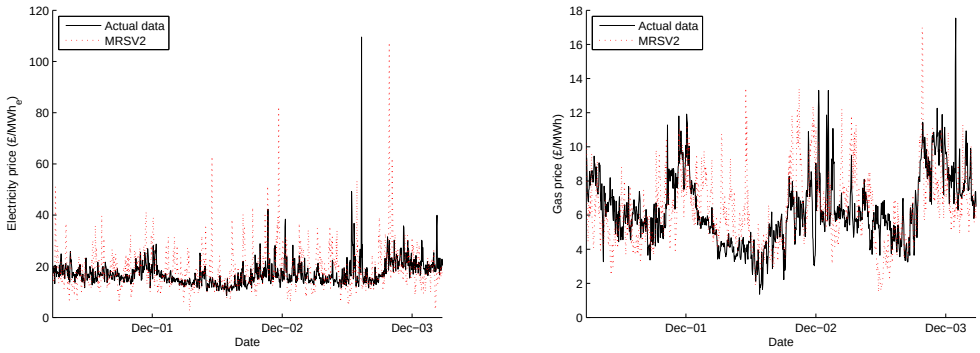

(a) Electricity (b) Gas

Figure 2.10: Simulation of electricity (a) and gas (b) spot prices over the in-sample period via model MRSV2

2.5 Valuing the Gas-Fired Power Plant over the Out-of-Sample Period

The four stochastic models that will be assessed on the basis of valuing a gas-fired power plant are redefined here[17]:

- Mean reversion for both logarithms of electricity and gas prices (MR)

- Mean reversion with Markov regime switching for the logarithm of the electricity price and simple linear mean reversion for the logarithm of the gas price (MRRS)

- Mean reversion with stochastic volatility for the logarithm of the electricity price and deterministic volatility for the logarithm of the gas price (MRSV1)

[17]The focus of our thesis is on comparing ordinary linear models with regime switching approaches and models with stochastic volatility with the aim of valuing a gas-fired power plant. Some other non-linear models that are not examined in this thesis, such as mean-reverting jump-diffusion (MRJD) processes, may also be able to capture the high energy price spikes. In an MRJD process, the normal, continuous changes in price (diffusion process) are modeled by a mean-reverting process, while the abnormal, discontinuous changes (jump process) are modeled by a Poisson distribution (for more details see, e.g., Cartea & Figueroa (2005); Clewlow *et al.* (2005); Deng (2000)). Moreover, in this study we do not model spark spreads directly because not only we may lose some information about the spark spreads' uncertainty structure, but also modelling the spark spread directly implies a constant heat rate, which makes it cumbersome to do sensitivity analysis.

- Mean reversion with stochastic volatility for both logarithms of electricity and gas prices (MRSV2)

2.5.1 Assumptions

We assume that the gas-fired power plant produces electricity with a constant capacity of 100 MW_e. The value of the plant depends only on the spark spread each day, and it can be switched on and off depending on its profitability in a particular day. The total number of daily running hours are twenty-four with an operating heat rate, ϵ, of 2.5 (MWh/MWh_e). We use a constant risk-adjusted annual interest rate $r = 0.06$[18], which results in a daily interest rate of $d = 0.0002$. The profit of the power plant without operational flexibility each day is

$$P_t = H \times K(E_t - \epsilon G_t) \tag{2.48}$$

which may be negative, while the profit of the plant with operational flexibility as in the following equation would never be negative:

$$P_t = \begin{cases} H \times K(E_t - \epsilon G_t) & if\ E_t - \epsilon G_t > 0 \\ 0 & if\ E_t - \epsilon G_t \leq 0 \end{cases} \tag{2.49}$$

where H, ϵ, and K denote, respectively, the daily operating hours, the heat rate, and the capacity of the plant.

Using this profit function, the present value (PV) of the power plant with and without the flexibility over the out-of-sample period can be calculated via the following equation[19]:

$$PV = P_{n+1} + \frac{P_{n+2}}{(d+1)} + \frac{P_{n+3}}{(d+1)^2} + \ldots + \frac{P_{n+T}}{(d+1)^{T-1}} \tag{2.50}$$

The expected PV for the linear model can be calculated directly by computing the expected price at time t (from $n+1$ to $n+T$); however, it is not possible

[18] In case of using forward prices, risk-neutral pricing (Cox & Ross (1976)) can be used instead because the risk is directly taken into account in forward prices rather than in the net cash flow discount rate.

[19] Since the in-sample period includes n observations, the out-of-sample period starts from the $(n+1)^{st}$ observation.

to calculate it for the non-linear models using the analytical formula. In order to have more consistent results, we use Monte Carlo simulation for both linear and non-linear models. A total of M sample paths are drawn from each model, $\{\tilde{\mathbf{y}}_{n+1}^{(j)}, \tilde{\mathbf{y}}_{n+2}^{(j)}, \ldots, \tilde{\mathbf{y}}_{n+T}^{(j)}; j = 1, \ldots, M\}$. The PV of the power plant can then be calculated by starting at the last date $n+T$ and working backward to the initial time, step by step. The only profit the plant will receive at time $n+T$ is P_{n+T} (Deng *et al.* (2001)), which helps us to find the PV of the plant at time $n+T-1$,

$$PV_{n+T-1}^{(j)} = P_{n+T-1}^{(j)} + \frac{PV_{n+T}^{(j)}}{(d+1)} = P_{n+T-1}^{(j)} + \frac{P_{n+T}^{(j)}}{(d+1)} \tag{2.51}$$

where the superscript j denotes the sample path. This new information is used to calculate the expected value of the plant at time $n+T-2$ and is worked backward successively until the initial time period $(n+1)$ using recursive Equation (2.51):

$$PV_{n+1}^{(j)} = \sum_{i=1}^{T} \frac{P_{n+i}^{(j)}}{(1+d)^{i-1}} \tag{2.52}$$

Finally, the expected PV of the plant can be estimated by calculating the mean of the PVs of the plant for all sample paths:

$$\hat{PV} = \frac{1}{M} \sum_{j=1}^{M} PV_{n+1}^{(j)} \tag{2.53}$$

2.5.2 Forecasting Comparison

Before assessing the proposed models with regard to their abilities in valuing the gas-fired power plant, we calculate their ERMSEs over the out-of-sample period. For this, we first simulate N sample paths of the out-of-sample price forecasts, $\{\tilde{\mathbf{y}}_{n+1}^{(j)}, \tilde{\mathbf{y}}_{n+2}^{(j)}, \ldots, \tilde{\mathbf{y}}_{n+T}^{(j)}; j = 1, \ldots, N\}$, from each model and then calculate the ERMSE value as follows:

$$ERMSE = \frac{1}{N} \sum_{j=1}^{N} \sqrt{\frac{1}{2T} \sum_{t=n+1}^{n+T} (\mathbf{y}_t - \tilde{\mathbf{y}}_t^{(j)})'(\mathbf{y}_t - \tilde{\mathbf{y}}_t^{(j)})} \tag{2.54}$$

The results reported in Table 2.8 reveal that the linear model, mean reversion without capturing either the spikes or stochastic volatility, has the best forecasting

Table 2.8: ERMSE over the out-of-sample period

	MR	MRRS	MRSV1	MRSV2
ERMSE	0.4280	0.4280	0.4537	0.4820

performance[20] among the others. As this model is also the simplest one, most decision-makers apply it in analysing investments.

On the other hand, simulations of electricity and gas spot prices for these four models, graphed in Figures 2.11 and 2.12, reveal that although the linear model can be considered a good model for short-term periods, i.e., less than a year, it is the worst one for long-term forecasting. Meanwhile the mean-reversion model with stochastic volatility for both logarithms of electricity and gas prices is better able to capture the behaviour of prices, specifically electricity prices, with respect to long-term forecasts.

The actual PV of the gas-fired power plant with and without flexibility over the out-of-sample period is £10.423 million and £6.992 million, respectively (see Tables 2.9 and 2.10 for the expected PVs). Contrary to our expectations from the previous comparison based on price forecasts, the simple linear model provides the least accurate expected value of the plant with and without flexibility because we have seen before that this model is not able to capture the spikes, specifically in electricity prices. Similarly, since the regime-switching model is not able to capture high spikes of electricity prices, it also underestimates the expected PV of the plant. The mean-reverting model with stochastic volatility for both electricity and gas, on the other hand, provides the best forecast of the PV for both situations with and without flexibility because it is able to predict spikes with the correct frequency, although not with the right timing, which results in the high value of the ERMSE. It is also revealed from these results that the expected PV calculated by each model is less than the actual PV of the plant over the out-of-sample data. This may have resulted from the fact that our in-sample data set is less volatile than the out-of-sample data.

In order to verify the accuracy of this seemingly counterintuitive result, we use the forecasting procedure similar to that of Kosater & Mosler (2006). Using the

[20]It should be mentioned that the forecasting performance refers to the direct energy price performance rather than the power plant valuation performance.

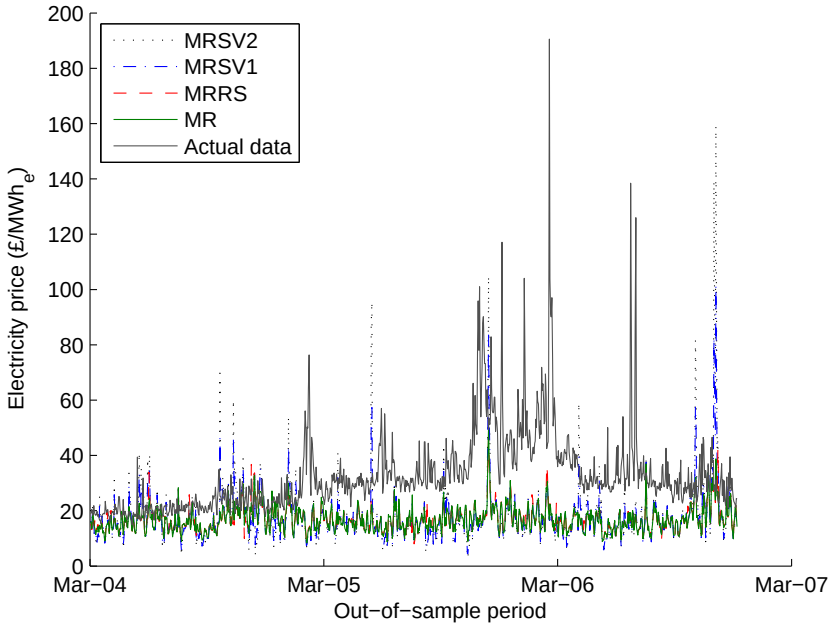

Figure 2.11: Simulation of electricity spot prices over the out-of-sample period (two years and forty weeks)

Table 2.9: The expected PV of the gas-fired power plant with flexibility together with the lower and upper quartiles (in million £)

	MR	MRRS	MRSV1	MRSV2
PV	6.4882	6.5001	7.8869	8.6068
Lower quartile	6.0783	6.0776	7.2923	7.9229
Upper quartile	6.8974	6.9228	8.4445	9.1219

Table 2.10: The expected PV of the gas-fired power plant without flexibility together with the lower and upper quartiles (in million £)

	MR	MRRS	MRSV1	MRSV2
PV	3.7959	3.8408	4.6698	4.5013
Lower quartile	3.1416	3.1797	3.7988	3.5032
Upper quartile	4.4751	4.5180	5.5438	5.4681

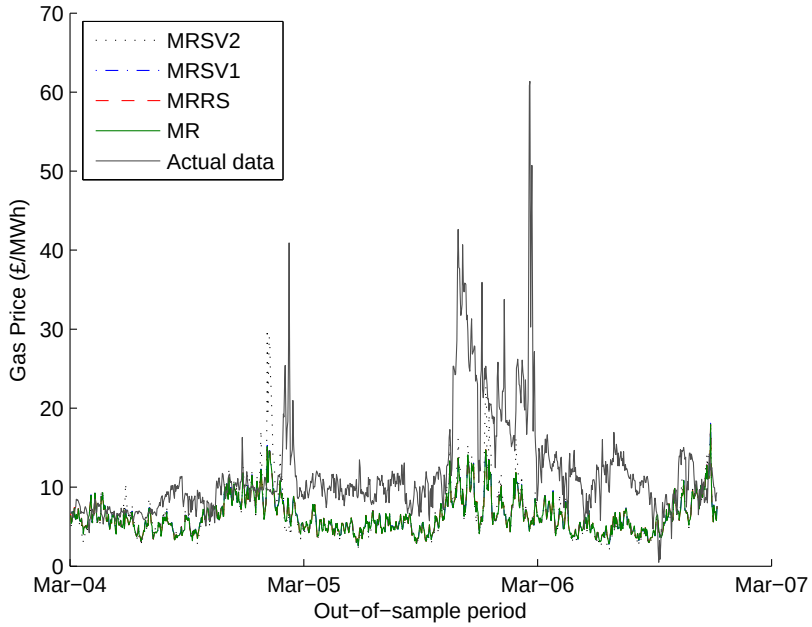

Figure 2.12: Simulation of gas spot prices over the out-of-sample period (two years and forty weeks)

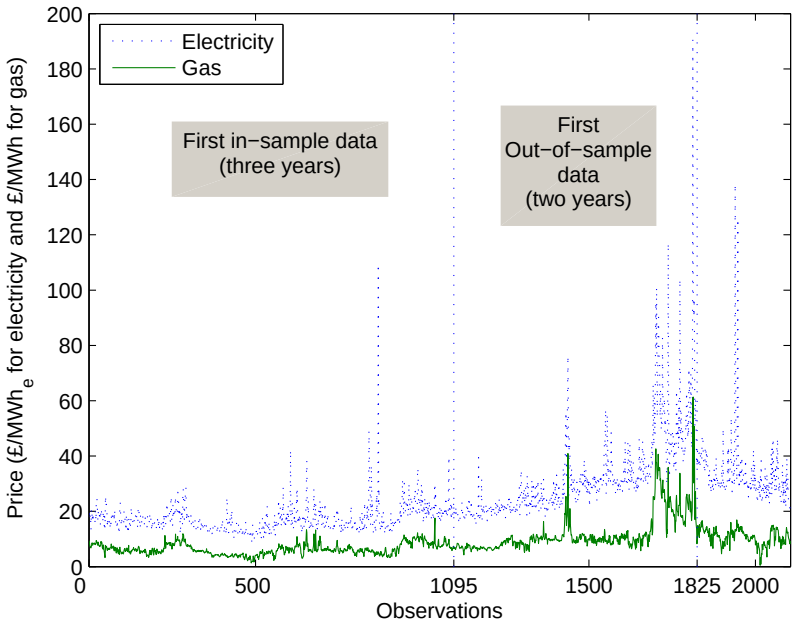

Figure 2.13: In-sample and out-of-sample periods

first 1095 observations as the in-sample data (see Figure 2.13), we estimate the parameters of the models of interest. Then, we make out-of-sample forecasts up to two years ahead and calculate the out-of-sample expected PV of the plant for those models, both with and without flexibility. The ERMSEs of these models are also calculated. Next, the in-sample data are enlarged by seven observations (one week) and again forecasts and required calculations for the new out-of-sample data (two years ahead) are made[21]. This procedure is repeated forty times.

The results are plotted in Figures 2.14 and 2.15. These results are entirely consistent with our previous findings, i.e., the non-linear models MRSV1 and MRSV2 are better able to capture the value of the power plant. We observe that before the tenth week is added to the in-sample data, the expected PV of the power plant under the MRSV2 model is greater than that under the MRSV1 model. This occurs because the estimated correlation coefficient between the logarithms of the electricity and gas price processes (see Figure 2.16) is lower

[21]Each time we enlarge the in-sample period, the out-of-sample period contains prices for two years ahead.

under the MRSV2 model during the first ten weeks and is higher from this point onwards. Since a lower correlation coefficient results in a more dispersed spark spread, which can be capitalised upon by operational flexibility, the expected PV of a flexible power plant is inversely proportional to its correlation coefficient. Hence, the expected PV of the power plant is greater under the MRSV2 model for the first ten weeks and then lower thereafter.

For a power plant without operational flexibility, a more dispersed spark spread will not necessarily lead to an increase in expected PV. Instead, we find that the expected plant PV under the MRSV1 model eventually becomes greater than that under the MRSV2 model (see Figure 2.15) because more volatile gas prices are added to the in-sample data from week 20 onwards, i.e., corresponding to observation 1235 (see Figure 2.13). Even though the eventually higher estimated correlation coefficient under the MRSV2 model reduces the risk of losses, the added in-sample data, nevertheless, imply higher expected natural gas price forecasts under the MRSV2 model than the MRSV1 model, thereby leading to a lower expected plant PV.

2.5.3 Sensitivity Analysis

2.5.3.1 Heat Rate

In order to determine how the results change with respect to the heat rate, we calculate the out-of-sample (from 27 March 2004 to 31 December 2006) expected PV of the plant with operational flexibility for different values of heat rate (ranging from 2 to 3) with all other factors are fixed (see Figures 2.17 and 2.18). It is revealed that for low values of the heat rate, both MRSV1 and MRSV2 are unlikely to capture the exact value of the out-of-sample PV of the plant, which may result from a low volatility of profit function. Figure 2.17 shows that for heat rate values of more than 2.8, model MRSV1 forecasts the PV of the plant with flexibility better than MRSV2 does, whereas neither MRSV1 nor MRSV2 is able to capture the PV of the plant without flexibility when the heat rate is larger than 2.8.

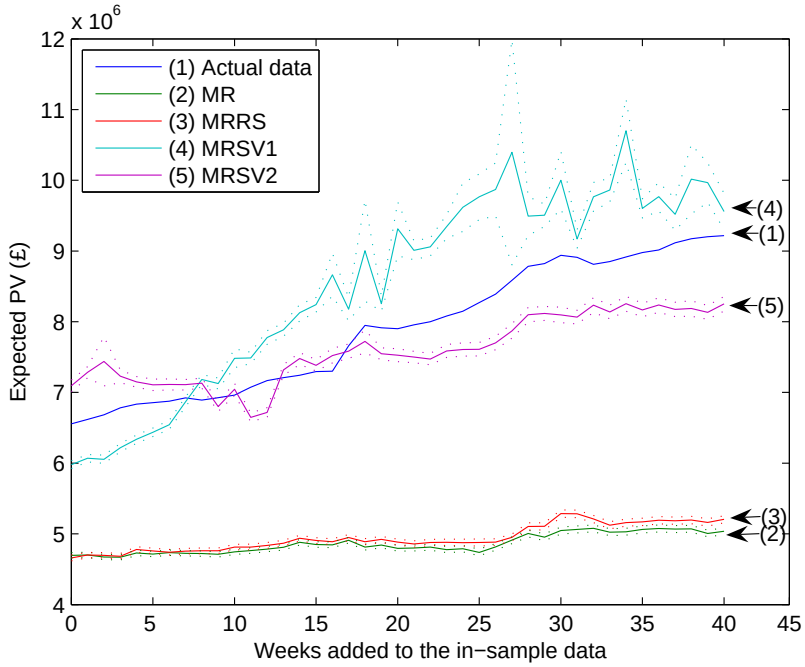

Figure 2.14: Expected PV and 95% CIs of the flexible plant with rolling expansion of the in-sample period

2.5.3.2 Stochastic Volatility of Electricity Prices via Changes in γ_E

Here, we would like to see how the expected PV of the plant would change if we modify the coefficient γ_E in the volatility function of electricity prices, $\gamma_E e^{Z_t^E}$, in either MRSV1 or MRSV2[22]. Figures 2.19 and 2.20 illustrate that the more (less) volatile the volatility of the electricity prices, the greater (lower) the expected plant PV. This dependence of the expected plant PV on γ_E is stronger in MRSV2 than in MRSV1 due to the presence of stochastic volatility in gas prices. Recall from Section 2.5.2 that the expected plant PV under the MRSV2 model is initially greater due to a lower correlation coefficient between electricity and gas prices, which results in a more dispersed spark spread under MRSV2. Since a flexible power plant is able to benefit from such variability, its expected PV is greater. On the other hand, considering the plant without flexibility (see Figure 2.20), it

[22]It must be mentioned that by increasing (decreasing) $\gamma_E e^{Z_t^E}$, we assume that the data are more (less) volatile, i.e., the analysis in this section is not directly connected to the real data.

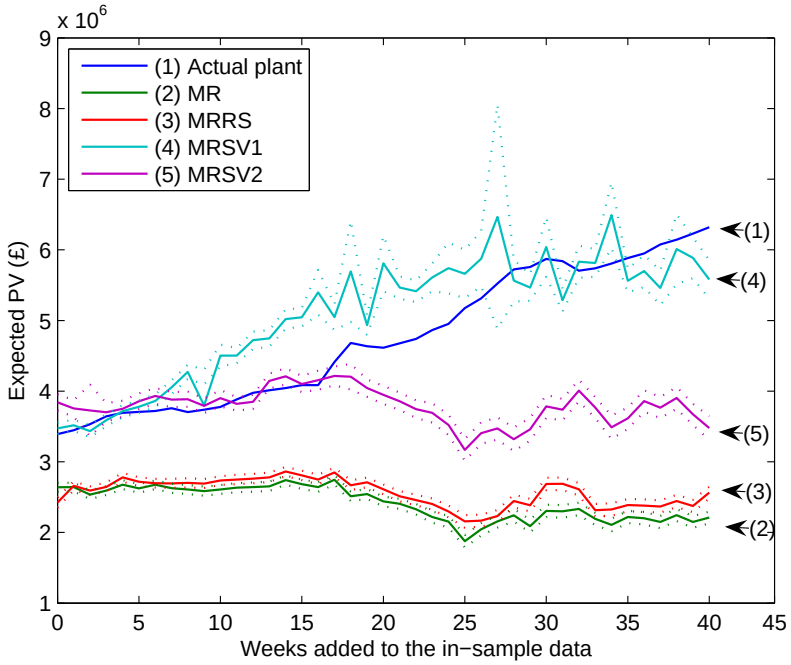

Figure 2.15: Expected PV and 95% CIs of the inflexible plant with rolling expansion of the in-sample period

is revealed that for small values of γ_E, the expected PV estimated by MRSV1 is larger than that estimated by MRSV2. This occurs because gas prices with stochastic volatility are more likely to produce high price spikes that will not be offset by corresponding spikes in electricity prices when γ_E is low. Thus, a power plant without operational flexibility will be at risk of losing money in such a situation.

2.6 Conclusions

After the liberalisation of the electricity industry, exploring the behaviour of energy prices, such as highly unexpected spikes and stochastic volatility, has become a main issue in energy economics in many countries. This chapter provides a comprehensive set of both linear and non-linear multivariate models for electricity and gas prices. A comparison study is carried out using UK electricity and

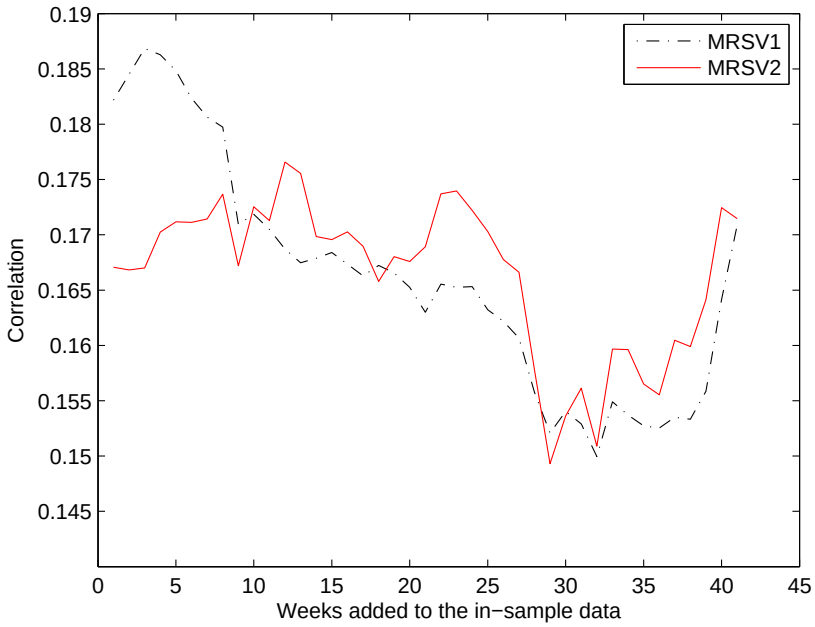

Figure 2.16: Estimated correlation between the logarithms of electricity and gas prices with rolling expansion of the in-sample period

gas spot prices to evaluate the forecasting performance of the proposed models in decision-making such as valuing a gas-fired power plant. We split our data set into two periods: the in-sample period that is used to estimate the models of interest and the out-of-sample period that is used to assess the forecasting performance of each model.

We first propose four linear models for logarithms of the data based on mean-reverting and geometric Brownian motion processes. Consistent with previous studies, such as Cortazar & Schwartz (1994), Laughton & Jacoby (1993), and Smith & McCardle (1998), we show that the mean-reverting model for both logarithms of electricity and gas not only is the best-fit linear model, but also has the best out-of-sample forecasting performance. However, due to its weakness in capturing the high-value sudden spikes of energy prices, we then allow for three non-linear models: a) mean reversion with Markov regime-switching with two independent regimes (the stable regime and the spike regime), b) mean reversion with stochastic volatility for the logarithm of the electricity price and

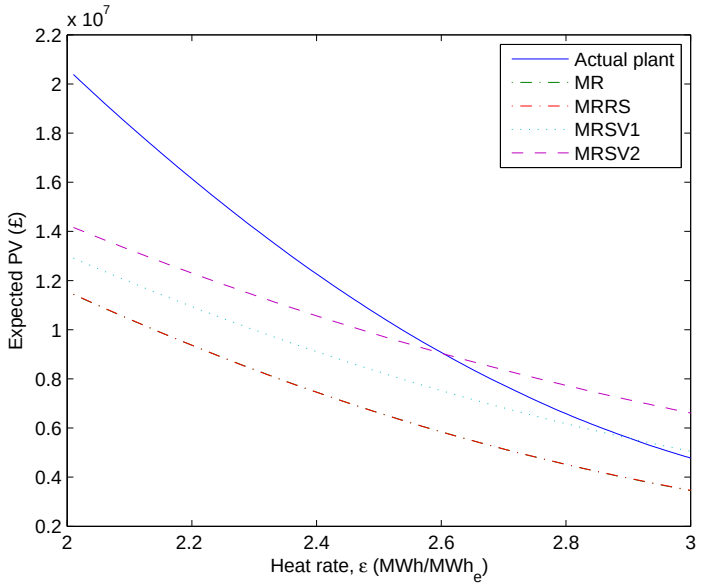

Figure 2.17: Expected PV of the plant with flexibility for different values of heat rate

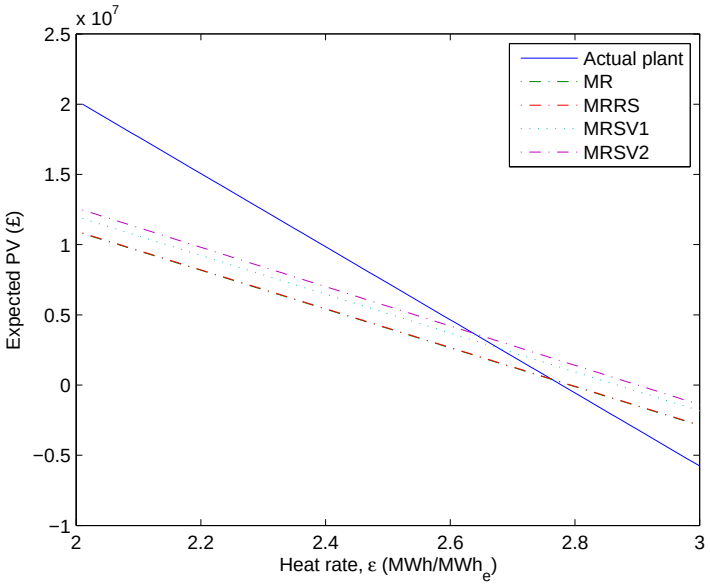

Figure 2.18: Expected PV of the plant without flexibility for different values of heat rate

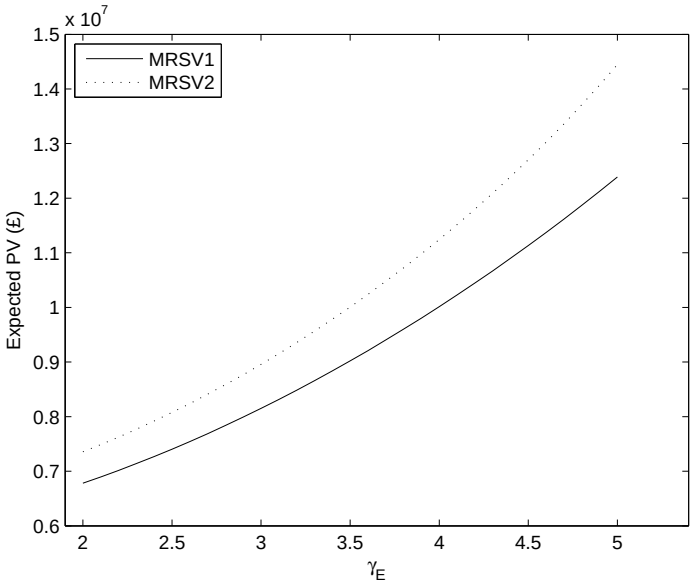

Figure 2.19: Expected PV of the plant with flexibility for different values of γ_E

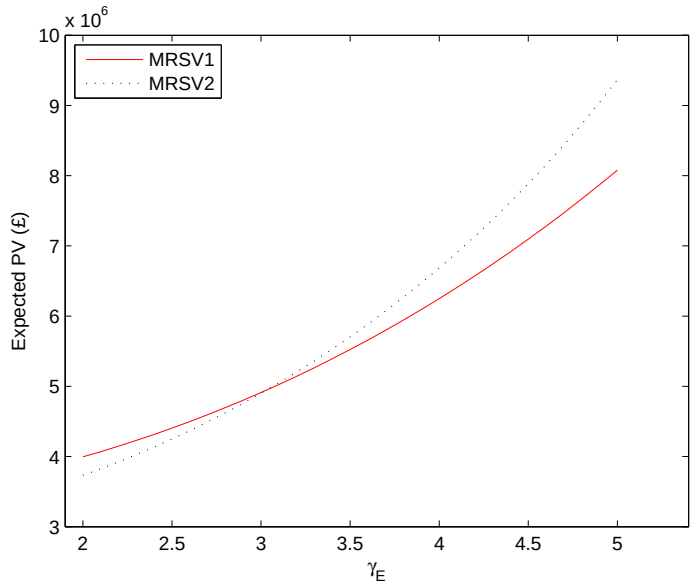

Figure 2.20: Expected PV of the plant without flexibility for different values of γ_E

deterministic volatility for the logarithm of the gas price, and c) mean reversion with stochastic volatility for both logarithms of electricity and gas prices. We next take the viewpoint of an investor in a gas-fired power plant with operational flexibility and compare the ability of linear and non-linear models in valuing the power plant over the out-of-sample period.

The study suggests that the linear model provides out-of-sample price forecasts with the lowest ERMSE in comparison to the non-linear models because it does not forecast any spikes at all, while the non-linear forecasts generate a large number of spikes with different levels and on different time locations. It seems clear that appearance of high spikes in forecasts with correct frequency and value, but not with right timing, may lead to large RMSEs when compared to the historical data; however, it would result in more accurate long-term decision-making in energy investments. Among the non-linear models, in contrast to earlier findings (e.g., Karakatsani & Bunn (2008); Kosater & Mosler (2006)), the regime-switching model is unlikely to capture long-term volatile electricity price behaviour over long-term periods. This may have resulted from different levels of spikes in electricity prices. For example, in UK electricity spot prices, the spikes range from about £40/MWh$_e$ to £180/MWh$_e$, while the equilibrium price is around £20/MWh$_e$. This behaviour of electricity prices is strong evidence of the presence of stochastic volatility. Consequently, the non-linear models with stochastic volatility for logarithms of electricity prices perform better than both the linear and the regime-switching models in terms of valuing a gas-fired power plant. The volatility of gas prices, on the other hand, does not seem to be stochastic, such that the model MRSV1 is able to capture the PV of the gas-fired power plant better than model MRSV2 over the different two-year out-of-sample periods (Figures 2.14 and 2.15), although it does not provide better results over the specific out-of-sample period ranges from 27 March 2004 to 31 December 2006 (Tables 2.9 and 2.10). Moreover, since the model MRSV1 is simpler than MRSV2, it is chosen as the best model among both the linear and non-linear models. In the next chapter, we focus on the importance of timing and technology choice rather than price modelling in making investment decisions in the energy sector.

Chapter 3

Real Options Analysis of Investment in Carbon Capture and Sequestration Technology

Among a comprehensive scope of mitigation measures for climate change, CO_2 capture and sequestration (CCS) plays a potentially significant role in industrialised countries. In this chapter, we develop an analytical real options model that values the choice between two emissions-reduction technologies available to a coal-fired power plant. Specifically, the plant owner may decide to invest in either full CCS (FCCS) or partial CCS (PCCS) retrofits given uncertain electricity, CO_2, and coal prices.We first assess the opportunity to upgrade to each technology independently by determining the option value of installing a CCS unit as a function of CO_2 and fuel prices. Next, we value the option of investing in either FCCS or PCCS technology. If the volatilities of the prices are low enough, then the investment region is dichotomous, which implies that for a given fuel price, retrofitting to the FCCS (PCCS) technology is optimal if the CO_2 price increases (decreases) sufficiently. The numerical examples using current market data suggest that neither retrofit is optimal immediately. Finally, we observe that the optimal stopping boundaries are highly sensitive to CO_2 price volatility.

3.1 Carbon Capture and Sequestration (CCS) Technology

CCS is a process by which CO_2 is separated from industrial and energy-related sources. It is then transported for geological storage, ocean storage, or mineral carbonation in order to be isolated permanently from the atmosphere or for use in industrial processes (IPCC (2005)). A power plant equipped with CCS technology requires additional energy for capture, transport, and storage, which causes a reduction in overall efficiency of the plant.

According to IPCC (2005), there are three types of CO_2 capture systems:

- Post-combustion, which captures CO_2 from the flue gas and is applied in existing power plants;

- Pre-combustion, in which CO_2 in the fuel is separated before combustion, which is more costly and applicable only to new fossil fuel plants;

- Oxyfuel combustion, which uses high purity of oxygen that causes CO_2 with high concentrations in flue gas to be easily separated. However, it is more expensive because of a higher energy requirement to produce pure oxygen.

After CO_2 is captured, it can be transported from the source to the storage site either through pipelines or using ships. However, for a large amount of CO_2 over short distances, pipelines are preferred, although smaller volumes of CO_2, specifically for larger distances overseas, may be transported with ships (IPCC (2005)).

Installing FCCS technology with access to geological or ocean storage, a coal-fired power plant can capture up to 85-95% of its CO_2 emissions (IPCC (2005)), while using approximately 10-40% more energy than before. However, achieving this CO_2 capture is likely to be too expensive and almost impossible in near term. With regard to this difficulty, Hildebrand & Herzog (2008) considers a lower rate of capturing, PCCS, as a reasonable first step in putting CCS into action. A coal-fired power plant equipped with PCCS could lower its CO_2 emissions to a gas-fired power plant's, i.e., a capture of nearly 45-65%. FCCS technology could cause up to a 60% increase in the capital cost of a pulverised coal power plant,

while this increase for PCCS is extremely less. Moreover, a power plant with PCCS requires less energy than a power plant with FCCS, thereby limiting the efficiency loss.

3.2 Problem Formulation

3.2.1 Assumptions

We take the perspective of the owner of a baseload coal-fired power plant with infinite lifetime[1] intending to reduce its CO_2 emissions by investing in either PCCS or FCCS technology. Since the timing of the retrofit is at the discretion of the owner, the option is perpetual. Additionally, we assume that the investment is entirely irreversible and cannot be scrapped once installed, nor is it possible to suspend the CCS unit to allow venting. The option of switching from one technology to another is also assumed to be impracticable in this study. Three sources of uncertainty are taken into consideration: fuel input price, F_t (in \$/MWh), electricity output price, E_t (in \$/MWh_e), and CO_2 permit price, C_t (in \$/tCO_2). Future revenues and costs of the investment are discounted at a subjective constant annual rate, μ. After investing in either technology, the electricity production of the plant, Q (in MWh_e/year), would remain the same as before; however, the overall efficiency of the plant will decline due to further energy requirements. Finally, once the retrofit decision is made, the CCS technology is installed immediately, i.e., there is no time-to-build problem as in Majd & Pindyck (1987).

3.2.2 NPV of Mitigation Projects

We assume that E_t, F_t, and C_t evolve stochastically according to the following GBM processes:[2]

[1] Although a coal-fired power plant has a typical lifetime of forty years, for simplicity, in this thesis, we assume that it has an infinite lifetime. This is justified by the impact of discounting the cashflows that are several decades in the future. Plus, assuming that all equipment lasts forever removes any complication from having to compare technologies with different lifetimes.

[2] As suggested in Pindyck (1999), although long-run energy prices are mean-reverting, since their rate of mean reversion is low, the GBM assumption may be acceptable in many applications.

$$dE_t = \alpha_E E_t dt + \sigma_E E_t dz_t^E \tag{3.1}$$

$$dF_t = \alpha_F F_t dt + \sigma_F F_t dz_t^F \tag{3.2}$$

$$dC_t = \alpha_C C_t dt + \sigma_C C_t dz_t^C \tag{3.3}$$

where $\{\alpha_i < \mu; i = E, F, C\}$[3] and $\{\sigma_i; i = E, F, C\}$ are, respectively, the drift and the volatility parameters, and dz_t^i stands for the increment of standard Brownian motion process. Moreover, we suppose that the prices are correlated, i.e., $\mathbb{E}(dz_t^i dz_t^j) = \rho_{ij} dt$ for $\{(i, j) = (E, F), (E, C), (F, C)\}$. Therefore, the net expected discounted profit of an existing power plant without any CCS, conditional on current prices E, F, and C, is given by:

$$\begin{aligned} & V(E, F, C) \\ &= Q\mathbb{E}\left[\int_0^\infty (E_t e^{-\mu t} - \epsilon_F F_t e^{-\mu t} - \epsilon_C C_t e^{-\mu t}) dt | E_0 = E, F_0 = F, C_0 = C\right] \\ &= Q\left[\frac{E}{\mu - \alpha_E} - \frac{\epsilon_F F}{\mu - \alpha_F} - \frac{\epsilon_C C}{\mu - \alpha_C}\right] \end{aligned} \tag{3.4}$$

where ϵ_F and ϵ_C represent the heat rate (in MWh/MWh_e) and the emission rate (in $\text{tCO}_2/\text{MWh}_e$), respectively, of a power plant without CCS. Thus, the expected net present value (NPV) of investing in retrofit project $j = \{pccs, fccs\}$ can be calculated as follows:

$$\begin{aligned} V^{(j)}(E, F, C) &= Q\left[\frac{E}{\mu - \alpha_E} - \frac{\epsilon_F^{(j)} F}{\mu - \alpha_F} - \frac{\epsilon_C^{(j)} C}{\mu - \alpha_C}\right] - I^{(j)} - V(E, F, C) \quad \Rightarrow \\ V^{(j)}(F, C) &= Q\left[\frac{(\epsilon_F - \epsilon_F^{(j)})F}{\mu - \alpha_F} + \frac{(\epsilon_C - \epsilon_C^{(j)})C}{\mu - \alpha_C}\right] - I^{(j)} \end{aligned} \tag{3.5}$$

[3]The interest rate must be greater than the output price's drift rate; otherwise, waiting longer would always be a better policy, and the optimal time of invest would never exist (the integral in Equation (3.4) could be indefinitely large by choosing a large T). It must also be greater than the cost's drift rate; otherwise, if it is not optimal to invest now, it would never be optimal (the integral in Equation (3.4) could be indefinitely small by choosing a large T).

where $I^{(j)}$ includes the initial sunk capital cost of the retrofit to technology j together with all other costs, such as additional operating and maintenance costs, which are discounted at the constant rate μ. Here, $\epsilon_C^{(j)}$ and $\epsilon_F^{(j)}$ are the CO_2 emissions and heat rate, respectively, with retrofit j. From Equation (3.5), it is revealed that the expected NPV of mitigation no longer depends on the electricity price since the plant's electricity output is unaffected. As we could expect, the expected NPV is decreasing in F and increasing in C because of the negative coefficient $(\epsilon_F - \epsilon_F^{(j)})$ and the positive coefficient $(\epsilon_C - \epsilon_C^{(j)})$, respectively. Intuitively, CCS technology reduces the plant's efficiency, which increases its post-retrofit heat rate while decreasing its CO_2 emissions rate. Accordingly, the value of the opportunity to mitigate, $W^{(j)}(F, C)$, depends only on the fuel price and CO_2 permit price.

3.2.3 Valuation of the Mitigation Options

3.2.3.1 Optimal Stopping, Value Matching, and Smooth Pasting

Since the plant owner can either invest in retrofit project $j = \{pccs,\ fccs\}$ (stopping region) and receive $V^{(j)}(F, C)$ calculated in Equation (3.5) or wait (continuation region), the choice in every instant is binary. Therefore, the Bellman equation[4], as the primary equation of optimisation theory, becomes

$$W^{(j)}(F, C) = \max\{V^{(j)}(F, C), \frac{\mathbb{E}[dW^{(j)}(F, C)]}{\mu dt}\} \tag{3.6}$$

Intuitively, there is an optimal stopping boundary, $C^{*(j)}(F)$, that separates the state space into stopping and continuation regions, i.e., it is the two-dimensional analogue of the trigger in the canonical real options problem. For $C < C^{*(j)}(F)$, it is optimal to wait, i.e., the second term on the right-hand side is the larger of the two or $\mu W^{(j)}(F, C) = \frac{\mathbb{E}[dW^{(j)}(F,C)]}{dt}$. On the other hand, for $C \geq C^{*(j)}(F)$ it is optimal to invest immediately in retrofit project j, i.e., $W^{(j)}(F, C) = V^{(j)}(F, C)$ for all values of F. Therefore by continuity, we can impose the value-matching

[4]Bellman's Principle of Optimality: An optimal policy has the property that, whatever the initial action, the remaining choices constitute an optimal policy with respect to the subproblem starting at the state that results from the initial actions (Dixit & Pindyck (1994)).

condition, which states that the value lost equals the value gained, as follows:

$$W^{(j)}(F, C^{*(j)}(F)) = V^{(j)}(F, C^{*(j)}(F)) \tag{3.7}$$

Moreover, the values $W^{(j)}(F, C)$ and $V^{(j)}(F, C)$, regarded as functions of F and C, should meet tangentially at the free boundary $C^{*(j)}(F)$. We then have the two smooth-pasting conditions as the first-order conditions of optimisation as follows (see Dixit & Pindyck (1994) for an argument on value-matching and smooth-pasting conditions):

$$W_F^{(j)}(F, C) = V_F^{(j)}(F, C) \qquad \text{on } C = C^{*(j)}(F) \tag{3.8}$$

$$W_C^{(j)}(F, C) = V_C^{(j)}(F, C) \qquad \text{on } C = C^{*(j)}(F) \tag{3.9}$$

where the subscripts denote the partial derivatives, e.g., $W_F^{(j)}(F, C) = \frac{\partial W^{(j)}(F,C)}{\partial F}$.

3.2.3.2 Individual Investment Options

Using dynamic programming, we first derive the value of the option to invest in PCCS and FCCS, independently. The Bellman equation, explained in the previous section, states that when it is optimal to wait, i.e., $C < C^{*(j)}(F)$, the rate of return on the option, $\mu W^{(j)}(F, C)$, must equal the expected rate of capital gain on it, $\mathbb{E}[dW^{(j)}(F, C)]/dt$:

$$\mu W^{(j)}(F, C) = \mathbb{E}[dW^{(j)}(F, C)]/dt \tag{3.10}$$

Thus, by applying Itô's lemma to the right-hand side of Equation (3.10) given that F and C evolve according to the GBM processes (3.2) and (3.3), the option to invest in j must satisfy the following partial differential equation (PDE):

$$\begin{aligned} \mu W^{(j)}(F, C) \;=\; & \alpha_F F W_F^{(j)}(F, C) + 0.5\sigma_F^2 F^2 W_{FF}^{(j)}(F, C) + \alpha_C C W_C^{(j)}(F, C) \\ & + 0.5\sigma_C^2 C^2 W_{CC}^{(j)}(F, C) + \rho\sigma_F\sigma_C F C W_{FC}^{(j)}(F, C) \end{aligned} \tag{3.11}$$

where $\rho = \frac{\mathbb{E}(dz_t^F dz_t^C)}{dt}$.[5]

[5]Since the electricity price is not relevant to retrofits, from now on, we define $\rho = \rho_{FC}$.

A general solution to the PDE, Equation (3.11), is of the power form as follows:

$$W^{(j)}(F,C) = A^{(j)}F^{\beta^{(j)}}C^{\eta^{(j)}}; \qquad 0 < F < \infty,\ 0 < C < C^{*(j)}(F) \tag{3.12}$$

where $A^{(j)}$, $\beta^{(j)}$, and $\eta^{(j)}$ are endogenous coefficients, depending on F, which are to be determined together with the free boundary, $C^{*(j)}(F)$. Substituting Equation (3.12) into Equation (3.11) yields:

$$\begin{aligned} H(\beta^{(j)},\eta^{(j)}) = \ & \alpha_F\beta^{(j)} + 0.5\sigma_F^2\beta^{(j)}(\beta^{(j)}-1) + \alpha_C\eta^{(j)} + 0.5\sigma_C^2\eta^{(j)}(\eta^{(j)}-1) \\ & +\rho\sigma_F\sigma_C\beta^{(j)}\eta^{(j)} - \mu = 0 \end{aligned} \tag{3.13}$$

Equation (3.13) is that of an ellipse in η and β that passes through all four axes (Adkins & Paxson (2010)) and is graphed in Figure 3.1 using the data provided in Table 3.1. This implies that Equation (3.12) can have the form:

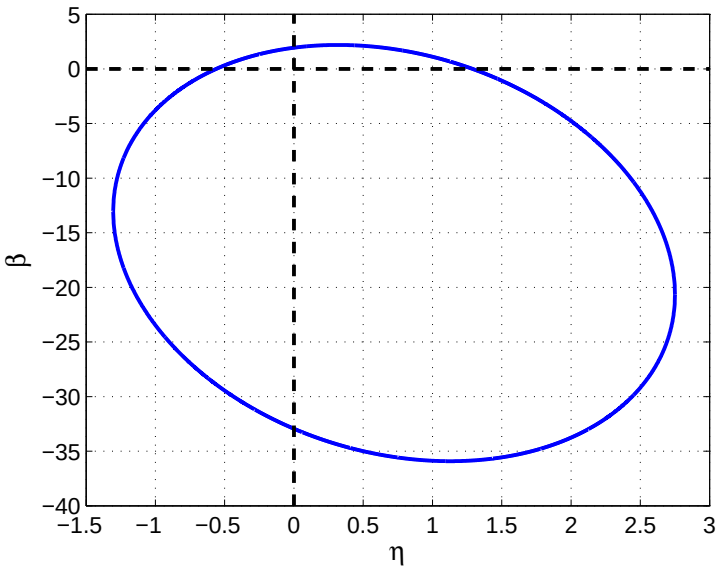

Figure 3.1: Function $H(\beta,\eta) = 0$

$$W^{(j)}(F,C) = A_1^{(j)}F^{\beta_1^{(j)}}C^{\eta_1^{(j)}} + A_2^{(j)}F^{\beta_2^{(j)}}C^{\eta_2^{(j)}} + A_3^{(j)}F^{\beta_3^{(j)}}C^{\eta_3^{(j)}} + A_4^{(j)}F^{\beta_4^{(j)}}C^{\eta_4^{(j)}} \tag{3.14}$$

where,

$$\begin{aligned} \eta_1^{(j)} > 0 \text{ and } \beta_1^{(j)} < 0 \\ \eta_2^{(j)} < 0 \text{ and } \beta_2^{(j)} > 0 \\ \eta_3^{(j)} > 0 \text{ and } \beta_3^{(j)} > 0 \\ \eta_4^{(j)} < 0 \text{ and } \beta_4^{(j)} < 0 \end{aligned} \tag{3.15}$$

However, by imposing limiting boundary conditions on F and C, we can eliminate the last three terms in Equation (3.14). When the fuel price, F, tends to infinity, the option value becomes worthless; therefore, the coefficients $A_2^{(j)}$ and $A_3^{(j)}$ in Equation (3.14) must be zero to prevent from diverging. Similarly, for low values of C (close to zero) it is not justifiable to invest in any CCS technology, i.e., the option value is worthless and the coefficient $A_4^{(j)}$ in Equation (3.14) must be zero, too. We then end up with the following option value function:

$$W^{(j)}(F,C) = A_1^{(j)} F^{\beta_1^{(j)}} C^{\eta_1^{(j)}} \qquad 0 < F < \infty,\ 0 < C < C^{*(j)}(F) \tag{3.16}$$

which can be rewritten as:

$$W^{(j)}(F,C) = A^{(j)} F^{\beta^{(j)}} C^{\eta^{(j)}} \qquad 0 < F < \infty,\ 0 < C < C^{*(j)}(F) \tag{3.17}$$

where $\eta^{(j)} > 0$ and $\beta^{(j)} < 0$. To prove uniqueness of the solution, standard techniques for such elliptic PDEs usually rely on proof by contradiction, which are outlined in Appendix G.

We now use one value-matching and two smooth-pasting conditions along with Equation (3.13) to solve for the four unknowns:

$$A^{(j)} F^{\beta^{(j)}} C^{\eta^{(j)}} = Q \left[\frac{(\epsilon_F - \epsilon_F^{(j)})}{\mu - \alpha_F} F + \frac{(\epsilon_C - \epsilon_C^{(j)})}{\mu - \alpha_C} C \right] - I^{(j)} \quad \text{on } C = C^{*(j)}(F) \tag{3.18}$$

$$A^{(j)} \beta^{(j)} F^{\beta^{(j)}-1} C^{\eta^{(j)}} = Q \frac{(\epsilon_F - \epsilon_F^{(j)})}{\mu - \alpha_F} \quad \text{on } C = C^{*(j)}(F) \tag{3.19}$$

$$A^{(j)}\eta^{(j)}F^{\beta^{(j)}}C^{\eta^{(j)}-1} = Q\frac{(\epsilon_C - \epsilon_C^{(j)})}{\mu - \alpha_C} \quad \text{on } C = C^{*(j)}(F) \tag{3.20}$$

Rearranging Equation (3.20), we obtain the coefficient $A^{(j)}$ as follows:

$$A^{(j)} = \frac{Q(\epsilon_C - \epsilon_C^{(j)})}{\eta^{(j)}(\mu - \alpha_C)}F^{-\beta^{(j)}}[C^{*(j)}(F)]^{1-\eta^{(j)}} \tag{3.21}$$

Substituting this into Equation (3.19) gives the following equation for the optimal stopping boundary:

$$C^{*(j)}(F) = \frac{\eta^{(j)}(\epsilon_F - \epsilon_F^{(j)})(\mu - \alpha_C)}{\beta^{(j)}(\epsilon_C - \epsilon_C^{(j)})(\mu - \alpha_F)}F \tag{3.22}$$

Finally, a linear relationship between $\beta^{(j)}$ and $\eta^{(j)}$ using Equation (3.18) is given by:

$$\beta^{(j)} = \frac{Q(\epsilon_F - \epsilon_F^{(j)})(\eta^{(j)} - 1)F}{(\mu - \alpha_F)I^{(j)} - Q(\epsilon_F - \epsilon_F^{(j)})F}, \tag{3.23}$$

which is decreasing in $\eta^{(j)}$, because of the negative coefficient $(\epsilon_F - \epsilon_F^{(j)})$ and the positive denominator.[6] If we impose this line on $H(\beta^{(j)}, \eta^{(j)}) = 0$, then it intersects the function at two points, which we now try to obtain. It must be mentioned that in Adkins & Paxson (2010), this part of the process is solved numerically, i.e., it does not provide the following analytical solution for calculating η_1. In Figure 3.2, using the data for PCCS technology, provided in Table 3.2, we show the intersections of the two lines, for the lowest and the highest value of F in our range of data, and the ellipse $H(\beta^{(j)}, \eta^{(j)}) = 0$.

After substituting the exponent $\beta^{(j)}$ from Equation (3.23) into Equation (3.13), we end up with the following quadratic polynomial:

$$a(\eta^{(j)})^2 - b\eta^{(j)} - c = 0 \tag{3.24}$$

[6]The denominator, $[(\mu - \alpha_F)I^{(j)} - Q(\epsilon_F - \epsilon_F^{(j)})F]$, is positive because $(\mu - \alpha_F)$ is positive and $(\epsilon_F - \epsilon_F^{(j)})$ is negative.

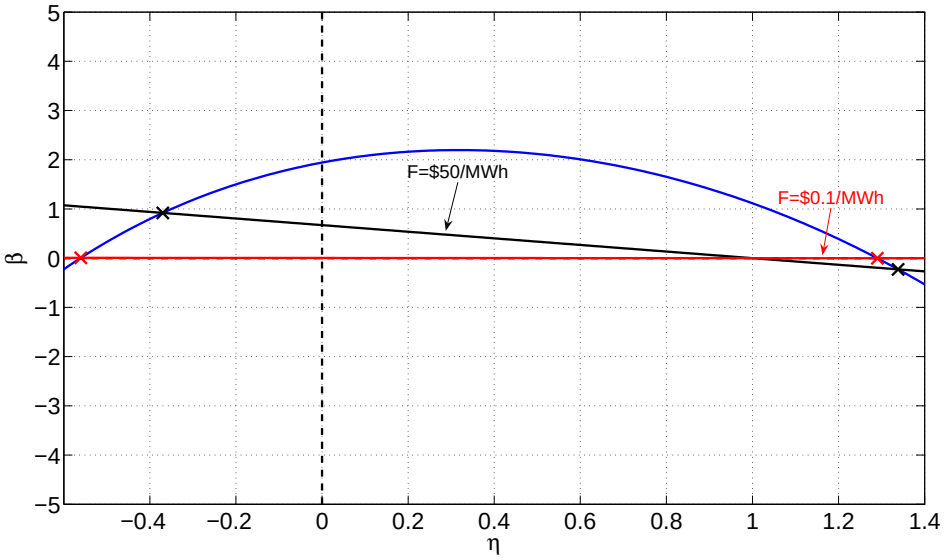

Figure 3.2: The intersection of function $H(\beta, \eta) = 0$ (data from Table 3.1) and Equation (3.23) for PCCS technology (data from Table 3.2), e.g., when $F = \$50/MWh$, $\eta_1^{(pccs)} = 1.33$ and $\beta_1^{(pccs)} = -0.21$.

where

$$\begin{aligned} a = \; & (0.5\sigma_F^2 + 0.5\sigma_C^2 - \rho\sigma_F\sigma_C)((\epsilon_F - \epsilon_F^{(j)})QF)^2 \\ & -(\sigma_C^2 - \rho\sigma_F\sigma_C)(\mu - \alpha_F)(\epsilon_F - \epsilon_F^{(j)})QI^{(j)}F \\ & +0.5\sigma_C^2(\mu - \alpha_F)^2(I^{(j)})^2 \end{aligned} \tag{3.25}$$

$$\begin{aligned} b = \; & (0.5\sigma_F^2 + 0.5\sigma_C^2 - \rho\sigma_F\sigma_C + \alpha_F - \alpha_C)((\epsilon_F - \epsilon_F^{(j)})QF)^2 \\ & -(\sigma_C^2 - \rho\sigma_F\sigma_C - 0.5\sigma_F^2 + \alpha_F - 2\alpha_C)(\mu - \alpha_F)(\epsilon_F - \epsilon_F^{(j)})QI^{(j)}F \\ & +(0.5\sigma_C^2 - \alpha_C)(\mu - \alpha_F)^2(I^{(j)})^2 \end{aligned} \tag{3.26}$$

$$\begin{aligned} c = \; & (\mu - \alpha_F)((\epsilon_F - \epsilon_F^{(j)})QF)^2 \\ & +(\alpha_F - 0.5\sigma_F^2 - 2\mu)(\mu - \alpha_F)(\epsilon_F - \epsilon_F^{(j)})QI^{(j)}F \\ & +\mu(\mu - \alpha_F)^2(I^{(j)})^2 \end{aligned} \tag{3.27}$$

Since $(\epsilon_F - \epsilon_F^{(j)}) < 0$, $(\mu - \alpha_F) > 0$, and the volatility of coal price is assumed to

be less than that of the CO_2 price ($\sigma_F < \sigma_C$)[7], coefficients a and c are positive. The discriminant $\Delta = b^2 + 4ac$ is, therefore, positive, which ensures the existence of two real and distinct roots:

$$\eta_1^{(j)} = \frac{b + \sqrt{b^2 + 4ac}}{2a} \tag{3.28}$$

$$\eta_2^{(j)} = \frac{b - \sqrt{b^2 + 4ac}}{2a} \tag{3.29}$$

In Appendix H, we prove that $\eta_1^{(j)}$ is always greater than 1; as a result, the corresponding $\beta_1^{(j)}$ calculated from Equation (3.23) is negative. On the other hand, $\eta_2^{(j)}$ is negative; thus, the corresponding $\beta_2^{(j)}$ is positive. It is observed that the boundary condition $W^{(j)}(F, C) \to 0$ as $F \to \infty$ appears superfluous and seems entirely guaranteed by value-matching and smooth-pasting conditions. Therefore, the unknowns $\eta^{(j)}$, $\beta^{(j)}$, and $A^{(j)}$ in Equation (3.17) are calculated, respectively, via Equations (3.28), (3.23), and (3.21). Figure 3.2 shows that, for this choice of data, $\eta_1^{(j)}$ is increasing in F while $\beta_1^{(j)}$ is decreasing. Equation (3.23) also substantiates the inverse relationship between $\beta_1^{(j)}$ and $\eta_1^{(j)}$. A list of the calculated unknowns for some values of F are reported in Appendix I.

We may, finally, be interested in simplifying the option value function by substituting $A^{(j)}$ into Equation (3.17) and combining Equations (3.23) and (3.22). We then have:

$$W^{(j)}(F, C) = \frac{Q(\epsilon_C - \epsilon_C^{(j)})}{\eta^{(j)}(\mu - \alpha_C)} [C^{*(j)}(F)]^{1-\eta^{(j)}} C^{\eta^{(j)}}, \begin{cases} 0 < F < \infty \\ 0 < C < C^{*(j)}(F) \end{cases} \tag{3.30}$$

where $\eta^{(j)}$ is calculated from Equation (3.28) and

$$C^{*(j)}(F) = \frac{\eta^{(j)}(\mu - \alpha_C)}{(\eta^{(j)} - 1)(\mu - \alpha_F)} \frac{(\mu - \alpha_F) I^{(j)} - Q(\epsilon_F - \epsilon_F^{(j)}) F}{Q(\epsilon_C - \epsilon_C^{(j)})} \tag{3.31}$$

[7] CO_2 price volatility is likely to be greater than currently suggested, which is higher than that of coal price, and is even tending to exceed natural gas price volatility (Celebi & Graves (2009)).

3.2.3.3 Mutually Exclusive Options

Now, we would like to consider the mutually exclusive option to retrofit with either PCCS or FCCS technology. By plotting the expected NPV of each technology, we note that there will be an indifference curve, $C_I(F)$, where they intersect, and if the volatilities are low enough, then it may be the case that the option value for investment in PCCS technology is greater than that for the FCCS technology. In this event, an indifference region will open up around the indifference curve, in which case it is optimal to wait before investing in either technology. This dichotomous option, which includes the option value functions of both technologies, must satisfy the Bellman equation (Equation (3.13)). Following the same methodology as in Section 3.2.3.2, over the indifference region, $\{(F, C) \mid 0 < F < \infty,\ C_L^*(F) < C < C_U^*(F)\}$, it must have the form:

$$\Psi(F, C) = D_1 F^{\delta_1} C^{\gamma_1} + D_2 F^{\delta_2} C^{\gamma_2} + D_3 F^{\delta_3} C^{\gamma_3} + D_4 F^{\delta_4} C^{\gamma_2} \tag{3.32}$$

where,

$$\begin{gathered} D_1,\ D_2\ , D_3,\ D_4\ > 0 \\ \delta_1 < 0 \text{ and } \gamma_1 > 0 \\ \delta_2 > 0 \text{ and } \gamma_2 < 0 \\ \delta_3 > 0 \text{ and } \gamma_3 > 0 \\ \delta_4 < 0 \text{ and } \gamma_4 < 0 \end{gathered} \tag{3.33}$$

However, the limiting boundary conditions of F help us to get rid of the last two terms in Equation (3.32). For low values of F (close to zero), the option value of investing in PCCS becomes worthless, and the mutually exclusive option value equals the option value of investing in FCCS. This occurs if $D_4 = 0$ and the coefficients D_1, δ_1, and γ_1 tend to, respectively, $A_1^{(fccs)}$, $\beta_1^{(fccs)}$, and $\eta_1^{(fccs)}$. On the other hand, for large values of F ($F \to \infty$), the option value of investing in FCCS becomes worthless and the mutually exclusive option value approaches the option value of investing in PCCS. This condition holds if $D_3 = 0$ and the coefficients D_2, δ_2, and γ_2 tend to $A_2^{(pccs)}$, $\beta_2^{(pccs)}$, and $\eta_2^{(pccs)}$, respectively.[8] We,

[8]Since the FCCS technology by using more fuel than the PCCS technology, captures more CO_2, when fuel price is close to zero, it is optimal to invest in FCCS, while for large values of F, it is not economical at all to invest in FCCS.

finally, end up with the following option value:

$$\Psi(F,C) = D_1 F^{\delta_1} C^{\gamma_1} + D_2 F^{\delta_2} C^{\gamma_2} \tag{3.34}$$

where,

$$\begin{gathered} D_1,\ D_2\ > 0 \\ \delta_1 < 0 \text{ and } \gamma_1 > 0 \\ \delta_2 > 0 \text{ and } \gamma_2 < 0 \end{gathered} \tag{3.35}$$

Intuitively, in the indifference region, when the fuel price decreases and the CO_2 permit price increases, investment in FCCS becomes more likely. Therefore, for any value of (F,C) in this region, the first term on the right-hand side of Equation (3.34) can be interpreted as the value of the option to upgrade to FCCS. On the other hand, since the PCCS technology requires less energy than the FCCS one and captures less CO_2, it is more profitable when the fuel price increases and CO_2 permit price decreases. Thus, we interpret the second term on the right-hand side of Equation (3.34) as the value of the option to upgrade to PCCS for any value of (F,C) in the indifference region. Now, the power coefficients, which are the two roots of Equation (3.13), are to be determined along with the endogenous coefficients, D_1 and D_2, as well as the upper, $C_U^*(F)$, and lower, $C_L^*(F)$, free boundaries that indicate where the intermediate option value curve value-matches and smooth-pastes with the expected NPV curves of the FCCS and PCCS technologies, respectively.

Substituting Equation (3.34) into Equation (3.11) yields:

$$\begin{aligned} &\left(\alpha_F\delta_1 + 0.5\sigma_F^2\delta_1(\delta_1-1) + \alpha_C\gamma_1 + 0.5\sigma_C^2\gamma_1(\gamma_1-1) + \rho\sigma_F\sigma_C\delta_1\gamma_1 - \mu\right) \\ &\times D_1 F^{\delta_1} C^{\gamma_1} + \left(\alpha_F\delta_2 + 0.5\sigma_F^2\delta_2(\delta_2-1) + \alpha_C\gamma_2 + 0.5\sigma_C^2\gamma_2(\gamma_2-1)\right. \\ &\left.+\rho\sigma_F\sigma_C\delta_2\gamma_2 - \mu\right) D_2 F^{\delta_2} C^{\gamma_2} = 0 \end{aligned} \tag{3.36}$$

which holds if and only if

$$\alpha_F\delta_1 + 0.5\sigma_F^2\delta_1(\delta_1-1) + \alpha_C\gamma_1 + 0.5\sigma_C^2\gamma_1(\gamma_1-1) + \rho\sigma_F\sigma_C\delta_1\gamma_1 - \mu = 0 \tag{3.37}$$

$$\alpha_F\delta_2 + 0.5\sigma_F^2\delta_2(\delta_2-1) + \alpha_C\gamma_2 + 0.5\sigma_C^2\gamma_2(\gamma_2-1) + \rho\sigma_F\sigma_C\delta_2\gamma_2 - \mu = 0 \quad (3.38)$$

These two equations together with the following six value-matching and smooth-pasting conditions are used to solve for the eight unknowns (D_1, D_2, δ_1, γ_1, δ_2, γ_2, $C_L^*(F)$, and $C_U^*(F)$):

$$\Psi(F,C) = Q\left[\frac{(\epsilon_F - \epsilon_F^{(pccs)})}{\mu-\alpha_F}F + \frac{(\epsilon_C - \epsilon_C^{(pccs)})}{\mu-\alpha_C}C\right] - I^{(pccs)} \quad \text{on } C = C_L^*(F) \quad (3.39)$$

$$\Psi_F(F,C) = Q\frac{(\epsilon_F - \epsilon_F^{(pccs)})}{\mu-\alpha_F} \quad \text{on } C = C_L^*(F) \quad (3.40)$$

$$\Psi_C(F,C) = Q\frac{(\epsilon_C - \epsilon_C^{(pccs)})}{\mu-\alpha_C} \quad \text{on } C = C_L^*(F) \quad (3.41)$$

$$\Psi(F,C) = Q\left[\frac{(\epsilon_F - \epsilon_F^{(fccs)})}{\mu-\alpha_F}F + \frac{(\epsilon_C - \epsilon_C^{(fccs)})}{\mu-\alpha_C}C\right] - I^{(fccs)} \quad \text{on } C = C_U^*(F) \quad (3.42)$$

$$\Psi_F(F,C) = Q\frac{(\epsilon_F - \epsilon_F^{(fccs)})}{\mu-\alpha_F} \quad \text{on } C = C_U^*(F) \quad (3.43)$$

$$\Psi_C(F,C) = Q\frac{(\epsilon_C - \epsilon_C^{(fccs)})}{\mu-\alpha_C} \quad \text{on } C = C_U^*(F) \quad (3.44)$$

From Equations (3.43) and (3.44), which are linear functions of D_1 and D_2, we can calculate D_1 and D_2 in terms of the other unknowns:

$$D_1 = Q\frac{(\epsilon_C - \epsilon_C^{(fccs)})(\mu-\alpha_F)\delta_2 C_U^*(F) - (\epsilon_F - \epsilon_F^{(fccs)})(\mu-\alpha_C)\gamma_2 F}{(\mu-\alpha_F)(\mu-\alpha_C)(\gamma_1\delta_2 - \gamma_2\delta_1)F^{\delta_1}C_U^*(F)^{\gamma_1}} \quad (3.45)$$

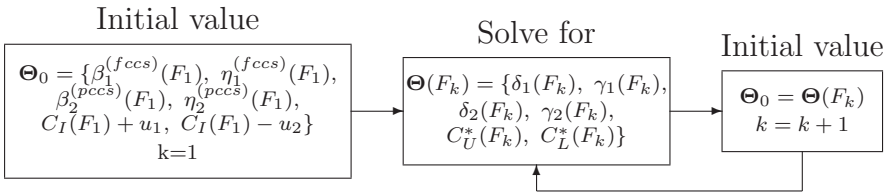

Figure 3.3: Numerical solution heuristic

$$D_2 = Q\frac{(\epsilon_F - \epsilon_F^{(fccs)})(\mu-\alpha_C)\gamma_1 F - (\epsilon_C - \epsilon_C^{(fccs)})(\mu-\alpha_F)\delta_1 C_U^*(F)}{(\mu-\alpha_F)(\mu-\alpha_C)(\gamma_1\delta_2-\gamma_2\delta_1)F^{\delta_2}C_U^*(F)^{\gamma_2}} \tag{3.46}$$

By substituting these coefficients into Equations (3.39-3.42), we reduce the system of eight equations to a new system of six non-linear equations with six unknowns, $\boldsymbol{\Theta}(F)$=$\{\delta_1(F),\ \gamma_1(F),\ \delta_2(F),\ \gamma_2(F),\ C_U^*(F),\ C_L^*(F)\}$, which must be solved numerically.

With an appropriate guess of the starting values using the `fsolve` command in Matlab, we can solve this system numerically. First, we discretise the values of the fuel price, e.g., in the ascending set $\{0, F_1, F_2, F_3, \cdots\}$. Starting from F_1, the most reasonable guess for the initial values of $\delta_1(F_1)$ and $\gamma_1(F_1)$ might be $\beta_1^{(fccs)}(F_1)$ and $\eta_1^{(fccs)}(F_1)$, respectively, calculated from Equations (3.28) and (3.23). Similarly, we can use $\beta_2^{(pccs)}(F_1)$ and $\eta_2^{(pccs)}(F_1)$, Equations (3.29) and (3.23), as an appropriate choice for the initials of $\delta_2(F_1)$ and $\gamma_2(F_1)$, respectively. However, the only information we have on the initials of $C_U^*(F_1)$ and $C_L^*(F_1)$ is that they surround the indifference point, $C_I(F_1)$. Therefore, we consider $C_I(F_1)+u_1$ and $C_I(F_1)-u_2$ as the initials of $C_U^*(F_1)$ and $C_L^*(F_1)$, respectively. Here, u_1 and u_2 may be chosen randomly, e.g., from the interval (0,1)\$/tCO_2. Using these initial values, we solve the problem for $\boldsymbol{\Theta}(F_1)$. Next, we use the calculated $\boldsymbol{\Theta}(F_1)$ as the initial values for the unknown parameters $\boldsymbol{\Theta}(F_2)$ and solve for them similarly. Successively, in each step k, the previous calculated $\boldsymbol{\Theta}(F_{k-1})$ can be used as the initial value of the current step and solve the system for $\boldsymbol{\Theta}(F_k)$ (see Figure 3).

3.3 Data

Data are reported in Tables 3.1 and 3.2. Parameters of CO_2 and coal price models and the data for FCCS technology are roughly adopted with Abadie & Chamarro (2008a) and Abadie & Chamarro (2008b)'s choice of parameters. The coal price in our study evolves according to a GBM process, while the electricity price, which represents the efficiency loss from the CCS retrofit, follows a GMR process with a low rate of mean reversion (0.125) in Abadie & Chamarro (2008b). The PCCS technology is proposed considering emissions reduction and initial capital cost provided by Hildebrand & Herzog (2008).

Parameter	Description	Value
α_F	Growth rate of coal price	0.04
α_C	Growth rate of CO_2 price	0.03[a]
σ_F	Volatility of coal price	0.05[b]
σ_C	Volatility of CO_2 price	0.47[a]
ρ	Correlation between coal and CO_2 prices	0.20[c]
μ	Discount rate	0.08
Φ	Capacity of the plant (MW_e)	500
Q	Annual energy production of the plant (MWh_e)	4380000
F_0	Current price of coal (\$/MWh)	15.5[d]
C_0	Current price of CO_2 (\$/tCO_2)	25.59[a]

[a] Abadie & Chamarro (2008a)'s data (using daily futures price data from ICE).

[b] Abadie & Chamarro (2008b)'s data (using yearly average prices gathered by the US Energy Information Administration).

[c] Since there is little information on CO_2 permit prices, we first assume a reasonable positive correlation coefficient between CO_2 and fuel prices. We then show how any changes in this coefficient may affect the results.

[d] The current price of coal is \$95/tCoal. According to ORNL (2009), a ton of coal on average produces 22 GJ (6.11 MWh) of energy. Thus, \$95/tCoal divided by 6.11 MWh/tCoal yields approximately \$15.5/MWh.

Table 3.1: Price and plant parameter values

Parameter	Description	PC	PC with PCCS	PC with FCCS
ϵ_C	Emission rate (tCO_2/MWh_e)	0.80	0.32[a]	0.08[b]
ϵ_F	Heat rate (MWh/MWh_e)	2.42	2.55	2.8
O&M	Additional operation and maintenance ($/$MWh_e$)	-	1.4	1.5
T&S	Transport and storage ($/$tCO_2$)	-	9	9
K	Initial capital cost of retrofit (m$)	-	130	331.57
$I^{(j)}$[c]	Total retrofit investment cost (m$)	-	443.17	768.475

[a] Capture of nearly 60% of the CO_2 emissions.
[b] Capture of nearly 90% of the CO_2 emissions.
[c] $I^{(j)} = K^{(j)} + \frac{Q}{\mu}(\text{O\&M}) + \frac{Q}{\mu}(\text{T\&S})(\epsilon_C - \epsilon_C^{(j)})$

Table 3.2: CCS parameter values

3.4 Numerical Examples

3.4.1 Individual Investment Options

We first consider a super critical pulverised coal power plant that has the option to invest in PCCS/FCCS technology in order to reduce its CO_2 emissions. Given current prices, we find the optimal stopping boundaries for independently investing in PCCS and FCCS as follows:

$$C^{*(pccs)}(F_0) = \$66.33/\text{tCO}_2$$

$$C^{*(fccs)}(F_0) = \$92.12/\text{tCO}_2$$

As we would expect, the critical CO_2 price for investing in PCCS technology is noticeably less than that for investing in FCCS technology. This difference between the free boundaries can be attributed to the high option value of waiting (the difference between the option value and the NPV, which are reported in Table 3.3) for FCCS ($608.53m) in comparison to that for PCCS ($196.72m). Both technologies are in-the-money, i.e., if the plant owner has to invest now or never, then she would invest immediately. On the other hand, she would lose a large amount of money by killing the waiting opportunity, specifically by investing in FCCS technology. Clearly, the NPVs of investing in FCCS and PCCS are more sensitive to C than to F, because the coefficient of C, in Equation (3.5), is larger

than the coefficient of F for both technologies.

The optimal stopping boundaries for each technology are graphed in Figures 3.4 and 3.5. As expected, these boundaries are strictly increasing with respect to F, i.e., the higher the fuel price is, the less likely the plant owner is to adopt the emission-reducing policy. It is also revealed that the boundaries are approximately linear with respect to F. This results from small changes in $\eta^{(j)}$ for different values of F, e.g., in Table I.1, it is observed that $\eta^{(pccs)}$ ranges from 1.2919 to 1.3339, which causes an approximate linear relationship between $C^{*(j)}(F)$ and F in Equation (3.31). These lines can be estimated as follows:

$$C^{*(pccs)}(F) = 46.8520 + 1.2570F \tag{3.47}$$

$$C^{*(fccs)}(F) = 54.1245 + 2.4523F \tag{3.48}$$

The NPV and the option value of investing in PCCS and FCCS are, respectively, graphed in Figures 3.6 and 3.7. From these graphs, the distinction between the NPV and the option value of investing in FCCS compared with PCCS is clearly visible. Furthermore, the expected NPV for FCCS is more sensitive to both F and C.

Our results for investing in the FCCS technology are similar to those of Abadie & Chamarro (2008a). Although the option value of investing in such CCS technology in both studies are nearly equal, the NPV calculated in Abadie & Chamarro (2008a) is almost twice as much as the value calculated in this thesis, which may be due to our different choice of model for the fuel price as the source of cost in our model. The use of a GMR process with high volatility (50%) and high mean-reversion rate (0.96) for the electricity price in Abadie & Chamarro (2008a) precipitates adoption in comparison with our study with the assumption of a GBM process for the fuel price. This results in a higher NPV and, thus, a lower critical threshold ($\$73.54/\text{tCO}_2$) calculated in Abadie & Chamarro (2008a) in comparison with the value calculated in our study ($\$92.12/\text{tCO}_2$).

Mitigation technology (j)	NPV (m$) $V^{(j)}(F_0, C_0)$	Option value (m$) $W^{(j)}(F_0, C_0)$
PCCS	412.20	608.92
FCCS	200.59	809.12

Table 3.3: NPV and option values

3.4.1.1 Sensitivity Analysis

Figure 3.8 shows the optimal stopping boundary, $C^{*(fccs)}(F)$, for different values of σ_F and σ_C. The solid line shows the boundary for the base case values of the volatilities, $\sigma_F = 0.05$ and $\sigma_C = 0.47$. It is revealed that $C^{*(fccs)}(F)$ is more sensitive to changes in the CO_2 price volatility than in the fuel price volatility. By letting σ_C to be fixed at its base value, if we increase the value of σ_F to 0.2 (a 300% increase), then a negligible increase in $C^{*(fccs)}(F)$ is observed. On the other hand, a 75% decrease in σ_C (to 0.1175) can make a significant downward change in $C^{*(fccs)}(F)$. This is intuitively because the CCS technology is more exposed to the CO_2 price than to the fuel price. In general, increasing uncertainty over the prices raises the value of waiting and, thus, shifts the optimal stopping boundary upward.

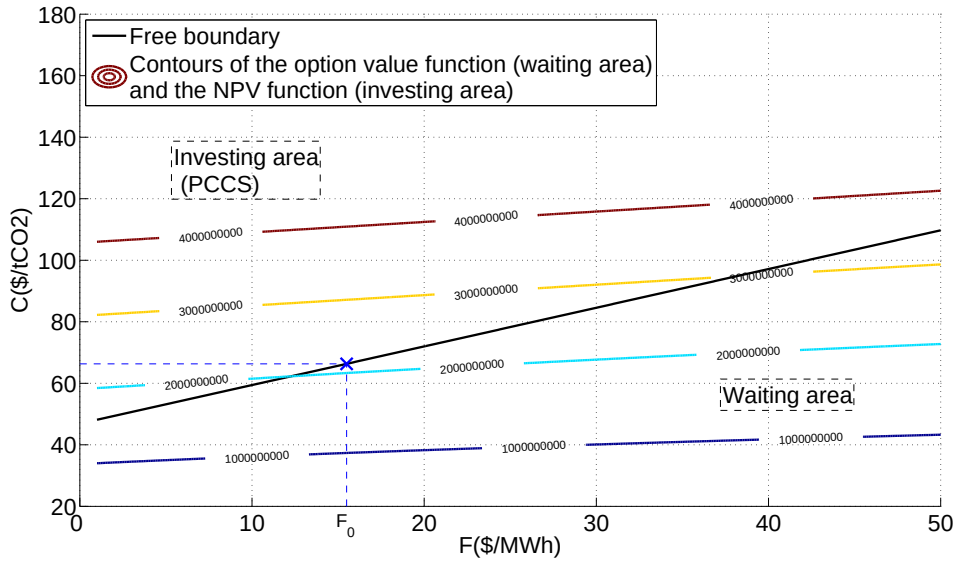

Figure 3.4: Free boundary $C^{*(pccs)}(F)$ as a function of F for PCCS retrofit

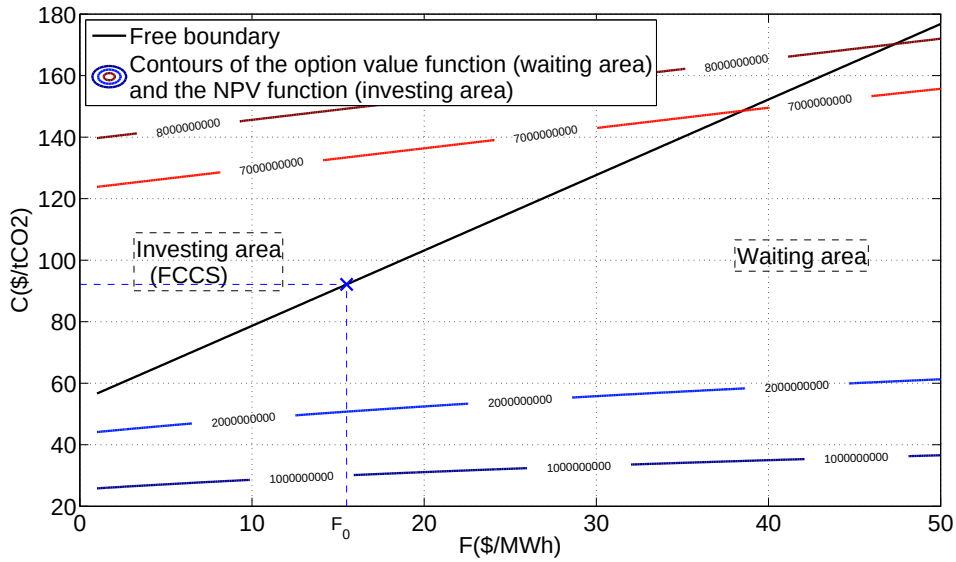

Figure 3.5: Free boundary $C^{*(fccs)}(F)$ as a function of F for FCCS retrofit

The correlation between the two stochastic variables may also affect the value and the time of adopting the emission-reduction policy. Figure 3.9 shows that a high positive correlation between the two GBM processes makes the adoption more accessible by reducing the critical threshold. Intuitively, high positive correlation reduces the risk of large differences between the two variables because any increase (decrease) in one variable may be accompanied by an increase (decrease) in the other. Hence, due to decrease in overall uncertainty, investment is optimal sooner. On the other hand, with a high negative correlation, an increase (decrease) in one variable is associated with a decrease (increase) in the other, i.e., we need to wait longer to receive more information about the prices. In this case, the overall uncertainty increases.

As we would expect, the larger the sunk capital cost of the investment is, the less likely the plant owner is to invest. This is illustrated in Figure 3.10 that compares the optimal stopping boundary for the base value of the capital cost with the boundaries for an increase of 100% as well as a decrease of 50%. Finally, we can generalise the results from the sensitivity analysis of the FCCS technology to that of the PCCS one.

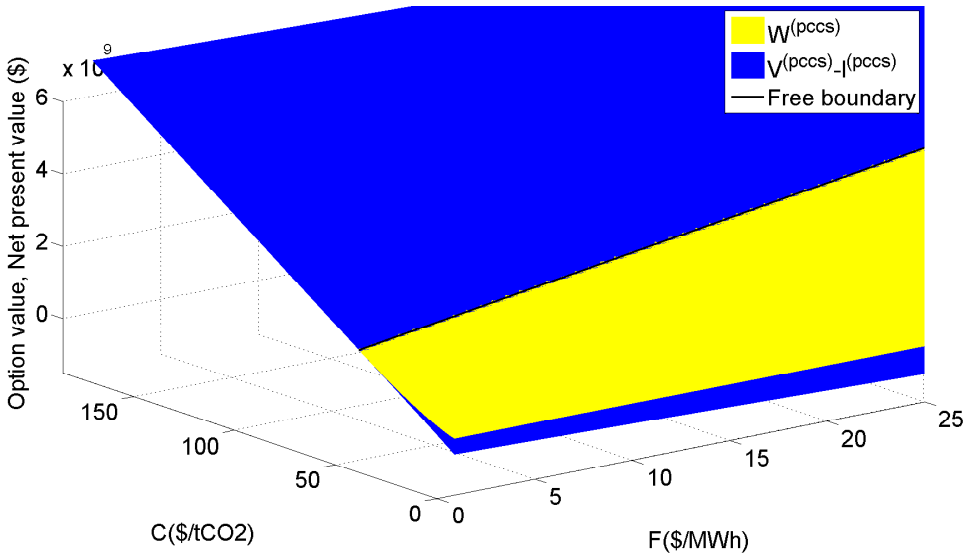

Figure 3.6: NPV and option value for PCCS

3.4.2 Mutually Exclusive Options

Now, suppose that the PC power plant has to choose between two alternative technologies: PCCS or FCCS. As discussed earlier in Section 3.2.3.3, using the data provided in Section 3.3, we first plot the expected PVs of both technologies to determine whether or not their intersection can lead to an indifference region. Figure 3.11 illustrates that the PCCS technology, which has a lower sunk capital cost, is uniformly dominated by the FCCS one. In this case, for CO_2 prices greater than the optimal boundary of FCCS ($C^{*(fccs)}(F)$), we invest immediately in FCCS, while for those prices less than this critical boundary, we wait.

Although the data here suggest that the PCCS technology would be skipped, it may be plausible that future innovations favour it. In order to determine how the methodology of Section 3.2.3.3 may cope with such an outcome, we modify the data such that the optimal investment region becomes dichotomous. As discussed in Décamps *et al.* (2006), a sufficient condition in order to have a dichotomous optimal investment region is that the PCCS retrofit generate slightly lower output flow than the FCCS retrofit, but at a considerably lower sunk capital cost. We would also require the volatilities of the prices to be relatively low, otherwise the optimal investment region would never be dichotomous. Concerning this, we

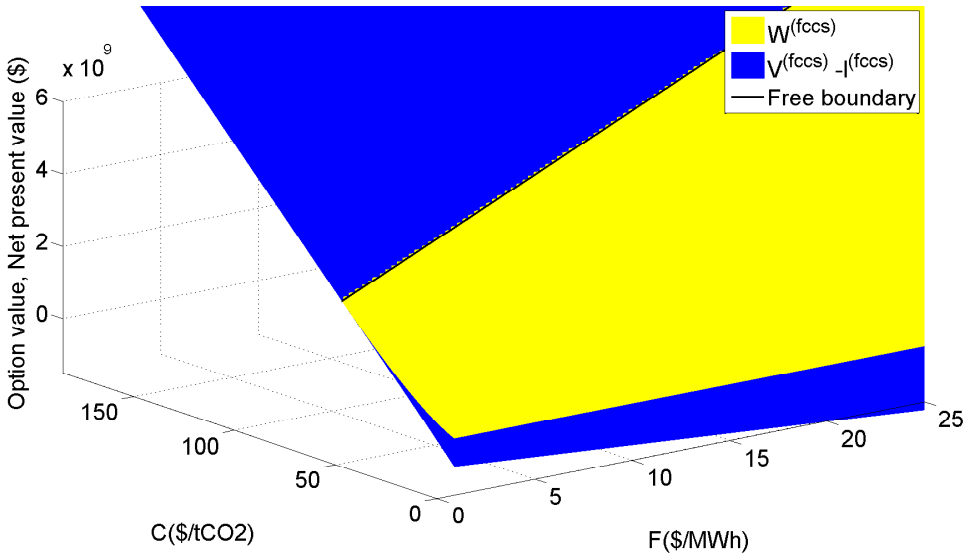

Figure 3.7: NPV and option value for FCCS

propose a superior PCCS technology in which the CO_2 emissions rate drops to 0.14 tCO_2/MWh_e (capture of nearly 82%), while the initial capital cost is reduced to \$75m. All other parameters are kept unchanged. We now plot the expected NPV of each technology in Figure 3.12. It is observed that the option value of investing in PCCS is greater than that of investing in FCCS. This fact results in an indifference region opening up around the indifference line in which it is optimal for the investor to wait[9] before investing in either technology. It should be mentioned that our solution to the individual investment options holds over the range $[0, C^{*(pccs)}(F)]$. We now need to evaluate the intermediate option and to find the two thresholds: C_L^* and C_U^*.

The intermediate option value as well as the thresholds are calculated using the algorithm in Figure 3 and graphed in Figures 3.13 and 3.14, respectively. It is revealed that for low values of CO_2: (i) for a constant CO_2 price, when the fuel price increases, it is more attractive to wait for PCCS, and when it decreases, it is more attractive to invest immediately; (ii) for a constant fuel price, increasing the CO_2 price results in investing in PCCS technology in order to reduce plant's

[9]Over the indifference region the investor has to wait because the NPVs of both technologies are equal and she cannot decide whether to invest in FCCS or PCCS. Therefore, she has to wait and see how the prices change in the future.

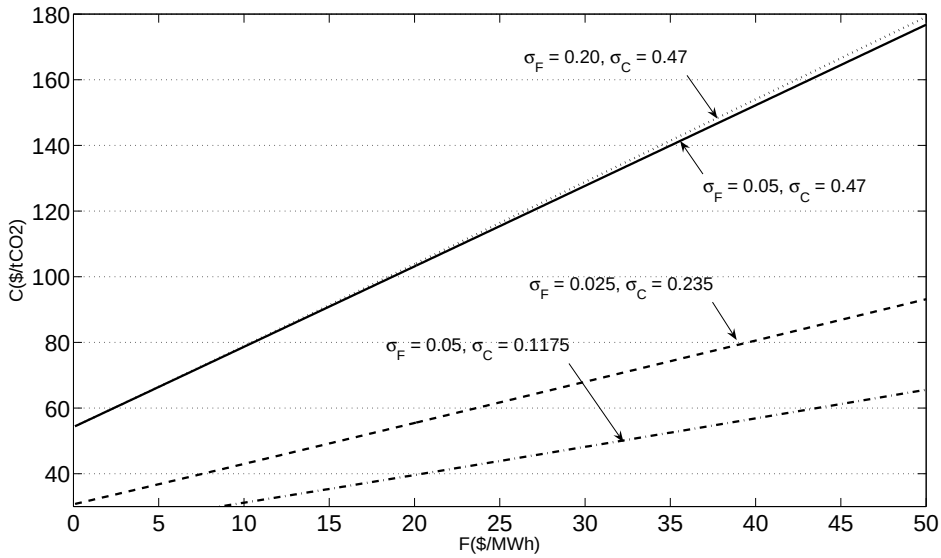

Figure 3.8: FCCS Free boundary sensitivity analysis with respect to volatilities

CO_2 emissions. Over the indifference region: (i) for any constant CO_2 price, as the fuel price increases, investing in PCCS becomes more economical, and as it decreases, investing in FCCS is preferred; (ii) for a constant fuel price, when the CO_2 price increases, it is more attractive to invest in FCCS, and when it decreases, it is more attractive to invest in PCCS because FCCS technology captures more CO_2 emissions than the PCCS technology does. Given the current price $F_0 = 15.5$ (\$/MWh), we find the PCCS retrofit threshold $C^{*(pccs)}(F_0) = \$50.83/\text{tCO}_2$. As the CO_2 price ($\$25.59/\text{tCO}_2$) is currently below this threshold, no retrofit is immediately adopted. However, suppose that the current CO_2 price given $F_0 = \$15.5$/MWh is located exactly on the indifference line, i.e., $C_I(F_0) = \$136.21/\text{tCO}_2$. The expected NPVs of investing in FCCS and PCCS, which are identical, and the mutually exclusive intermediate option value of investing in either technology are given in Table 3.4. The option value of waiting before investing in either technology is then \$20.042m which shows that by investing in any technology without considering this waiting opportunity we may lose an amount equal to 0.28% of the NPV of investing. Although such a high CO_2 price is not currently plausible, future international agreements on emissions may make result in such prices. For example, in Sweden, the CO_2 tax is $\$145/\text{tCO}_2$ (Swedish

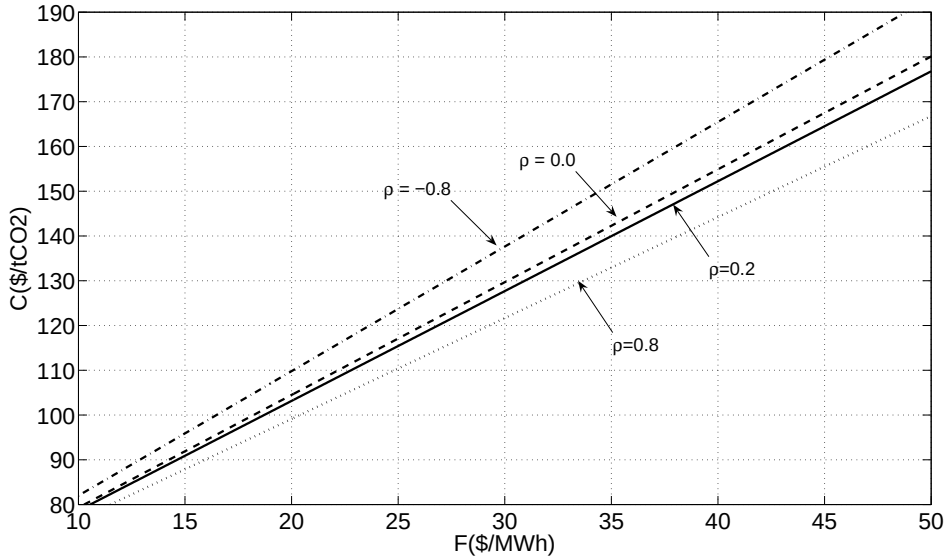

Figure 3.9: FCCS free boundary sensitivity analysis with respect to the correlation coefficient

Government Budget Bill (2008)).

$V^{(pccs)}(F_0, C_I(F_0))$	\$7.1776 billion
$V^{(fccs)}(F_0, C_I(F_0))$	\$7.1776 billion
$\Psi(F_0, C_I(F_0))$	\$7.1976 billion
$C_L^*(F_0)$	\$121.45/tCO$_2$
$C_U^*(F_0)$	\$151.96/tCO$_2$

Table 3.4: NPVs, option value, and thresholds with enhanced PCCS technology and higher initial CO_2 price

3.4.2.1 Sensitivity Analysis

From the previous example with the models of irreversible investments, decreasing the price volatilities reduces the waiting value. This can be seen from Figure 3.15, which depicts the optimal stopping boundaries with a 40% decrease in the base values of the price volatilities. Comparing these boundaries to those for the base values, it is observed that both the postponing areas are narrower for the reduced volatilities. On the other hand, the mutually exclusive intermediate

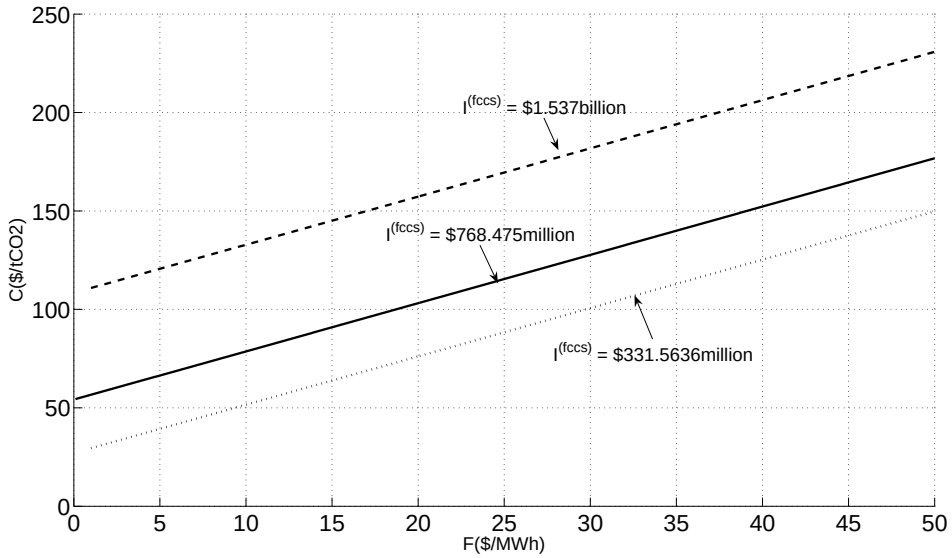

Figure 3.10: FCCS free boundary sensitivity analysis with respect to the capital cost

option value at the indifference point, $\Psi(F_0, C_I(F_0))$, reduces to \$7.1848 billion which is equivalent to losing 0.10% of the NPV of investing by killing the waiting opportunity. This value, however, rises to \$7.2167 billion with a 40% increase in the base values of the price volatilities, which reveals that we may lose 0.55% of the NPV of investing if we fail to take advantage of waiting. Furthermore, in Figure 3.16 we plot the NPVs of FCCS and PCCS technologies and their option values with the price volatilities twice as much as the base values. It is observed that even the enhanced PCCS technology, which has a lower sunk capital cost, is uniformly dominated by the FCCS one. In this case, for CO_2 prices greater than the optimal boundary of FCCS ($C^{*(fccs)}(F)$), we invest immediately in FCCS.

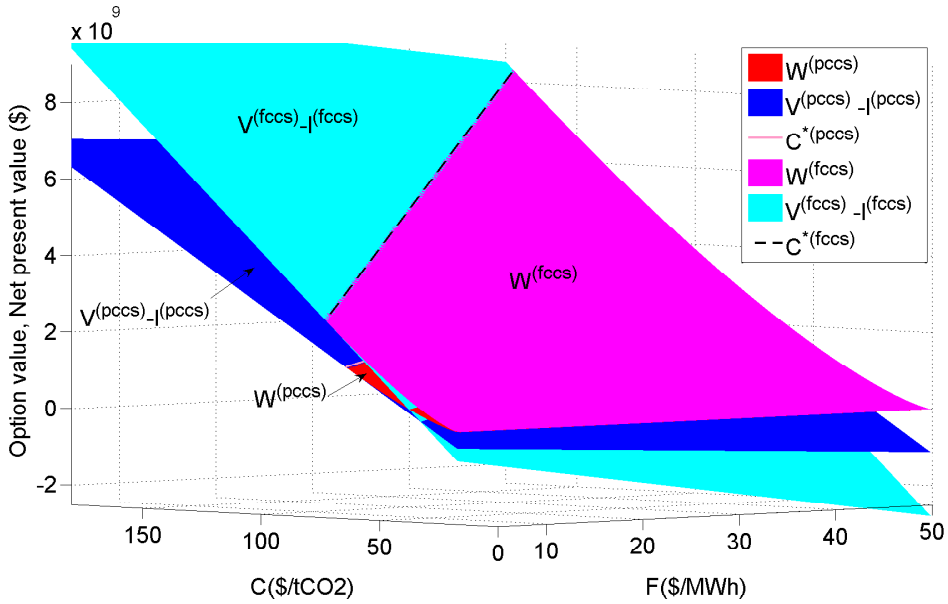

Figure 3.11: NPV and option value (separate valuation) indicate that the PCCS technology is uniformly dominated by the FCCS one ($\sigma_F = 0.05$ and $\sigma_C = 0.47$)

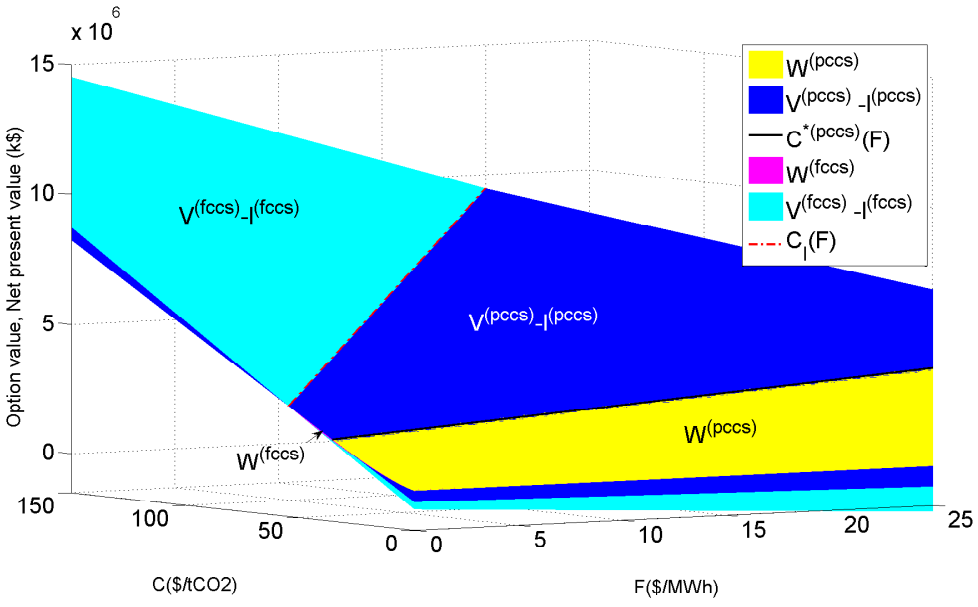

Figure 3.12: NPV and option value with enhanced PCCS technology (separate valuation) indicate that the option value of investing in PCCS ($W^{(pccs)}$) is greater than that of investing in FCCS ($W^{(fccs)}$), thereby resulting in an indifference region around the indifference line ($C_I(F)$) ($\sigma_F = 0.05$ and $\sigma_C = 0.47$)

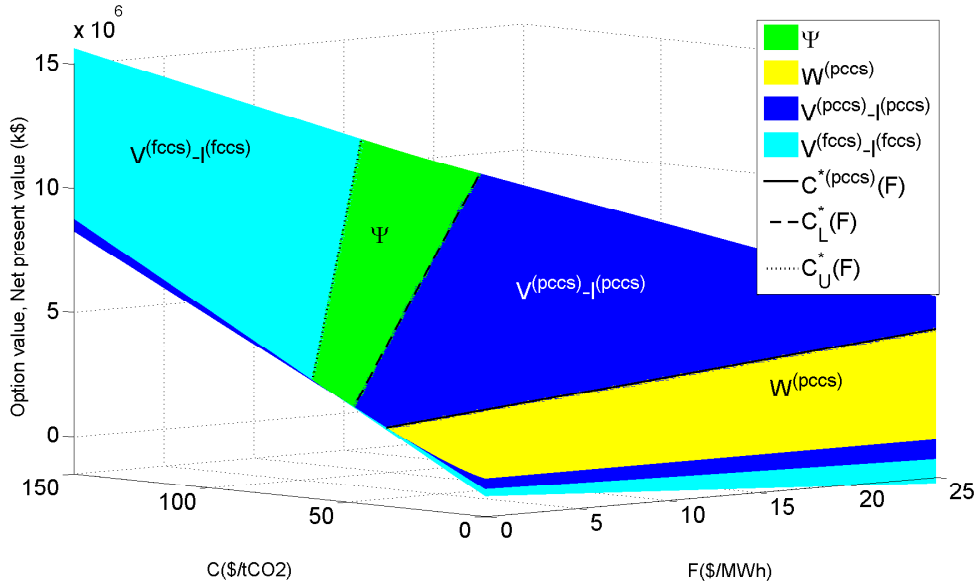

Figure 3.13: NPV and option value with enhanced PCCS technology (mutually exclusive options) show that for CO_2 prices less than $C^{*(pccs)}(F)$, we wait for PCCS, while for those prices between $C^{*(pccs)}(F)$ and $C^*_L(F)$, we invest immediately in PCCS; over the indifferent region (Ψ), we wait to invest either in PCCS or FCCS, and for CO_2 prices greater than $C^*_U(F)$, we invest immediately in FCCS ($\sigma_F = 0.05$ and $\sigma_C = 0.47$)

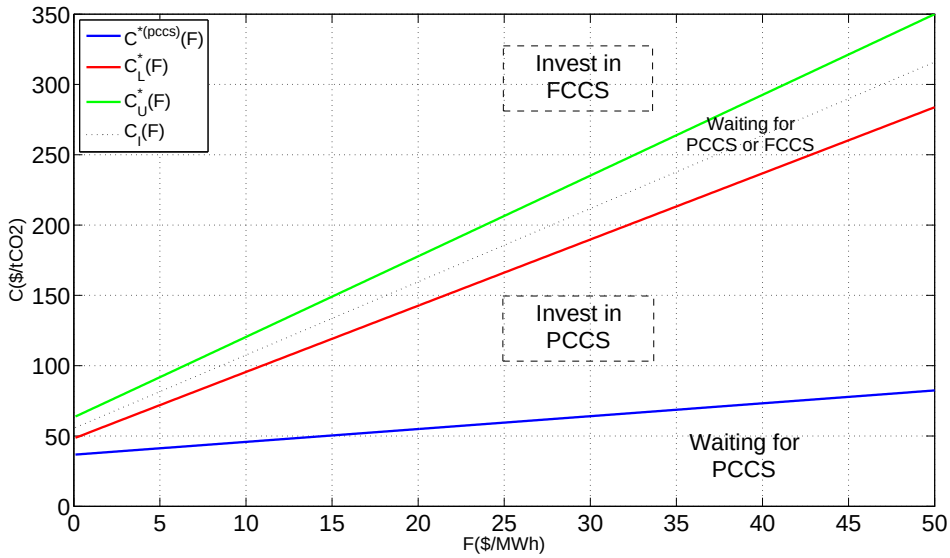

Figure 3.14: Free boundaries with enhanced PCCS technology ($\sigma_F = 0.05$ and $\sigma_C = 0.47$)

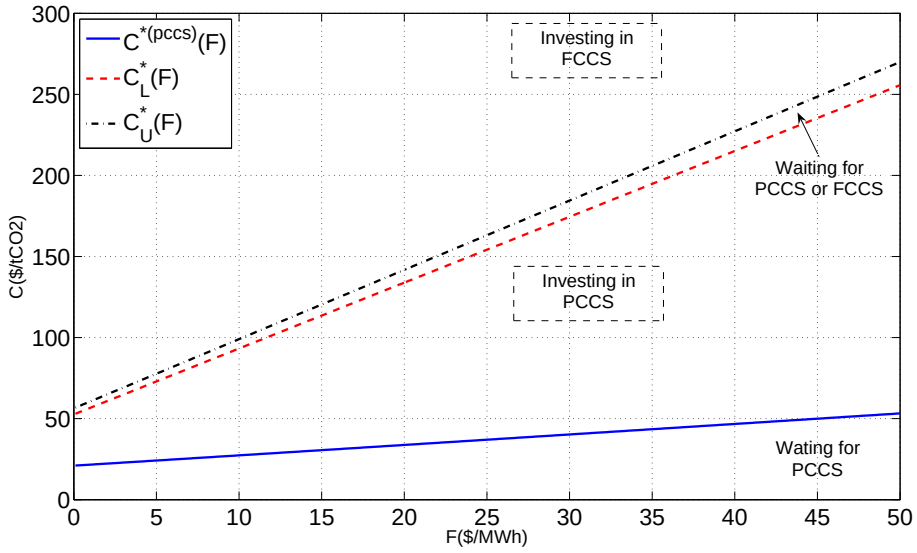

Figure 3.15: Free boundaries with enhanced PCCS technology ($\sigma_F = 0.030$ and $\sigma_C = 0.282$)

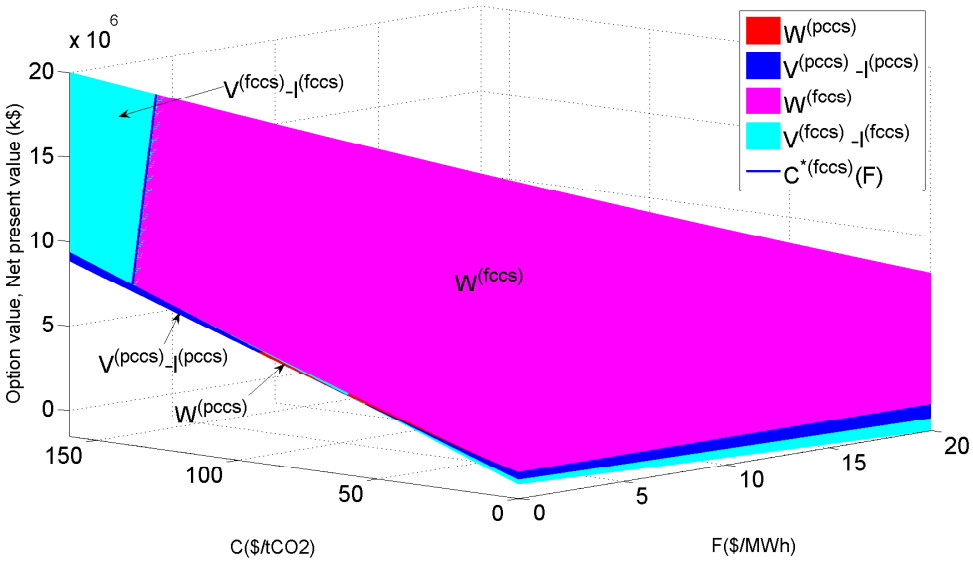

Figure 3.16: NPV and option value with enhanced PCCS technology (separate valuation) indicate that the PCCS technology is uniformly dominated by the FCCS one and for CO_2 prices greater (less) than $C^{*(fccs)}(F)$, we invest immediately in (wait for) FCCS ($\sigma_F = 0.10$ and $\sigma_C = 0.94$)

3.5 Conclusions

As industrialised countries have agreed to reduce their CO_2 emissions, which is assumed to be the most critical anthropogenic GHG, a wide range of mitigation options have been proposed. Among these, the CCS technology is of high importance because fossil fuels continue to be the dominant energy resources in the near term. Capturing almost all emissions is the main objective of policymakers; however, it may critically alter the technology, operation, and economics of a power plant. As a result, in this chapter we analyse both full and partial capture technologies under uncertainty over CO_2 permit and coal prices.

We first take the perspective of a coal-fired power plant that has to decide whether to invest, now or any time in the future, in an emission-reduction technology. Thus, we examine the opportunity to invest in FCCS and PCCS technologies separately. The options to invest in such technologies are valued as well as the optimal stopping boundaries. Using current market data, we find that invest-

ing in any CCS technology is not optimal. The critical threshold for investing in FCCS given current coal price is \$92.12/tCO_2, while the current CO_2 price is \$25.59/tCO_2. By proposing a more achievable PCCS technology, although we could reduce the critical threshold to \$56.70/tCO_2, it is still not optimal to invest immediately.

We then assume that the plant owner has to decide simultaneously between investing in either FCCS or PCCS technology and introduce the required conditions under which the investment region becomes dichotomous. Regarding these conditions, we propose an enhanced PCCS technology such that its calculated option value from the separate valuation is greater than that of the FCCS technology. Therefore, their NPVs intersect each other at an indifference curve that leads us to value a postponing area where we wait before investing in either technology. Unlike our analytical solution to the separate valuation, this mutually exclusive option value, depending on more than one stochastic variable, must be solved numerically. As such, our solution method is a quasi-analytical one.

The sensitivity of the investment opportunities to changes in the volatilities and the correlation of the stochastic prices as well as in the sunk capital cost is analysed in this chapter. Our numerical examples show that the investment option is highly sensitive to alterations in the volatility of CO_2 price. Generally, increases in volatilities cause increases in optimal boundaries as well as in option values. However, the correlation between the two prices has an opposite impact on the optimal boundaries, such that high positive correlation between prices makes the waiting area narrower.

On the whole, the outcome of this chapter is twofold. Firstly, we demonstrate that investing in any CCS technology is not economically advisable in the near term. It would be, however, more attractive should more rigorous climate policies be imposed, e.g., which either increases the CO_2 price level or reduces the uncertainty in the CO_2 price. Secondly, from a theoretical point of view, we develop a two-factor real options model for mutually exclusive investment under uncertainty over two correlated variables. In the next chapter, we focus on optimal operational decision-making under uncertainty in the energy sector.

Chapter 4

Real Options Analysis of Multiple-Exercise Interruptible Load Contracts

In deregulated electricity industries, load-serving entities (LSEs) provide electricity to their consumers at fixed retail rates, while they procure this electricity from wholesale electricity markets. Taking the perspective of such an LSE, we assume that a representative consumer is on an interruptible-load (IL) contract that allows the LSE to curtail electricity provision multiple times for a specified duration at a defined capacity payment. Given that the wholesale electricity price follows a geometric Brownian motion process, a relevant policy question is: how high should the wholesale electricity price be before the LSE exercises each interruption opportunity? We proceed by first finding the optimal interruption policy for a single-exercise IL contract before extending the model to consider many interruptions. While the generalised model does not have a closed-form analytical solution, it is, nevertheless, possible to solve it numerically to obtain an optimal interruption policy. Our numerical example of valuing a twenty-exercise IL contract, using the data provided by PG&E and NERC, suggests that interruption is desirable at relatively high electricity prices. Moreover, we show that the optimal value of the contract and the optimal interruption thresholds are highly sensitive to the volatility such that uncertainty favours a delay in interrupting. For comparison, we show that a deterministic approximation captures most of the value

of the IL contract as long as the volatility is low and the exercise constraints are not too severe.

4.1 IL Contracts

As a consequence of peak demand and supply constraints during hot summer and cold winter days, the electricity spot price increases significantly relative to its normal level. Therefore, LSEs, which purchase electricity from wholesale electricity spot markets and sell it to consumers at fixed retail rates, become exposed to huge losses. Over time, this may result in the interruption of electricity over the entire service area due to rationing. Although building enough power plants looks a reasonable resolution to this scenario, it may not be viable because besides the policy resistance to construction of new power plants and transmission lines, it would impact tariff rates and the environment. By contrast, demand response programmes are designed to be both fiscally and environmentally responsible solutions to temporary peak demand periods. Consumers' voluntary participation in demand response programmes helps enhance electricity reliability not only for their own businesses, but also for the entire service territory. Moreover, they will be offered appropriate incentives for their contribution to such programmes.

An IL contract between an LSE and a representative consumer allows the LSE to interrupt a portion or all of the load over some period of time in exchange for a pecuniary compensation. Clearly, such an LSE would exercise the interruption when the electricity spot price is significantly higher than the retail price. On the other hand, the LSE has to offer appropriate incentives to those consumers who participate in such programmes. In practice, no physical interruption occurrs as consumers are required to curtail their load. Several types of IL contracts offered by LSEs are now available, the most common of which are pay-in-advance and pay-as-you-go contracts. In the former, the consumer receives a discount on the retail price of electricity for the entire load, while in the latter, a compensation is paid per unit of load interrupted. Baldick *et al.* (2006) shows that retailers prefer to sign pay-as-you-go contracts because they always have a positive value due to payment, and interruptions that are made to the benefit of the retailers. Consumers will be notified of an interruption event between thirty minutes to two calendar days prior to the event. Each interruption may continue for two to six

hours, and the maximum number of interruptions is limited, e.g., for a programme provided by PG&E operating over the summer season (from 1 May through 31 October), the maximum number of interruptions is twenty-five, and the maximum number of interruption hours is seventy-five. Consecutive interruption days may also be restricted to a maximum of one, two, or three days. Customers who are involved in this programme would be paid compensation of $100-1000/MWh depending on the type of contract (PG&E (2008b) and PG&E (2009)).

4.2 Problem Formulation

4.2.1 Assumptions

In this chapter, we focus on the pay-as-you-go contract with infinite lifetime[1] where a customer responds to the interruptions 100% of time. We first consider a single-exercise IL contract on a continuous, flat load of a unit MW, in which the LSE has a perpetual option to interrupt the consumer's electricity supply for T years at a cost of $\$I$. Then, we suppose that a contract with N interruptions exists with interruption n lasting for T_n years and having a capacity payment of $\$I_n$, $n = 1, \ldots, N$. Moreover, the minimum lag between each two interruptions assumed to be h years, i.e., the $(n+1)$st interruption is available $T_n + h$ years after exercising the nth interruption. The retail price is fixed at C (in \$/MWh), while the wholesale electricity spot price, $\{P_t,\ t \geq 0\}$ (in \$/MWh), follows the exogenous, stochastic GBM process[2]:

$$dP_t = \alpha P_t dt + \sigma P_t dZ_t \tag{4.1}$$

where α and σ are, respectively, the annual growth rate and volatility parameters, and dZ_t stands for the increment of a standard Brownian motion process. The current electricity spot price is P_0, and the future returns and costs are discounted at a subjective constant annual rate $\rho > \alpha$. We suppose that the LSE serves a

[1] Although an IL contract has an expiration time, for simplicity, in this chapter, we assume that each interruption can occur at any time in the future.

[2] It must be mentioned that all the analyses in this chapter rely on the assumption that the electricity spot price evolves according to a GBM process. In case of assuming other processes for the stochastic variable, in general, analytical solutions may not exist, and we would typically have to resort to numerical methods to obtain a solution.

small amount of load compared to the system, such that its interruption does not affect the spot price of electricity.

4.2.2 Single-Exercise IL Contract

There are two states in this setup: one in which the LSE has not exercised the interruption and, thus, realises no savings over its instantaneous profit, $\$(C - P_t)dt$, and the other in which the interruption has been exercised, thereby allowing the LSE to save $\$(P_t - C)dt$ for a capacity payment of $\$I$ for T years. Thus, its decision-making problem to select the optimal time, τ, at which to exercise the interruption is:

$$F(P_0) \equiv \sup_{\tau \in \mathcal{S}} \mathbb{E}_{P_0} \left[\int_{\tau}^{\tau+T} H(P_t - C)e^{-\rho t}dt - e^{-\rho\tau}I \right] \tag{4.2}$$

where $\mathcal{S}$ denotes the set of stopping times of the filtration generated by the price process and H refers to the number of hours in a year. Here, $F(P_0)$ is the maximised expected value of the option to exercise the interruption, where the expected payoff (in \$) from immediate exercise is:

$$\begin{aligned} V(P_0) &\equiv \mathbb{E}_{P_0} \left[\int_0^T H(P_t - C)e^{-\rho t}dt \right] \\ &= \int_0^T H(P_0 e^{-(\rho-\alpha)t} - Ce^{-\rho t})dt \\ &= aP_0 - bC \end{aligned} \tag{4.3}$$

where $a = \frac{H(1-e^{-(\rho-\alpha)T})}{\rho-\alpha}$ and $b = \frac{H(1-e^{-\rho T})}{\rho}$. By using the strong Markov property of the GBM process and the law of iterated expectations, we have:

$$\mathbb{E}_{P_0} \left[\mathbb{E}_{P_\tau} \left[\int_{\tau}^{\tau+T} H(P_t - C)e^{-\rho t}dt \right] \right] = \mathbb{E}_{P_0} \left[\int_{\tau}^{\tau+T} H(P_t - C)e^{-\rho t}dt \right] \tag{4.4}$$

Hence, Equation (4.2) may be re-written as:

$$F(P_0) \equiv \sup_{\tau \in \mathcal{S}} \mathbb{E}_{P_0} \left[\mathbb{E}_{P_\tau} \left[\int_{\tau}^{\tau+T} H(P_t - C)e^{-\rho t}dt \right] - e^{-\rho\tau}I \right]$$

$$
\begin{aligned}
&= \sup_{\tau \in \mathcal{S}} \mathbb{E}_{P_0} \left[\mathbb{E}_{P_\tau} \left[\int_0^T H(P_{t'+\tau} - C) e^{-\rho(t'+\tau)} dt' \right] - e^{-\rho\tau} I \right] \\
&= \sup_{\tau \in \mathcal{S}} \mathbb{E}_{P_0} \left[e^{-\rho\tau} \left\{ V(P_\tau) - I \right\} \right] \qquad (4.5)
\end{aligned}
$$

The second equality results from applying the transformation $t' = t - \tau$. According to Dixit & Pindyck (1994) (p. 315), the expected stochastic discount factor given the current price and optimal price threshold, P^*, is:

$$
\mathbb{E}_{P_0} \left[e^{-\rho\tau} \right] = \left(\frac{P_0}{P^*} \right)^{\beta} \qquad (4.6)
$$

where β is the positive root of the characteristic quadratic equation $\frac{1}{2}\sigma^2\beta(\beta - 1) + \alpha\beta - \rho = 0$. Thus, the optimal stopping time problem becomes a non-linear maximisation one:

$$
F(P_0) \equiv \max_{P^* \geq P_0} \left(\frac{P_0}{P^*} \right)^{\beta} \left\{ V(P^*) - I \right\} \qquad (4.7)
$$

The first-order necessary condition to this problem yields:

$$
\begin{aligned}
&\beta \left(\frac{P_0}{P^*} \right)^{\beta-1} \frac{P_0}{(P^*)^2} \left\{ aP^* - bC - I \right\} = \left(\frac{P_0}{P^*} \right)^{\beta} a \\
&\Rightarrow P^* = \left(\frac{\beta}{\beta - 1} \right) \frac{(I + bC)}{a} \qquad (4.8)
\end{aligned}
$$

The second-order sufficiency condition is verified in Appendix J. Since $\beta = \frac{1}{2} - \alpha/\sigma^2 + \sqrt{[\alpha/\sigma^2 - \frac{1}{2}]^2 + 2\rho/\sigma^2} > 1$ is a positive, exogenous constant, the fraction $\frac{\beta}{\beta-1}$ is also greater than one. This implies that $P^* > \frac{(I+bC)}{a} \equiv P^{det}$, which is the threshold at which to exercise the interruption from a now-or-never deterministic discounted cash flow (DCF) perspective. By re-arranging Equation (4.8), we obtain that it is optimal to interrupt electricity supply when the expected PV of the electricity price is greater than the PV of the cost of interruption, i.e., the capacity payment and the PV of the forgone retail rate:

$$
aP^* = \left(\frac{\beta}{\beta - 1} \right) (I + bC) \qquad (4.9)
$$

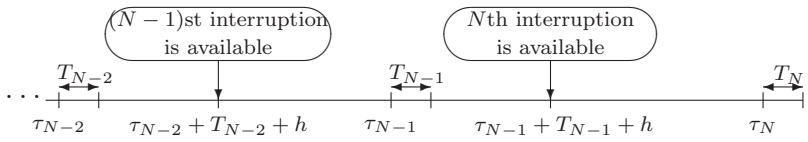

Figure 4.1: Decision-making timeline for τ_{N-1}

Hence, as expected, uncertainty favours a delay in the decision-making as the value of waiting imposes an additional (implicit) cost of action. In Appendix K, we prove analytically that both the optimal threshold, Equation (4.8), and the optimal value of the contract, Equation (4.7), are increasing functions of σ.

4.2.3 Multiple-Exercise IL Contract

4.2.3.1 Solve for the Nth and $(N-1)$st Interruptions

An optimal interruption policy for an N-exercise IL contract is a set of threshold prices, $\{P^{*(N)}_{\tau_1}, \ldots, P^{*(N)}_{\tau_n}, \ldots, P^{*(N)}_{\tau_N}\}$, where τ_n and $P^{*(N)}_{\tau_n}$, $n = 1, \ldots, N$, represent, respectively, the optimal time and the optimal threshold price of exercising the nth interruption from an N-exercise IL contract. Starting with the Nth interruption, we note that it offers the same opportunities as a single-exercise IL contract. Therefore, its value and exercise price should also be the same. We define the following $\forall n$:

$$a_n = H\frac{1-e^{-(\rho-\alpha)T_n}}{\rho-\alpha} \tag{4.10}$$

$$b_n = H\frac{1-e^{-\rho T_n}}{\rho} \tag{4.11}$$

$$V_n(P) \;=\; a_n P - b_n C \tag{4.12}$$

Thus, assuming that when the Nth interruption option is first available (see Fig. 1), it is still optimal to wait, i.e., $P^{*(N)}_{\tau_N} \geq P_{\tau_{N-1}+T_{N-1}+h}$, then the maximised value of the option to exercise the Nth interruption (discounted to time $\tau_{N-1}+T_{N-1}+h$

when it is first available) is:

$$\begin{aligned} F_N^{(N)}(P_{\tau_{N-1}+T_{N-1}+h}) &\equiv \sup_{\tau_N \in \mathcal{S}} \mathbb{E}_{P_{\tau_{N-1}+T_{N-1}+h}} \left[e^{-\rho(\tau_N - (\tau_{N-1}+T_{N-1}+h))} \right. \\ &\quad \left. \times \{V_N(P_{\tau_N}) - I_N\} \right] \\ &= \max_{P^{*(N)}_{\tau_N} \geq P_{\tau_{N-1}+T_{N-1}+h}} \left(\frac{P_{\tau_{N-1}+T_{N-1}+h}}{P^{*(N)}_{\tau_N}} \right)^{\beta} \left\{ V_N\left(P^{*(N)}_{\tau_N}\right) - I_N \right\} \end{aligned} \tag{4.13}$$

The solution to Equation (4.13) yields:

$$P^{*(N)}_{\tau_N} = \left(\frac{\beta}{\beta - 1} \right) \frac{(I_N + b_N C)}{a_N} \tag{4.14}$$

Working backwards to the $(N-1)$st interruption option (see Fig. 1), if it is still optimal to wait, i.e., $P^{*(N)}_{\tau_{N-1}} \geq P_{\tau_{N-2}+T_{N-2}+h}$, then the LSE's nested problem, i.e., the maximised value of the option to exercise the $(N-1)$st interruption onward (discounted to time $\tau_{N-2} + T_{N-2} + h$), is[3]:

$$\begin{aligned} F_{N-1}^{(N)}(P_{\tau_{N-2}+T_{N-2}+h}) \equiv \sup_{\tau_{N-1} < \tau_N} \mathbb{E}_{P_{\tau_{N-2}+T_{N-2}+h}} \left[e^{-\rho(\tau_{N-1} - (\tau_{N-2}+T_{N-2}+h))} \right. \\ \left. \times \left\{ V_{N-1}\left(P_{\tau_{N-1}}\right) - I_{N-1} + e^{-\rho(T_{N-1}+h)} \mathbb{E}_{P_{\tau_{N-1}}} \left[F_N^{(N)}\left(P_{\tau_{N-1}+T_{N-1}+h}\right) \right] \right\} \right] \end{aligned} \tag{4.15}$$

$$\begin{aligned} \Rightarrow F_{N-1}^{(N)}(P_{\tau_{N-2}+T_{N-2}+h}) = \max_{P^{*(N)}_{\tau_{N-1}} \geq P_{\tau_{N-2}+T_{N-2}+h}} \left(\frac{P_{\tau_{N-2}+T_{N-2}+h}}{P^{*(N)}_{\tau_{N-1}}} \right)^{\beta} \\ \times \left\{ V_{N-1}(P^{*(N)}_{\tau_{N-1}}) - I_{N-1} + e^{-\rho(T_{N-1}+h)} \mathbb{E}_{P^{*(N)}_{\tau_{N-1}}} \left[F_N^{(N)}\left(P_{\tau_{N-1}+T_{N-1}+h}\right) \right] \right\} \end{aligned} \tag{4.16}$$

The conditional expectation of the Nth interruption's option value at time $\tau_{N-1} + T_{N-1} + h$ given the information at time τ_{N-1} depends on whether or not the Nth

[3]When the $(N-1)$st interruption is first available at time $\tau_{N-2} + T_{N-2} + h$, if $P^{*(N)}_{\tau_{N-1}} \geq P_{\tau_{N-2}+T_{N-2}+h}$, then the LSE has to wait until the price reaches the optimal threshold $P^{*(N)}_{\tau_{N-1}}$. The LSE will then exercise the $(N-1)$st interruption and receive the immediate payoff $V_{N-1}(P^{*(N)}_{\tau_{N-1}}) - I_{N-1}$. Therefore, in order to find the $(N-1)$st optimal threshold, we need to maximise the immediate payoff at time τ_{N-1} plus the Nth interruption option value, which is available $T_{N-1} + h$ years later, discounted to time $\tau_{N-2} + T_{N-2} + h$. Since these values are random, we need to take their expectations given available information.

interruption is exercised immediately, i.e., whether or not $P_{\tau_{N-1}+T_{N-1}+h} \geq P^{*(N)}_{\tau_N}$:

$$F^{(N)}_N(P_{\tau_{N-1}+T_{N-1}+h}) = \begin{cases} a_N P_{\tau_{N-1}+T_{N-1}+h} - b_N C - I_N & \text{if } P_{\tau_{N-1}+T_{N-1}+h} \geq P^{*(N)}_{\tau_N} \\ \left(\frac{P_{\tau_{N-1}+T_{N-1}+h}}{P^{*(N)}_{\tau_N}}\right)^{\beta} \left[V_N\left(P^{*(N)}_{\tau_N}\right) - I_N\right] & \text{otherwise} \end{cases} \tag{4.17}$$

Thus:

$$\begin{aligned} \mathbb{E}_{P^{*(N)}_{\tau_{N-1}}}\left[F^{(N)}_N\left(P_{\tau_{N-1}+T_{N-1}+h}\right)\right] &= \mathbb{E}_{P^{*(N)}_{\tau_{N-1}}}\left[a_N P_{\tau_{N-1}+T_{N-1}+h}\right. \\ &\left. - b_N C - I_N\right] \times \mathbb{P}_{P^{*(N)}_{\tau_{N-1}}}\left[P_{\tau_{N-1}+T_{N-1}+h} \geq P^{*(N)}_{\tau_N}\right] \\ &+ \mathbb{E}_{P^{*(N)}_{\tau_{N-1}}}\left[\left(\frac{P_{\tau_{N-1}+T_{N-1}+h}}{P^{*(N)}_{\tau_N}}\right)^{\beta}\left[V_N\left(P^{*(N)}_{\tau_N}\right) - I_N\right]\right] \\ &\times \mathbb{P}_{P^{*(N)}_{\tau_{N-1}}}\left[P_{\tau_{N-1}+T_{N-1}+h} < P^{*(N)}_{\tau_N}\right] \end{aligned} \tag{4.18}$$

By the definition of conditional probability and optimal thresholds, and the characteristics of a GBM process (see Etheridge (2002)), we have:

$$\mathbb{P}_{P^{*(N)}_{\tau_{N-1}}}\left[P_{\tau_{N-1}+T_{N-1}+h} \geq P^{*(N)}_{\tau_N}\right] = \Phi\left(\frac{\left(\alpha - \frac{1}{2}\sigma^2\right)(T_{N-1}+h) - \ln\left(\frac{P^{*(N)}_{\tau_N}}{P^{*(N)}_{\tau_{N-1}}}\right)}{\sigma\sqrt{T_{N-1}+h}}\right) \tag{4.19}$$

where Φ is the cumulative distribution function (CDF) of a standard normal random variable.

Returning to Equation (4.18), we now calculate the conditional expectation as follows:

$$\begin{aligned} \mathbb{E}_{P^{*(N)}_{\tau_{N-1}}}\left[F^{(N)}_N\left(P_{\tau_{N-1}+T_{N-1}+h}\right)\right] &= \left[a_N P^{*(N)}_{\tau_{N-1}} e^{\alpha(T_{N-1}+h)} - b_N C - I_N\right] \\ &\times \Phi\left(R(T_{n-1}+h, P^{*(N)}_{\tau_N}, P^{*(N)}_{\tau_{N-1}})\right) + \left(\frac{P^{*(N)}_{\tau_{N-1}}}{P^{*(N)}_{\tau_N}}\right)^{\beta} e^{\gamma(T_{N-1}+h)} \\ &\times \left[a_N P^{*(N)}_{\tau_N} - b_N C - I_N\right]\left(1 - \Phi\left(R(T_{n-1}+h, P^{*(N)}_{\tau_N}, P^{*(N)}_{\tau_{N-1}})\right)\right) \end{aligned} \tag{4.20}$$

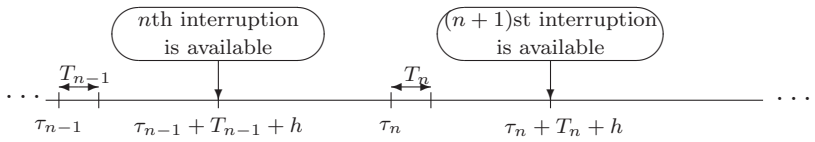

Figure 4.2: Decision-making timeline for τ_n

where $\gamma = \beta\alpha + \frac{1}{2}\beta(\beta-1)\sigma^2$ and $R(t,X,Y) = \frac{\left(\alpha-\frac{1}{2}\sigma^2\right)t - \ln\left(\frac{X}{Y}\right)}{\sigma\sqrt{t}}$. Inserting Equation (4.20) into the optimisation problem in Equation (4.16) and taking the first-order necessary condition yields (see Appendix L for more details):

$$\begin{aligned}
&P^{*(N)}_{\tau_{N-1}}(\beta-1)\left[a_{N-1}+a_N e^{-(\rho-\alpha)(T_{N-1}+h)}\left(\Phi\left(R(T_{N-1}+h,P^{*(N)}_{\tau_{N-1}},P^{*(N)}_{\tau_N})\right)\right.\right.\\
&\quad\left.\left.-\frac{\phi\left(R(T_{N-1}+h,P^{*(N)}_{\tau_{N-1}},P^{*(N)}_{\tau_N})\right)}{(\beta-1)\sigma\sqrt{T_{N-1}+h}}\left(1-\left(\frac{P^{*(N)}_{\tau_{N-1}}}{P^{*(N)}_{\tau_N}}\right)^{\beta-1}e^{(\gamma-\alpha)(T_{N-1}+h)}\right)\right)\right]\\
&=\beta\left[b_{N-1}C+I_{N-1}+(b_NC+I_N)e^{-\rho(T_{N-1}+h)}\left(\Phi\left(R(T_{N-1}+h,P^{*(N)}_{\tau_{N-1}},P^{*(N)}_{\tau_N})\right)\right.\right.\\
&\quad\left.\left.-\frac{\phi\left(R(T_{N-1}+h,P^{*(N)}_{\tau_{N-1}},P^{*(N)}_{\tau_N})\right)}{\beta\sigma\sqrt{T_{N-1}+h}}\left(1-\left(\frac{P^{*(N)}_{\tau_{N-1}}}{P^{*(N)}_{\tau_N}}\right)^{\beta}e^{\gamma(T_{N-1}+h)}\right)\right)\right] \qquad (4.21)
\end{aligned}$$

where, ϕ is the probability distribution function (PDF) of a standard normal random variable. Hence, given $P^{*(N)}_{\tau_N}$ from Equation (4.14), it is possible to solve Equation (4.21) numerically for $P^{*(N)}_{\tau_{N-1}}$ and then work backwards iteratively for $P^{*(N)}_{\tau_{N-2}},\ldots,P^{*(N)}_{\tau_1}$.

4.2.3.2 General Solution for the nth Interruption

Following the same methodology as in the previous section, when the nth interruption is available (see Fig. 2), if it is still optimal to wait, i.e., $P^{*(N)}_{\tau_n} \geq P_{\tau_{n-1}+T_{n-1}+h}$, then the maximised value of the option to exercise the nth interruption onward, discounted to time $\tau_{n-1}+T_{n-1}+h$, is:

$$\begin{aligned}
F^{(N)}_n(P_{\tau_{n-1}+T_{n-1}+h}) \equiv \sup_{\tau_{n-1}<\tau_n<\tau_{n+1}} &\mathbb{E}_{P_{\tau_{n-1}+T_{n-1}+h}}\left[e^{-\rho(\tau_n-(\tau_{n-1}+T_{n-1}+h))}\right.\\
&\left.\times\left\{V_n\left(P_{\tau_n}\right)-I_n+e^{-\rho(T_n+h)}\mathbb{E}_{P_{\tau_n}}F^{(N)}_{n+1}\left(P_{\tau_n+T_n+h}\right)\right\}\right]
\end{aligned}$$

$$\Rightarrow F_n^{(N)}(P_{\tau_{n-1}+T_{n-1}+h}) \equiv \max_{P_{\tau_n}^{*(N)} \geq P_{\tau_{n-1}+T_{n-1}+h}} \left(\frac{P_{\tau_{n-1}+T_{n-1}+h}}{P_{\tau_n}^{*(N)}}\right)^{\beta} \Big\{ a_n P_{\tau_n}^{*(N)} - b_n C - I_n + e^{-\rho(T_n+h)} \mathbb{E}\left[F_{n+1}^{(N)}\left(P_{\tau_n+T_n+h}\right) | P_{\tau_n} = P_{\tau_n}^{*(N)}\right]\Big\} \quad (4.22)$$

Taking the first-order necessary condition and simplifying the result yields:

$$P_{\tau_n}^{*(N)}(\beta-1)\left(a_n - \frac{e^{-\rho(T_n+h)}}{\beta-1} \left.\frac{\partial \mathbb{E}\left[F_{n+1}^{(N)}(P_{\tau_n+T_n+h}) | P_{\tau_n}\right]}{\partial P_{\tau_n}}\right|_{P_{\tau_n}=P_{\tau_n}^{*(N)}}\right) = \beta(b_n C + I_n - e^{-\rho(T_n+h)} \mathbb{E}\left[F_{n+1}^{(N)}(P_{\tau_n+T_n+h}) | P_{\tau_n} = P_{\tau_n}^{*(N)}\right]) \quad (4.23)$$

In Appendix M, we show that the conditional expectation of the $(n+1)$st interruption's option given $P_{\tau_n} = P_{\tau_n}^{*(N)}$ is calculated via the following equation:

$$\begin{aligned}\mathbb{E}\left[F_{n+1}^{(N)}(P_{\tau_n+T_n+h}) | P_{\tau_n} = P_{\tau_n}^{*(N)}\right] &= \Big(a_{n+1} e^{\alpha(T_n+h)} P_{\tau_n}^{*(N)} - b_{n+1} C - I_{n+1} \\ &+ e^{-\rho(T_{n+1}+h)} \mathbb{E}\left[F_{n+2}^{(N)}(P_{\tau_n+T_n+h+T_{n+1}+h}) | P_{\tau_n} = P_{\tau_n}^{*(N)}\right]\Big) \\ &\times \Phi\left(R(T_n+h, P_{\tau_n}^{*(N)}, P_{\tau_{n+1}}^{*(N)})\right) + \Big(a_{n+1} P_{\tau_{n+1}}^{*(N)} - b_{n+1} C - I_{n+1} \\ &+ e^{-\rho(T_{n+1}+h)} \mathbb{E}\left[F_{n+2}^{(N)}(P_{\tau_{n+1}+T_{n+1}+h}) | P_{\tau_{n+1}} = P_{\tau_{n+1}}^{*(N)}\right]\Big) e^{\gamma(T_n+h)} \\ &\times \left(\frac{P_{\tau_n}^{*(N)}}{P_{\tau_{n+1}}^{*(N)}}\right)^{\beta} \left(1 - \Phi\left(R(T_n+h, P_{\tau_n}^{*(N)}, P_{\tau_{n+1}}^{*(N)})\right)\right) \end{aligned} \quad (4.24)$$

Having the information that after exercising the last interruption, there is no interruption available at time $\tau_N + T_N + h$, i.e., $F_{N+1}^{(N)}(.) = 0$, and working backwards to time τ_n, we can solve this problem recursively. The now-or-never NPV of exercising the nth interruption at the current electricity price, P_0, can also be calculated from the following equation:

$$NPV_n^{(N)}(P_0) = a_n P_0 - b_n C - I_n + e^{-\rho(T_n+h)} \mathbb{E}\left[F_{n+1}^{(N)}(P_{\tau_n+T_n+h}) | P_{\tau_n} = P_0\right] \quad (4.25)$$

4.2.4 Approximate IL Contract Valuation

Since the exact valuation procedure in Section 4.2.3 does not yield closed-form solutions, we approximate the conditional expectation of the $(n+1)$st interruption's option value at time $\tau_n + T_n + h$ given the information at time τ_n using the conditional expectation of future electricity price given the information at time τ_n, i.e., $\mathbb{E}(P_{\tau_n+T_n+h}|P_{\tau_n})$. This is the approach taken in Fleten *et al.* (2007) when analysing sequential, lagged investment decisions in decentralised renewable power generation. We, thus, define the following maximised value function, which must be solved for the approximate price threshold, $P^{*(N)}_{\tau'_n}$:

$$J^{(N)}_n(P_{\tau'_{n-1}+T_{n-1}+h}) = \max_{P^{*(N)}_{\tau'_n} \geq P_{\tau'_{n-1}+T_{n-1}+h}} \left(\frac{P_{\tau'_{n-1}+T_{n-1}+h}}{P^{*(N)}_{\tau'_n}}\right)^{\beta} \left\{a_n P^{*(N)}_{\tau'_n} - b_n C - I_n + e^{-\rho(T_n+h)} J^{(N)}_{n+1}\left(\mathbb{E}\left[P_{\tau'_n+T_n+h}|P_{\tau'_n} = P^{*(N)}_{\tau'_n}\right]\right)\right\} \tag{4.26}$$

Clearly, this approximate approach does not affect valuation of the last interruption, i.e., $\tau'_N = \tau_N$, $P^{*(N)}_{\tau'_N} = P^{*(N)}_{\tau_N}$, and $J^{(N)}_N(.) = F^{(N)}_N(.)$. However, the remaining approximate thresholds, $\{P^{*(N)}_{\tau'_1}, \ldots, P^{*(N)}_{\tau'_{N-1}}\}$, are significantly higher than their corresponding thresholds calculated in Section 4.2.3.2, $\{P^{*(N)}_{\tau_1}, \ldots, P^{*(N)}_{\tau_{N-1}}\}$. The reason for this increase is explained mathematically in Appendix N using Jensen's inequality. Moreover, in Appendix O, we show how to obtain the closed-form solutions for the approximate price thresholds:

$$P^{*(N)}_{\tau'_n} = \frac{\beta}{\beta - 1} \frac{\sum_{j=n}^{S_{\tau'_n}} e^{-\rho T^{(n)}_{j-n}} (b_j C + I_j)}{\sum_{j=n}^{S_{\tau'_n}} e^{-(\rho-\alpha)T^{(n)}_{j-n}} a_j}, \qquad n = 1, \ldots, N \tag{4.27}$$

where $T^{(n)}_0 = 0$, $T^{(n)}_k = \sum_{j=n}^{n+k-1}(T_j + h)$ for $k = 1, \ldots, N-n$, and $S_{\tau'_n}$ is either the smallest value in set $S = \{n, n+1, \ldots, N-1\}$ for which the expected forward price at time $\tau'_n + T_{S_{\tau'_n}-n+1}$ given $P_{\tau'_n} = P^{*(N)}_{\tau'_n}$ is less than the $(S_{\tau'_n}+1)$st interruption threshold, i.e., $\mathbb{E}\left[P_{\tau'_n+T^{(n)}_{S_{\tau'_n}-n+1}}|P_{\tau'_n} = P^{*(N)}_{\tau'_n}\right] = e^{\alpha T_{S_{\tau'_n}-n+1}} P^{*(N)}_{\tau'_n} < P^{*(N)}_{S_{\tau'_n}+1}$, or N if $e^{\alpha T_{s-n+1}} P^{*(N)}_{\tau'_n} \geq P^{*(N)}_{s+1}$ for any $s \in S$. Evidently, since the approximation approach is much easier to calculate, it would be preferable to a retailer if it can

capture most of the value of a multiple-exercise IL contract.

4.3 Numerical Examples

4.3.1 Data

Using the IL contract data provided by PG&E (2008b) and PG&E (2009), we assume $C = \$60/\text{MWh}$ and $N = 20$ with each interruption option providing six hours of 1 MW curtailment for a capacity payment of about \$600.[4] In order to keep the limitation of occurring a maximum of one interruption in each day, we let $h = 1/365$. The parameters of the electricity spot price process, which are reported in Table 4.1, are estimated using the wholesale average annual electricity prices, from 2001 to 2007, by North American Electric Reliability Corporation (NERC (2008)), developed from the form EIA-861 (2008).

Table 4.1: Data

Parameter	Value
σ	0.20
α	0.03
P_0 (\$/MWh)	50
C (\$/MWh)	60
ρ	0.10
T_n (years)	6/8760
I_n (\$)	600
h (years)	1/365

4.3.2 Single-Exercise IL Contract

We first solve the problem for a single-exercise IL contract in which the LSE has one interruption opportunity. Using the results from Section 4.2.2, the optimal threshold, the expected NPV of interrupting, and the optimal value of the contract, which are graphed in Fig. 4.3, suggest that at the current electricity price, interrupting is neither in-the-money nor optimal to be exercised immediately.

[4] We assume that the LSE has to pay compensation of $P_{\text{fine}} = \$100/\text{MWh}$, which results in a capacity payment of $I_n = \int_0^{T_n} \left(e^{-\rho t} H \; P_{\text{fine}} \; dt\right) = \$599.99, \; n = 1, 2, \ldots, N$.

On the other hand, a positive optimal value of the contract ($23.44) results in a high option value of waiting ($683.41), i.e., the difference between the optimal value and the now-or-never NPV of exercising the interruption, as well as a high optimal threshold ($320/MWh).

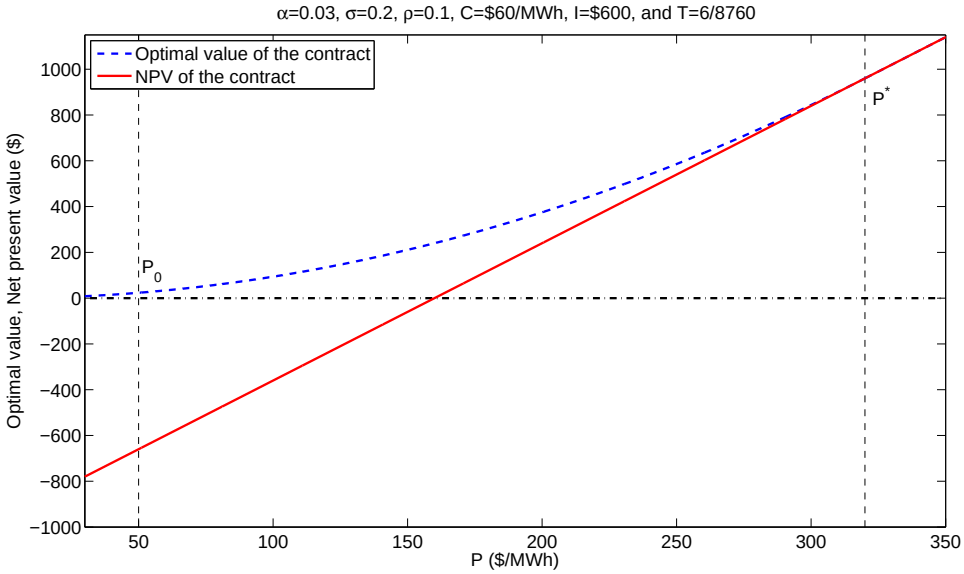

Figure 4.3: NPV and optimal value for a single-exercise IL contract

Fig. 4.4 indicates that uncertainty delays interruption because, intuitively, with more uncertainty, we are more likely to wait for new information. Consistently, Fig. 4.5 reveals that the optimal value of the contract is also increasing with respect to σ, i.e., with more uncertainty, the contract is more valuable. As we would expect, Figs. 4.4 and 4.5, respectively, demonstrate that when the capacity payment is high, exercising a contract is delayed and its optimal value decreases, which can be simply proven from Equations (4.8) and (4.9).

4.3.3 Two-Exercise IL Contract

Here, by adding another interruption to the single-exercise IL contract, we are interested in calculating the threshold of the first interruption together with the optimal value of the contract. From Section 4.2.3.2, we need to solve the problem starting from the second interruption. The results for the second interruption are

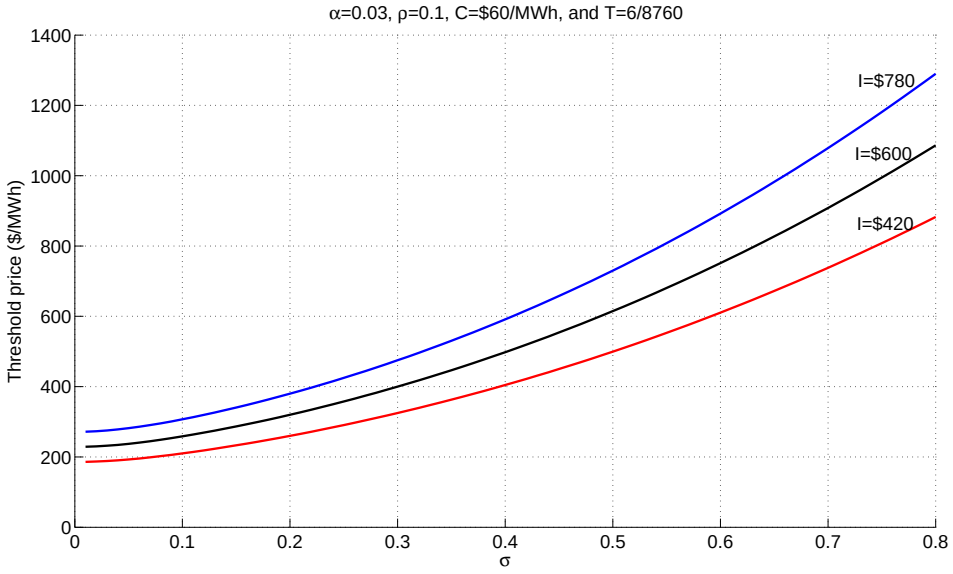

Figure 4.4: Optimal threshold of a single-exercise IL contract - sensitivity to the volatility

the same as what we obtained in Section 4.3.2. In order to calculate the optimal time of the first interruption, however, we have to solve Equation (4.23) when $n = 1$, which is a non-linear function of $P_{\tau_1}^{*(2)}$. From Equation (4.24), we have the conditional expected value of the second interruption:

$$\begin{aligned}\mathbb{E}\left[F_2^{(2)}(P_{\tau_1+T_1+h})|P_{\tau_1} = P_{\tau_1}^{*(2)}\right] = \\ (a_2 e^{\alpha(T_1+h)} P_{\tau_1}^{*(2)} - b_2 C - I_2)\mathbb{P}\left(P_{\tau_1+T_1+h} \geq P_{\tau_2}^{*(2)}|P_{\tau_1} = P_{\tau_1}^{*(2)}\right) + \\ \left(a_2 P_{\tau_2}^{(*)} - b_2 C - I_2\right) e^{\gamma(T_1+h)} \left(\frac{P_{\tau_1}^{*(2)}}{P_{\tau_2}^{*(2)}}\right)^{\beta} \left(1 - \mathbb{P}\left(P_{\tau_1+T_1+h} \geq P_{\tau_2}^{*(2)}|P_{\tau_1} = P_{\tau_1}^{*(2)}\right)\right)\end{aligned} \tag{4.28}$$

Inserting Equation (4.28) into Equation (4.23), we can solve for $P_{\tau_1}^{*(2)}$ numerically. The results, which are graphed in Fig. 4.6 using the data in Table 4.1, reveal that interrupting is not optimal immediately. Moreover, the thresholds of the first ($319.47/MWh) and the second ($320/MWh) interruption are significantly high, such that it is almost impossible to reach them in the near term, and the difference between the thresholds is negligible because the option values of waiting

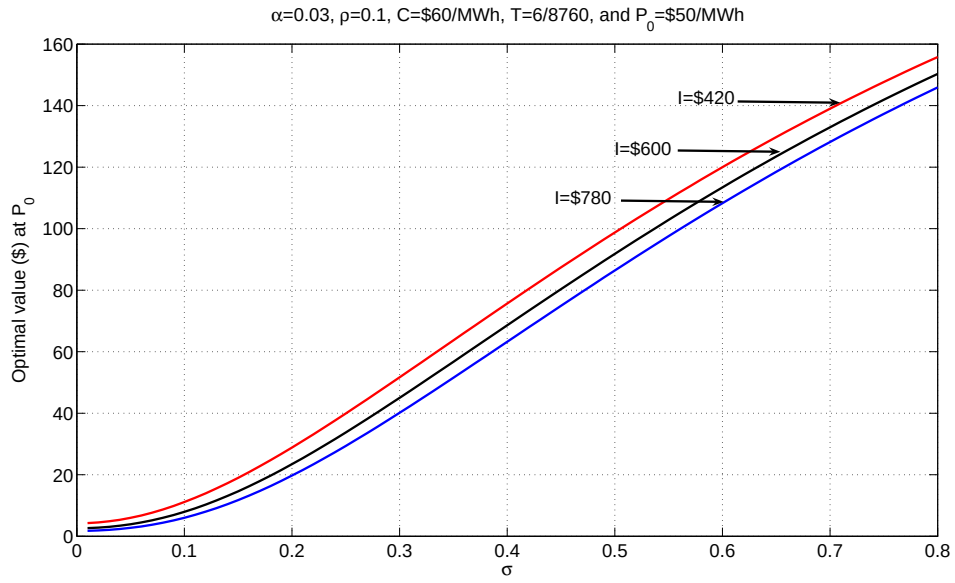

Figure 4.5: Optimal value for a single-exercise IL contract - sensitivity to the volatility

for both interruptions are almost equal. Therefore, in the following sections, we first do a sensitivity analysis by increasing the volatility and the minimum lag between each two interruptions as well as decreasing the retail price of electricity and the capacity payment. The altered data will be then used as the basis for the sensitivity analyses to the volatility, the capacity payment, and the interruption lag.

4.3.4 Multiple-Exercise IL Contract

In this section, we first provide the solutions using the results from Section 4.2.3.2. Then, a comparison with the approximation approach and sensitivity analyses to the volatility of electricity spot price, the capacity payment, and the interruption lag are carried out.

4.3.4.1 Estimations

Using the actual data, Figs. 4.7 and 4.8 reveal that the difference between the thresholds of the first and the last interruption is only $2/MWh and that exercis-

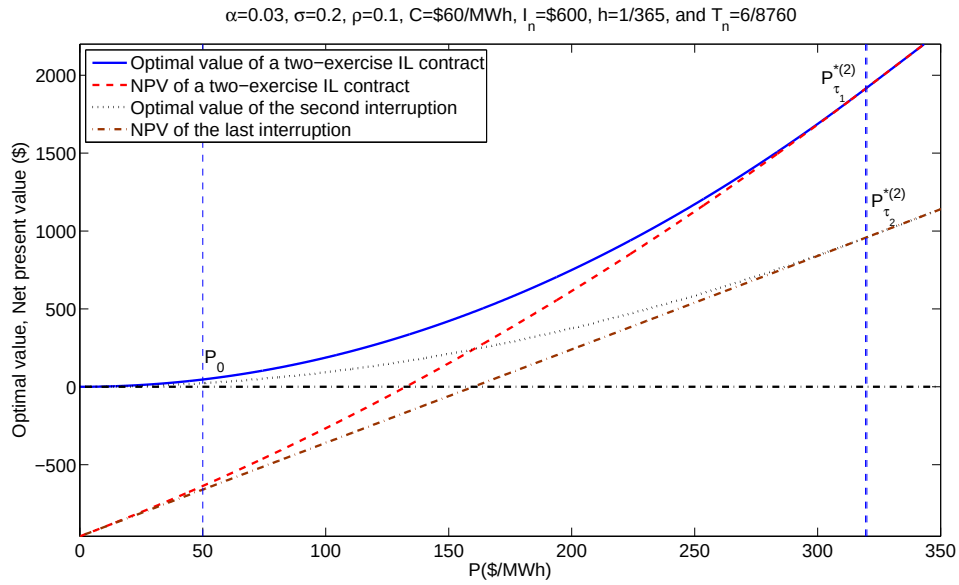

Figure 4.6: NPV and optimal value for a two-exercise IL contract

Table 4.2: Altered data for sensitivity analysis

Parameter	Value
σ	0.40
C (\$/MWh)	55
I_n (\$)	360[a]
h (years)	7/365

[a]Since the LSE has a limitation of one interruption each week, it pays less incentive to its customers, i.e., we assume that $P_{\text{fine}} = \$60/\text{MWh}$.

ing the first interruption is neither optimal nor in-the-money. On the other hand, after altering the data, which are reported in Table 4.2, Fig. 4.7 shows that although the first interruption is exercised at electricity spot price of \$347.91/MWh, the optimal threshold price of interrupting the last interruption is \$357.93/MWh. Interestingly, it can be seen that the optimal thresholds of the first nine interruptions tend to a value just below \$348/MWh, i.e., even by adding more interruptions to this contract the optimal threshold of exercising the first interruption does not lower than \$348/MWh. Fig. 4.9 shows that although the contract is currently in-the-money, it is not optimal to exercise the first interruption immediately, and we need to wait until the price reaches the first threshold.

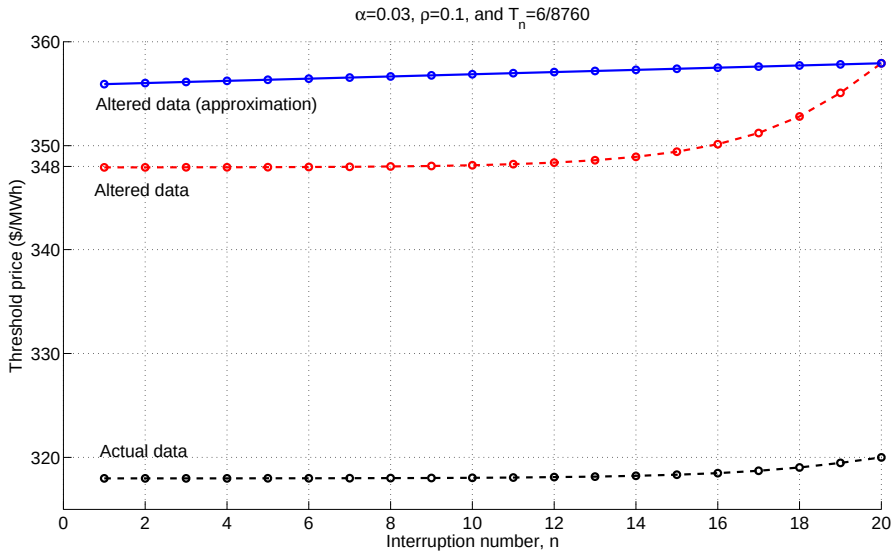

Figure 4.7: Optimal thresholds of a twenty-exercise IL contract for the actual and altered data

4.3.4.2 Comparison with the Approximate Approach

Using the results from Section 4.2.4, approximate optimal thresholds of the twenty interruptions are calculated and graphed in Fig. 4.7. We can see that the approximate thresholds are higher than those calculated in Section 4.3.4.1. A loss of about 1% ($20) in the optimal value of the contract is also observed after applying the approximation approach (Fig. 4.10) because in the approximate IL contract valuation, we use the expected future electricity price rather than the spot price of electricity, which results in a less precise optimal value. The reason for this reduction is also explained mathematically in Appendix N using Jensen's inequality.

4.3.4.3 Sensitivity Analysis to the Volatility (σ)

Reducing (increasing) the volatility, we show that the optimal thresholds significantly decrease (increase); however, the difference between the first and the last threshold becomes smaller (larger) (see Fig. 4.11). As discussed before, in Section 4.3.2, with more uncertainty, the LSE is more likely to wait for new information in the future, such that after exercising the first interruption it is still optimal to

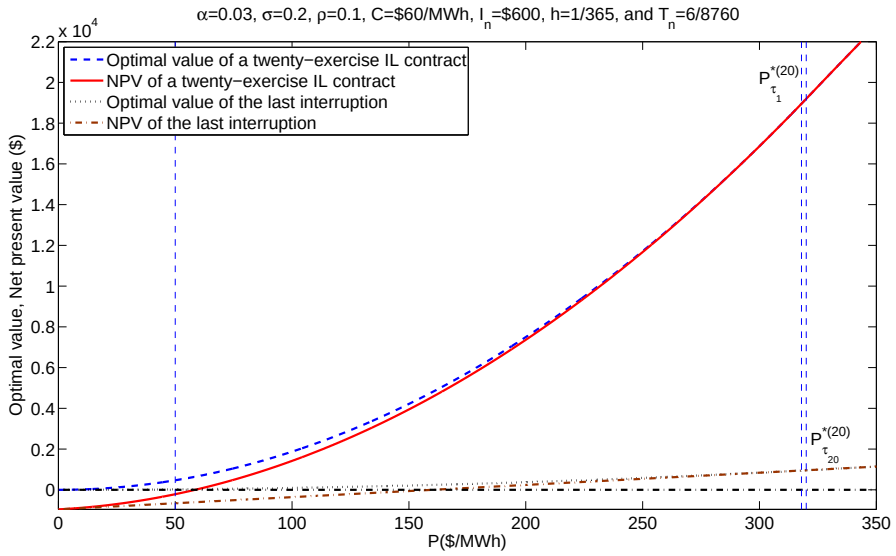

Figure 4.8: NPV and optimal value for a twenty-exercise IL contract for the actual data

wait before exercising the nth, $n = 2, 3, \ldots, N$, interruption. Moreover, any decrease (increase) in the volatility, shifts the thresholds and their approximations evenly down (up). Fig. 4.12 displays that the more the uncertainty, the higher the optimal value of the contract.

Furthermore, in Fig. 4.10, we demonstrate that the percentage loss in optimal value from the approximation approach is also increasing with respect to the volatility because with high uncertainty, the expected future electricity price fails to capture the behaviour of the spot price of electricity. This weakness of the approximation is even more significant when the interruption lag is very high. As a result, the loss from approximation becomes more critical for large interruption lags. In effect, since $\{P_t,\ t \geq 0\}$ follows a GBM process, the total amount of uncertainty is proportional to $\sigma^2(T_n + h)$. Thus, the greater the volatility or the interruption lag, the worse the approximation method.

4.3.4.4 Sensitivity Analysis to the Capacity Payment (I)

As we would expect, Fig. 4.13 shows that a contract with higher capacity payment is less likely to be interrupted. Changes in the capacity payment, however, slightly affect the differences between the thresholds and their approximations, and for

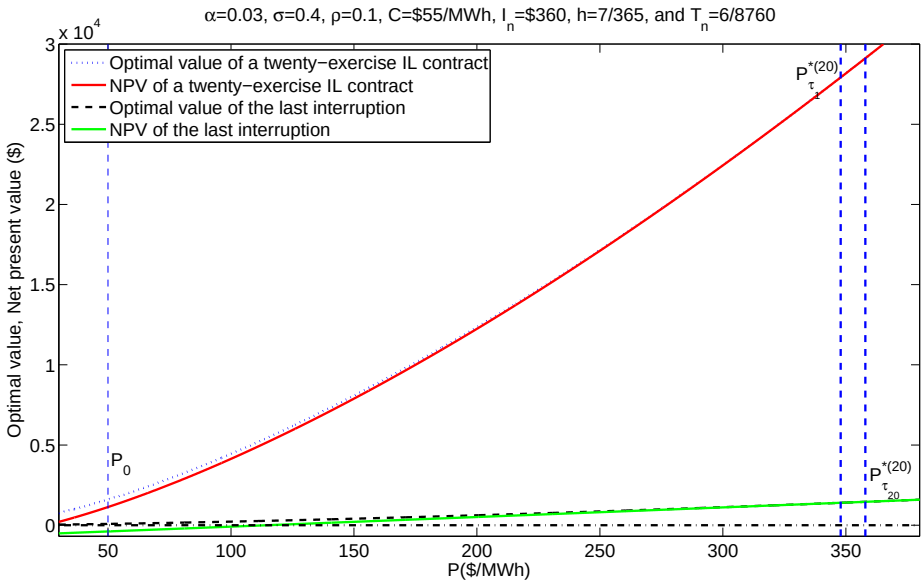

Figure 4.9: NPV and optimal value for a twenty-exercise IL contract for altered data

both approaches, the thresholds shift up/down equivalently. Similarly, Fig. 4.14 reveals that modifications in the capacity payment have no impact on the loss in the optimal value of the contract from approximation because both the optimal value and its approximation decrease equivalently for any increase in the capacity payment (see Fig. 4.15).

4.3.4.5 Sensitivity Analysis to the Interruption Lag (h)

On the other hand, by imposing more restrictions to the contract, i.e., increasing the interruption lag, the contract becomes less valuable (see Fig. 4.16) and is likely to be exercised earlier (see Fig. 4.17). This decrease in the optimal value is, however, more critical when we approximate the value of the contract. Therefore, when the interruption lag is very large, the approximation approach fails to capture accurately the value of the contract; consequently the LSE may lose a substantial amount of money from approximation (see Fig. 4.18). For example, in a situation where only one interruption is allowed per month and the volatility is high, up to 4.5% of the optimal value is lost. In contrast to the impacts of σ and I on moving the thresholds for both approaches almost identically, changes in the

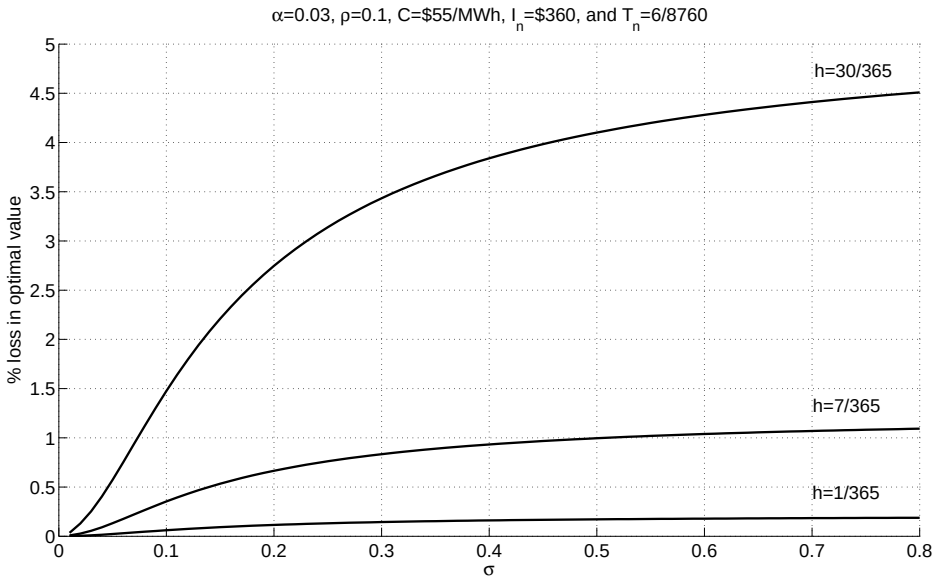

Figure 4.10: Percentage loss in optimal value of a twenty-exercise IL contract from approximation approach when $P_0 = \$50/MWh$ (sensitivity to the volatility)

interruption lag spread the thresholds and their approximations because the last threshold in both approaches is not affected by any changes in the interruption lag (see Fig. 4.17).

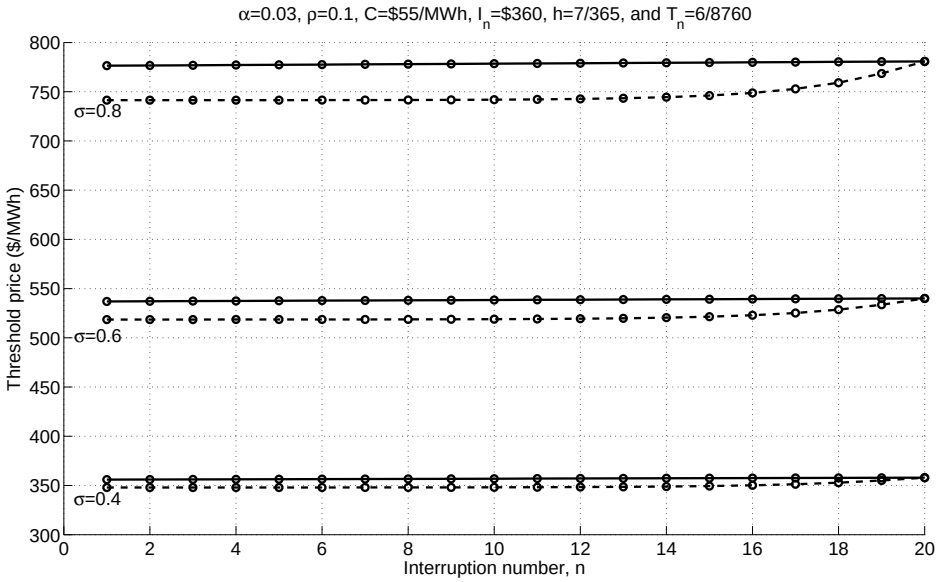

Figure 4.11: Optimal thresholds (dashed curve) and their approximations (solid curve) of a twenty-exercise IL contract for altered data (sensitivity to the volatility)

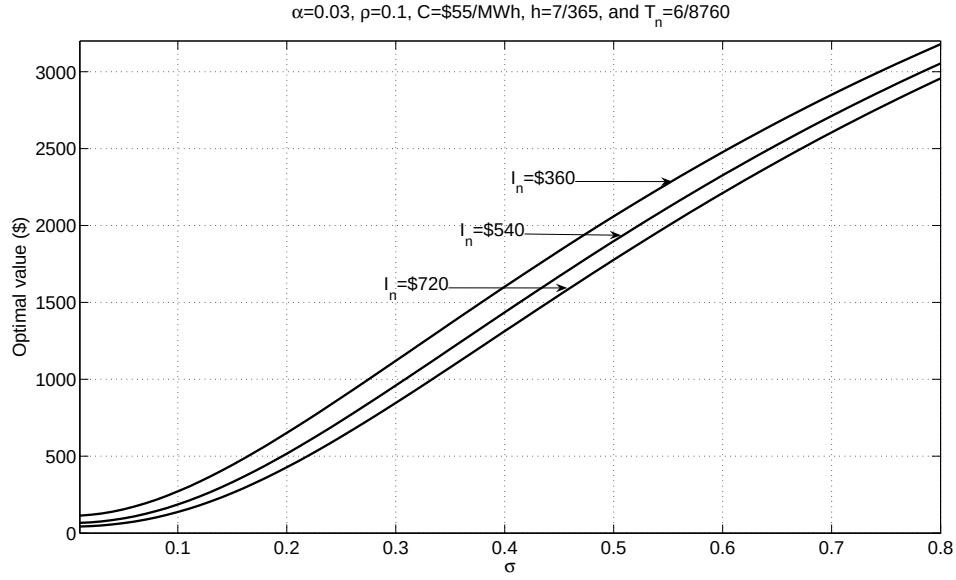

Figure 4.12: Optimal value of a twenty-exercise IL contract when current price is \$50/MWh (sensitivity to the volatility)

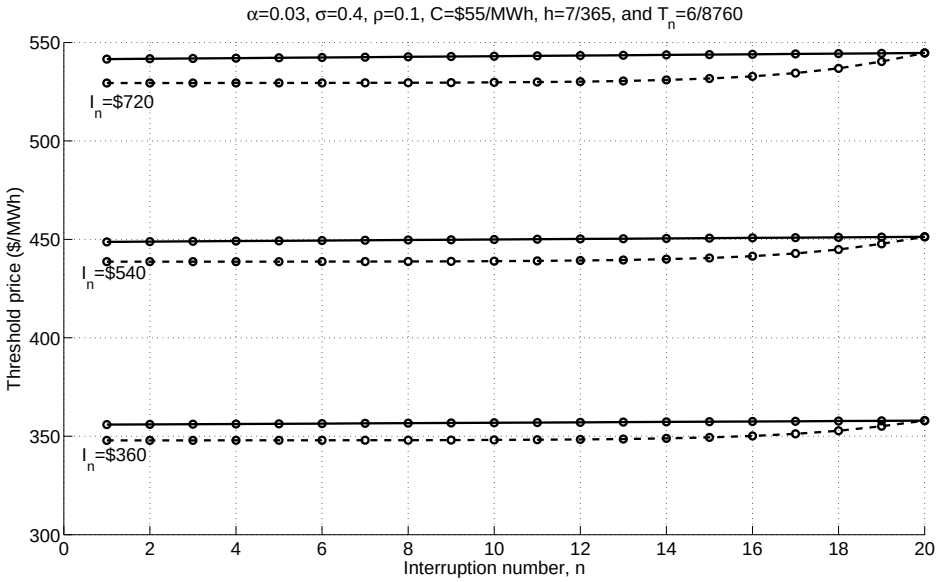

Figure 4.13: Optimal thresholds of a twenty-exercise IL contract (sensitivity to the capacity payment)

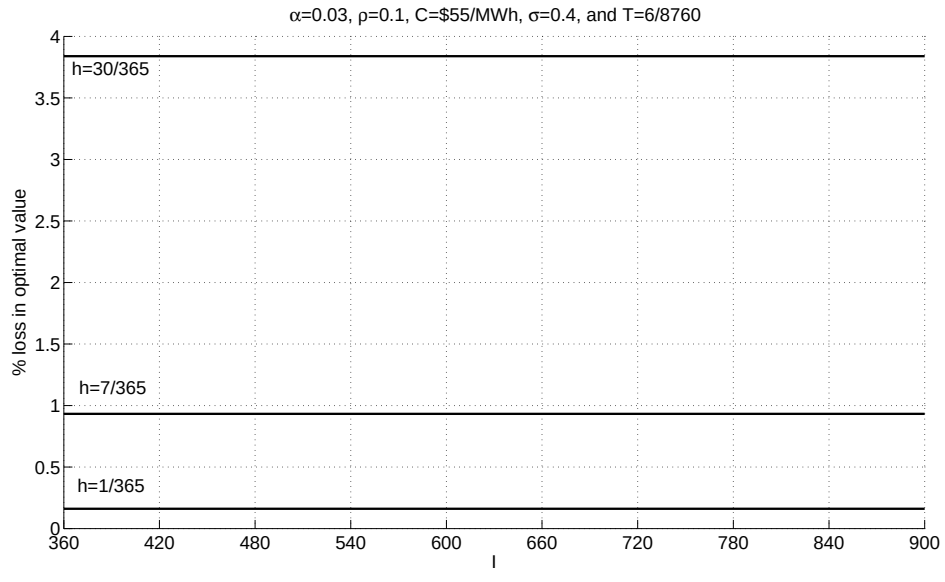

Figure 4.14: Percentage loss in optimal value of a twenty-exercise IL contract from approximation approach when $P_0 = \$50/MWh$ (sensitivity to the capacity payment)

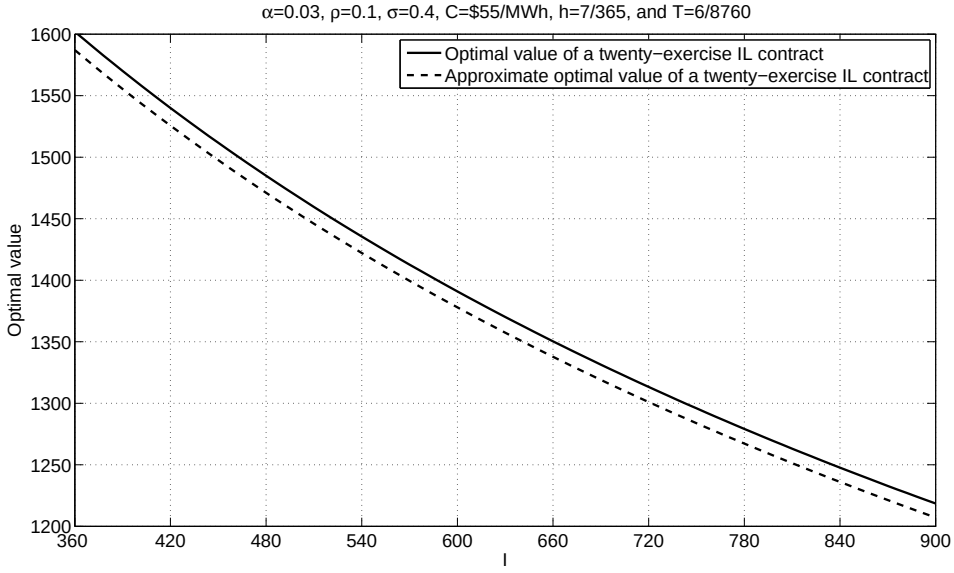

Figure 4.15: Optimal value of a twenty-exercise IL contract and its approximation when $P_0 = \$50/MWh$ (sensitivity to the capacity payment)

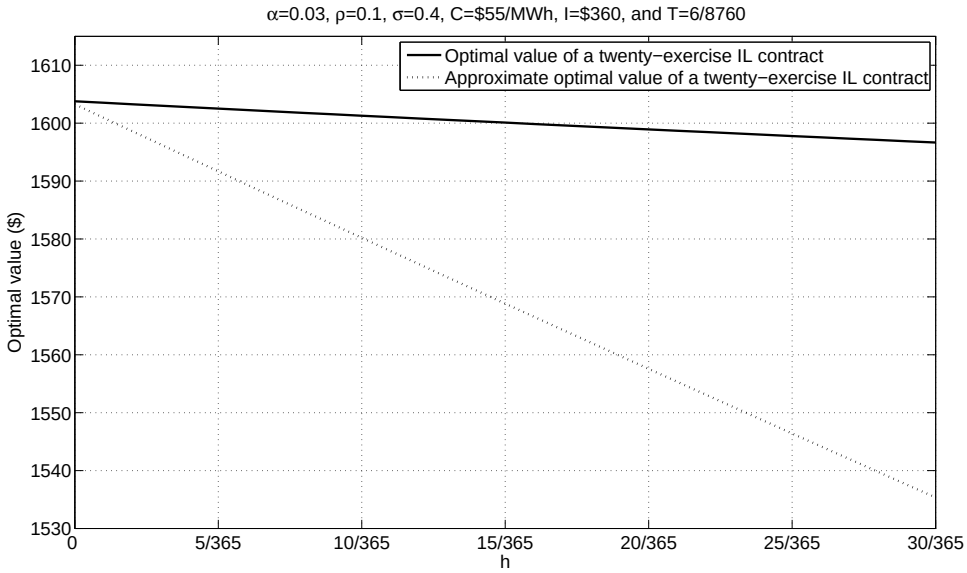

Figure 4.16: Optimal value of a twenty-exercise IL contract and its approximation when $P_0 = \$50/MWh$ (sensitivity to the interruption lag)

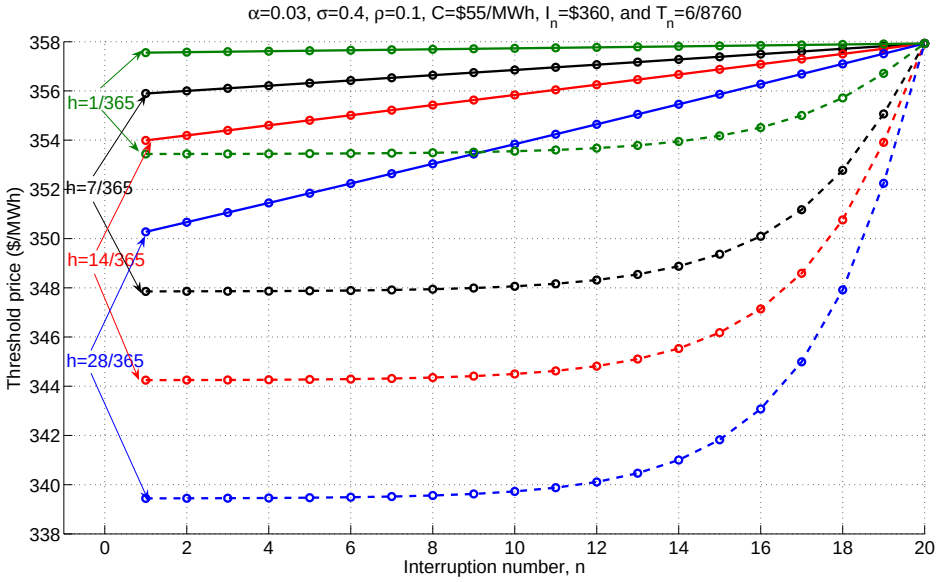

Figure 4.17: Optimal thresholds of a twenty-exercise IL contract (sensitivity to the gap between each two interruptions)

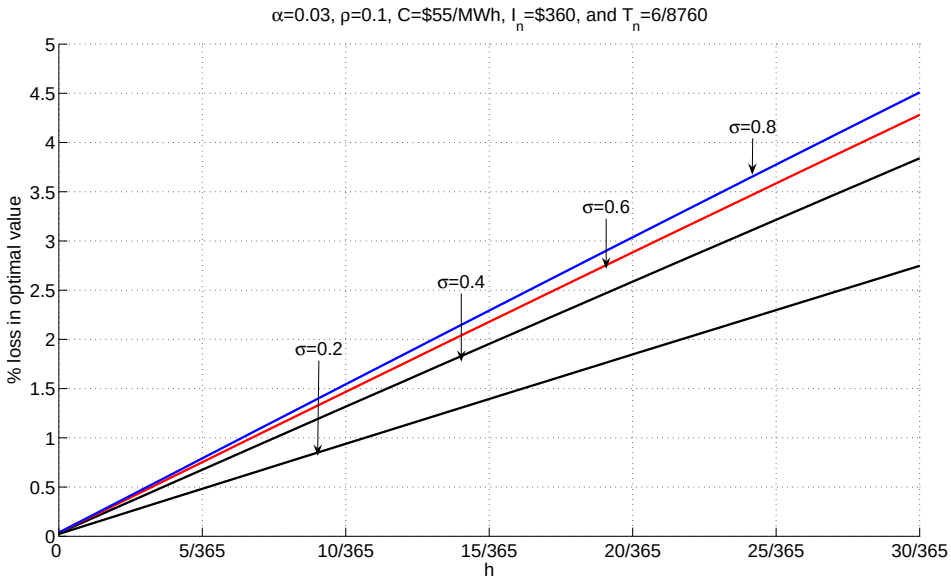

Figure 4.18: Percentage loss in optimal value of a twenty-exercise IL contract from approximation approach when $P_0 = \$50/MWh$ (sensitivity to the lag)

4.4 Conclusions

In order to alleviate financial risk from the deregulation of electricity industry around the world, recent financial instruments for management of supply and demand, such as IL contracts, are of high importance to LSEs. In this chapter, we take the perspective of an LSE that provides electricity to its consumers at a fixed retail rate, while it purchases this electricity from wholesale electricity markets. We first determine the optimal threshold price as well as the optimal value of a single-exercise IL contract. Thereafter, a sequential nested decision-making problem with lags is solved quasi-analytically. We also develop a simple approximate IL contract valuation, which, in many cases, may capture most of the value of the contract.

Using data provided by PG&E and NERC, our numerical examples suggest that for the current spot price of electricity, a twenty-exercise IL contract is neither in-the-money nor optimal to be interrupted immediately. Moreover, the difference between the thresholds of the first and the last interruption is not sig-

nificant because the value of waiting in all interruptions is almost equal. Thus, valuing each interruption separately from others would not have an important impact on the optimal time of interrupting. Nevertheless, we show that with a high volatility and large interruption lags, the difference between the first and the last interruption threshold becomes more distinguished. Greater uncertainty, however, delays the interruption because with more uncertainty, we wait longer in order to receive new information in the future. On the other hand, greater interruption lags reduce the optimal value of the contract, which results in an earlier optimal time of interruption. We also reveal that the deterministic approximation captures most of the value of the multiple-exercise IL contract as long as the volatility is low and the exercise constraints are not too severe.

Chapter 5

Conclusions

After the liberalisation of the electricity industry, market participants have been exposed to financial risks due to uncertain energy prices. Therefore, exploring the behaviour of energy prices, such as highly unexpected spikes and stochastic volatility, and optimal decision-making in energy projects have become main issues in energy economics in many countries. In this thesis, we first provide a comprehensive set of both linear and non-linear multivariate models for electricity and gas prices and carry out a comparison study using UK electricity and gas spot prices to evaluate the forecasting performance of the proposed models in decision-making such as valuing a gas-fired power plant. We, then, pursue a related line of research by taking the perspective of a coal-fired power plant owner that may decide to invest in either FCCS or PCCS retrofits given uncertain electricity, CO_2, and coal prices, and develop an analytical real options model that values the choice between the two technologies. Finally, we extend the use of real options to an operational decision-making problem. We value a multiple-exercise IL contract that allows an LSE to curtail electricity provision to a representative consumer multiple times for a specified duration at a defined capacity payment given uncertain wholesale electricity price from the viewpoint of the LSE. Here, we will summarise the results of this thesis, discuss its limitations, and offer directions for future research.

5.1 Modelling Electricity and Gas Prices

In Chapter 2, using UK electricity and natural gas daily spot prices, we show that the mean-reverting model for both logarithms of electricity and gas not only is the best-fit linear model, but also has the best out-of-sample forecasting performance. It is, however, not able to capture the high-value sudden spikes of energy prices. Therefore, Markov regime-switching approaches and a mean-reverting stochastic model are posited to improve upon this linear model. We then take the viewpoint of an investor in a gas-fired power plant with operational flexibility in order to compare the ability of linear and non-linear models in valuing the power plant over the out-of-sample period. The study suggests that although the linear model provides out-of-sample forecasts with the lowest ERMSE, the non-linear models with stochastic volatility for logarithms of electricity prices perform better than both the linear and the regime-switching models in terms of valuing a gas-fired power plant. On the other hand, since the volatility of gas prices does not seem to be stochastic, the model MRSV1 is chosen as the best model among both the linear and non-linear models.

In this study, our data set is restricted to average daily spot prices, which may result in losing the intra-day variation in price behaviour, e.g., the short-duration spikes may actually occur in half-hourly prices rather than in daily ones. Analysing the intra-day data, as in Karakatsani & Bunn (2008), would be a sensible resolution to any possible misleading references resulted from this feature. Moreover, a non-linear regime-switching model with time-varying parameters, a study similar to Mount *et al.* (2005), may improve the weakness of regime-switching models in capturing high-value spikes of electricity prices. It would also be interesting if the proposed models in this study could be replicated in other countries as well as for other commodity prices to see whether they would produce similar results. Finally, since in a CO_2-constrained environment, a gas-fired power plant has to purchase permits for its CO_2 emissions, further research regarding the role of stochastic CO_2 emissions permit prices as another source of cost, affecting the value of the power plant, would be of great help.

5.2 Carbon Capture and Sequestration Technology

From the viewpoint of a coal-fired power plant that has to decide whether to invest, now or any time in the future, in FCCS and PCCS technologies separately, in Chapter 3, using current market data, we show that investing in any CCS technology is not economically advisable in the near term. Then, supposing that the plant owner has to decide between investing in either FCCS or PCCS technology simultaneously, we introduce the required conditions under which the investment region becomes dichotomous. Regarding these conditions, we propose an enhanced PCCS technology that leads us to value a postponing area where we wait before investing in either technology. Unlike our analytical solution to the separate valuation, this mutually exclusive option value is solved quasi-analytically because it depends on more than one stochastic variable. Our numerical examples show that greater uncertainty delays the investment and makes the investment option more valuable. However, the correlation between the two prices has an opposite impact on the optimal boundaries, such that high positive correlation between prices makes the waiting area narrower.

Although GBM processes are commonly assumed to be good models for energy prices, as examined, e.g., in Pindyck (1999), they may not be suitable for CO_2 permit prices. Moreover, using alternative stochastic processes for energy prices, such as mean-reverting models, as in Abadie & Chamarro (2008a), may result in different outcomes. Considering other possible options, such as the option to suspend the CCS unit to allow venting or the option of switching from one technology to another, may also affect the option value. Finally, a complete model that accounts for the limited lifetime of the equipment, the time-to-build problem, or the market competition such as in Paxson & Pinto (2005), would be better able to capture the sequential decision-making challenges faced by a power plant. The methods in this study can be extended to any similar utilities faced with investing in alternative opportunities under uncertainty.

5.3 Multiple-Exercise Interruptible Load Contract

In Chapter 4, we take the perspective of an LSE that provides electricity to its consumers at a fixed retail rate, while it purchases this electricity from wholesale electricity markets. Given uncertainty in wholesale electricity spot price, we solve a sequential nested decision-making problem with lags quasi-analytically and develop a simple approximate IL contract valuation, which is much easier to calculate and, in many cases, may capture most of the value of the contract. Using the data provided by PG&E and NERC, we show that at the current spot price of electricity, a twenty-exercise IL contract is not optimal to be interrupted immediately and that with a high volatility and large interruption lags, the difference between the first and the last interruption threshold becomes more distinguished. Greater uncertainty, however, delays the interruption because with more uncertainty, we wait longer in order to receive new information in the future. On the other hand, greater interruption lags reduce the optimal value of the contract, which results in an earlier optimal time of interruption. Finally, we reveal that the deterministic approximation can be used instead of the exact valuation when the volatility is low and the exercise constraints are not too severe.

The assumption of a GBM process for the spot price of electricity would be either improved, e.g., by including jumps or spikes in the process, or replaced by alternative stochastic processes, such as a mean-reverting model. Moreover, a complete model that takes into account a fixed-term contract would be better able to capture the value of the contract. This would, however, require a solution approach based on finite differences. In such a contract, the interruptions are likely to be exercised at lower price thresholds closer to the end of the contract. Other possible options may also affect the optimal value of the contract, e.g., cancellation of the interruption once initiated would increase the value of the contract, while advance notification as in Kamat & Oren (2001), may be in favour of the consumer rather than the retailer.

Appendix A

Seasonality Function: Estimation

Table A.1: Estimations of the coefficients of weekly seasonality

j	$\gamma_{1j}^{(E)}$	$\gamma_{1j}^{*(E)}$	$\gamma_{1j}^{(G)}$	$\gamma_{1j}^{*(G)}$
1	-0.0114	0.1118	0.0078	0.0714
2	0.0236	0.0197	0.0155	-0.0003
3	0.0170	0.0178	0.0000	0.0043

Table A.2: Estimations of the coefficients of yearly seasonality

j	$\gamma_{2j}^{(E)}$	$\gamma_{2}^{*(E)}$	$\gamma_{2j}^{(G)}$	$\gamma_{2j}^{*(G)}$	j	$\gamma_{2j}^{(E)}$	$\gamma_{2}^{*(E)}$	$\gamma_{2j}^{(G)}$	$\gamma_{2j}^{*(G)}$
1	0.0049	-0.1238	0.0703	-0.2608	91	0.0038	0.0030	0.0047	-0.0071
2	-0.0479	0.0210	-0.0664	0.0624	92	-0.0145	0.0010	-0.0099	0.0021
3	0.0241	0.0085	0.0172	0.0044	93	0.0037	0.0040	0.0002	0.0043
4	-0.0265	-0.0009	-0.0165	-0.0114	94	0.0004	0.0030	0.0025	0.0037
5	0.0004	-0.0133	0.0107	0.0056	95	0.0013	-0.0052	0.0076	0.0000
6	-0.0046	-0.0179	-0.0413	0.0006	96	0.0027	0.0038	0.0016	-0.0055
7	0.0116	-0.0010	0.0209	-0.0110	97	0.0045	0.0050	-0.0003	0.0033
8	-0.0179	0.0115	-0.0241	0.0065	98	0.0025	-0.0046	-0.0063	-0.0038
9	-0.0126	0.0108	-0.0151	0.0082	99	-0.0069	0.0054	0.0005	0.0046
10	0.0003	-0.0086	0.0142	-0.0036	100	0.0026	0.0008	-0.0016	-0.0014
11	-0.0122	0.0066	-0.0104	0.0036	101	-0.0018	0.0025	0.0017	-0.0025
12	-0.0273	-0.0220	-0.0184	-0.0095	102	0.0005	-0.0092	0.0024	-0.0010
13	0.0087	0.0094	-0.0019	0.0215	103	0.0058	0.0009	0.0061	0.0054
14	0.0219	0.0211	0.0297	0.0061	104	-0.0024	0.0096	-0.0022	-0.0074
15	-0.0097	-0.0367	-0.0282	-0.0363	105	-0.0019	-0.0089	-0.0034	-0.0046
16	-0.0230	-0.0011	-0.0131	-0.0098	106	-0.0012	-0.0052	-0.0019	0.0065
17	-0.0191	0.0205	-0.0270	0.0145	107	-0.0085	0.0061	0.0003	0.0054
18	-0.0075	0.0040	0.0227	0.0001	108	-0.0025	-0.0062	-0.0016	-0.0051
19	0.0264	0.0007	0.0189	-0.0140	109	0.0047	-0.0036	0.0073	-0.0005
20	0.0088	0.0027	0.0005	0.0030	110	0.0010	0.0075	-0.0009	-0.0077
21	0.0052	-0.0107	-0.0047	0.0005	111	0.0022	-0.0086	-0.0022	0.0008
22	0.0021	0.0001	0.0193	0.0058	112	0.0006	0.0002	-0.0050	0.0023
23	0.0024	-0.0019	-0.0177	-0.0084	113	-0.0029	0.0007	-0.0069	-0.0003
24	0.0096	0.0091	0.0167	-0.0058	114	0.0040	0.0079	-0.0002	0.0063
25	-0.0116	0.0032	-0.0110	0.0090	115	-0.0027	-0.0036	0.0019	0.0046
26	-0.0024	-0.0080	0.0024	0.0149	116	0.0052	-0.0012	-0.0011	-0.0068
27	0.0128	0.0009	0.0203	-0.0169	117	-0.0036	0.0026	0.0013	-0.0001
28	0.0004	-0.0112	0.0116	0.0000	118	0.0043	-0.0014	0.0006	0.0032
29	0.0059	0.0033	-0.0006	0.0079	119	0.0100	0.0024	0.0003	-0.0002
30	0.0090	-0.0005	0.0207	0.0054	120	0.0009	0.0024	-0.0039	0.0023
31	0.0012	-0.0093	-0.0037	-0.0062	121	-0.0054	-0.0040	0.0004	-0.0053
32	-0.0069	0.0034	0.0015	0.0079	122	0.0023	-0.0012	0.0021	0.0000
33	-0.0097	0.0040	-0.0148	-0.0074	123	-0.0037	-0.0052	-0.0049	-0.0007
34	0.0145	-0.0100	0.0171	-0.0054	124	-0.0007	-0.0054	-0.0007	0.0018
35	-0.0035	-0.0172	-0.0073	0.0023	125	0.0016	0.0005	-0.0014	-0.0012
36	-0.0293	-0.0010	-0.0267	0.0091	126	-0.0136	0.0024	0.0034	0.0007
37	0.0069	0.0103	0.0055	0.0041	127	0.0060	-0.0035	-0.0052	0.0038
38	0.0040	-0.0008	-0.0006	0.0100	128	-0.0064	-0.0015	0.0020	0.0051
39	0.0012	-0.0102	0.0099	-0.0096	129	-0.0067	-0.0021	-0.0048	-0.0029
40	-0.0087	0.0129	-0.0079	-0.0098	130	-0.0018	-0.0034	-0.0022	-0.0074
41	-0.0147	0.0007	-0.0038	-0.0006	131	-0.0001	0.0052	-0.0017	0.0012
42	-0.0032	-0.0109	-0.0014	0.0037	132	0.0002	-0.0021	-0.0043	0.0008
43	0.0011	0.0037	0.0077	-0.0004	133	-0.0007	0.0035	0.0058	0.0035
44	-0.0050	0.0041	0.0013	0.0010	134	0.0003	-0.0031	0.0039	0.0024
45	0.0061	-0.0006	0.0057	0.0054	135	0.0028	-0.0035	-0.0028	-0.0030

Table A.3: Estimations of the coefficients of yearly seasonality (continued)

j	$\gamma_{2j}^{(E)}$	$\gamma_{2}^{*(E)}$	$\gamma_{2j}^{(G)}$	$\gamma_{2j}^{*(G)}$	j	$\gamma_{2j}^{(E)}$	$\gamma_{2}^{*(E)}$	$\gamma_{2j}^{(G)}$	$\gamma_{2j}^{*(G)}$
46	0.0040	-0.0005	-0.0023	-0.0049	136	-0.0034	0.0062	-0.0024	0.0018
47	-0.0017	-0.0045	-0.0020	-0.0075	137	-0.0018	-0.0008	-0.0061	0.0042
48	-0.0090	0.0027	0.0019	-0.0035	138	-0.0017	-0.0007	-0.0024	0.0006
49	0.0123	-0.0093	-0.0013	0.0025	139	0.0035	0.0008	0.0032	-0.0072
50	0.0028	0.0012	0.0020	0.0062	140	0.0055	-0.0042	0.0009	0.0013
51	-0.0106	-0.0171	-0.0038	-0.0064	141	-0.0043	0.0025	-0.0057	-0.0048
52	-0.0346	-0.0166	-0.0169	0.0156	142	-0.0013	-0.0020	0.0065	-0.0007
53	-0.0021	0.0184	-0.0090	0.0022	143	0.0022	-0.0006	-0.0046	0.0011
54	0.0010	0.0005	-0.0009	-0.0105	144	0.0006	0.0035	-0.0039	0.0043
55	-0.0001	-0.0175	0.0040	-0.0014	145	-0.0060	-0.0037	-0.0017	-0.0004
56	-0.0030	-0.0023	0.0012	-0.0019	146	0.0055	0.0004	0.0000	-0.0006
57	-0.0122	-0.0012	-0.0019	0.0068	147	0.0059	-0.0026	-0.0019	-0.0020
58	0.0122	-0.0075	0.0110	0.0010	148	-0.0011	-0.0031	0.0015	0.0003
59	0.0057	0.0006	0.0011	-0.0016	149	0.0040	0.0078	0.0020	0.0050
60	-0.0116	0.0013	-0.0009	-0.0010	150	-0.0006	-0.0055	0.0030	-0.0015
61	0.0110	0.0210	0.0072	0.0083	151	-0.0009	0.0051	0.0009	-0.0034
62	0.0026	-0.0042	0.0008	-0.0020	152	0.0039	-0.0028	-0.0030	0.0001
63	0.0009	0.0019	0.0011	0.0025	153	-0.0003	0.0020	0.0011	0.0021
64	-0.0031	0.0020	-0.0048	-0.0061	154	0.0082	0.0020	0.0022	0.0001
65	-0.0082	-0.0030	0.0067	0.0055	155	-0.0041	-0.0090	-0.0045	-0.0021
66	0.0163	0.0050	0.0038	-0.0012	156	-0.0063	0.0061	-0.0046	0.0031
67	0.0084	0.0099	-0.0081	0.0000	157	-0.0015	0.0167	0.0024	0.0068
68	-0.0028	-0.0162	-0.0022	0.0002	158	0.0048	-0.0032	0.0014	0.0009
69	-0.0068	-0.0005	-0.0058	0.0130	159	0.0037	-0.0040	0.0027	0.0004
70	0.0000	0.0055	-0.0046	-0.0096	160	-0.0037	0.0032	0.0010	-0.0050
71	0.0084	0.0003	0.0036	0.0070	161	0.0032	-0.0086	-0.0038	-0.0033
72	0.0014	-0.0054	-0.0030	-0.0010	162	-0.0053	0.0028	0.0008	0.0016
73	-0.0034	-0.0035	-0.0001	0.0002	163	0.0052	-0.0002	0.0030	-0.0003
74	0.0076	-0.0029	0.0075	0.0015	164	0.0020	-0.0050	-0.0049	0.0016
75	0.0093	0.0003	-0.0014	0.0048	165	-0.0017	0.0049	-0.0015	-0.0018
76	-0.0023	-0.0075	-0.0053	-0.0058	166	0.0052	0.0027	0.0028	0.0014
77	-0.0069	-0.0020	0.0032	0.0013	167	0.0034	0.0048	0.0016	0.0012
78	-0.0033	0.0020	-0.0045	-0.0019	168	-0.0021	-0.0068	-0.0020	-0.0031
79	0.0014	-0.0022	-0.0023	0.0083	169	0.0023	-0.0073	-0.0018	-0.0012
80	-0.0021	-0.0015	0.0100	0.0065	170	-0.0034	0.0087	-0.0032	0.0029
81	-0.0086	-0.0023	-0.0076	-0.0019	171	-0.0046	-0.0034	0.0047	0.0010
82	0.0040	-0.0066	0.0016	-0.0065	172	0.0032	0.0021	-0.0007	0.0051
83	-0.0051	0.0042	-0.0016	-0.0001	173	-0.0009	0.0008	-0.0016	0.0009
84	0.0020	0.0041	-0.0104	0.0061	174	-0.0022	-0.0063	0.0038	-0.0035
85	-0.0071	0.0015	-0.0055	0.0027	175	-0.0033	0.0002	-0.0047	0.0033
86	-0.0040	-0.0057	0.0020	0.0030	176	-0.0002	-0.0044	-0.0005	-0.0011
87	0.0078	-0.0032	0.0004	0.0023	177	0.0020	0.0029	0.0007	0.0002
88	-0.0091	0.0077	-0.0034	0.0017	178	-0.0046	0.0098	0.0007	-0.0021
89	-0.0046	-0.0091	0.0056	0.0058	179	0.0010	-0.0047	0.0016	0.0031
90	0.0114	0.0016	-0.0005	-0.0052	180	0.0024	0.0058	0.0004	-0.0030

Appendix B

Standard Errors

Table B.1: Standard errors of estimated parameters reported in Table 2.2

Parameters		Model (1)	Model (2)	Model (3)	Model (4)
Electricity	σ_E	0.24	0.28	0.04	0.04
	μ_E		1.48	0.52	0.52
	κ_E	7.63			
	$\lambda_E\kappa_E$	21.53			
	$\rho\sigma_E\sigma_G$	0.15	0.16	0.03	0.05
Gas	σ_G	0.17	0.17	0.06	0.17
	μ_G			0.69	
	κ_G	4.68	4.67		4.67
	$\lambda_G\kappa_G$	8.43	8.41		8.41

Appendix C

Diagnostic Tests

In order to verify essential properties of the residuals, i.e., uncorrelated random variables with constant mean zero and constant variance, the quantile-quantile plot of the standardised residuals and also the residuals versus the order of observations are graphed in Figures C.1 and C.2, which indicate that the residuals are approximately normal with mean of zero and a roughly constant variance. Moreover, the chi-square goodness-of-fit tests of the standardised residuals against the standard normal distribution reported in Table C.1 are consistent with the normality of residuals.

Table C.1: Chi-square goodness-of-fit test

		Model (1)	Model (2)	Model (3)	Model (4)
Electricity	$\mathcal{X}^2$ [a]	35.5860	45.1298	47.3199	46.5964
	df [b]	36	36	36	36
	p [c]	0.4881	0.1415	0.0982	0.1111
Gas	$\mathcal{X}^2$ [a]	49.4747	50.1140	47.8951	49.9333
	df [b]	35	35	34	35
	p [c]	0.0533	0.0470	0.0574	0.0487

[a] Chi-square statistic

[b] Degrees of freedom = total number of cells - 3, cells with expected counts less than 5 are pooled to neighbouring cells

[c] Almost all p values are greater than 0.05 which means that the null hypothesis of having normal residuals can not be rejected

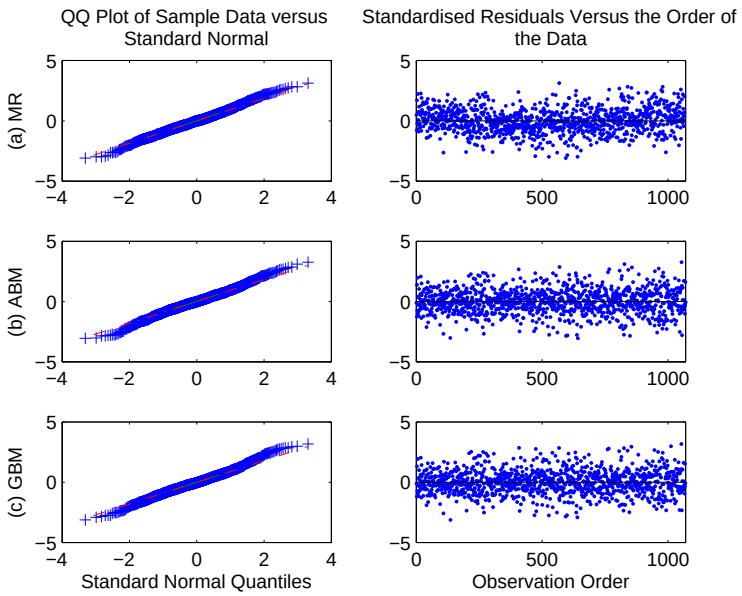

Figure C.1: Standardised residuals of logarithms of electricity prices

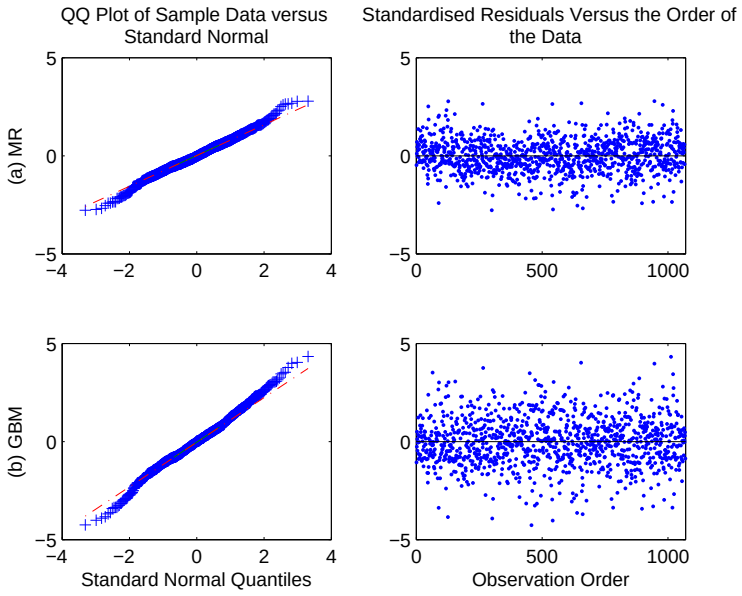

Figure C.2: Standardised residuals of logarithms of gas prices

Appendix D

Hamilton Filter

Here, we discuss the Hamilton-filter algorithm for a particular multivariate time series, Equation 2.18, where the second term on the right-hand side of this equation follows an AR(1) process with normally distributed innovations as

$$\begin{bmatrix} Z_t^{E(S_t)} \\ Z_t^{G(S_t)} \end{bmatrix} = \begin{bmatrix} \phi_E^{(S_t)} Z_{t-1}^{E(S_{t-1})} \\ \phi_G^{(S_t)} Z_{t-1}^{G(S_{t-1})} \end{bmatrix} + \mathbf{W}_t^{(S_t)} \tag{D.1}$$

where $\mathbf{W}_t$, conditional on information available at time t, is multivariate normally distributed with zero mean and the covariance matrix of $\Sigma^{(S_t)}$,

$$\Sigma^{(S_t)} = \begin{bmatrix} \sigma_E^{2(S_t)}\Delta t & \sigma_E^{(S_t)}\sigma_G^{(S_t)}\rho\Delta t \\ \sigma_E^{(S_t)}\sigma_G^{(S_t)}\rho\Delta t & \sigma_G^{2(S_t)}\Delta t \end{bmatrix} \tag{D.2}$$

which is dependent on the regime state.

In order to apply the Hamilton filter, we need to combine Equations 2.18 and D.1 into a single equation:

$$\mathbf{Y}_t = \begin{bmatrix} \alpha_E^{(S_t)} \\ \alpha_G^{(S_t)} \end{bmatrix} + \begin{bmatrix} \phi_E^{(S_t)} & 0 \\ 0 & \phi_G^{(S_t)} \end{bmatrix} (\mathbf{Y}_{t-1} - \begin{bmatrix} \alpha_E^{(S_{t-1})} \\ \alpha_G^{(S_{t-1})} \end{bmatrix}) + \mathbf{W}_t^{(S_t)}, \tag{D.3}$$

where

$$\mathbf{Y}_t = \begin{bmatrix} X_t^{E(S_t)} \\ X_t^{G(S_t)} \end{bmatrix} \tag{D.4}$$

Hence, $\mathbf{Y}_t$, given $\{S_t = s_t, S_{t-1} = s_{t-1}, \mathbf{Y}_{t-1} = \mathbf{y}_{t-1}\}$, is multivariate normally distributed with the probability density function

$$\begin{aligned} &f(\mathbf{Y}_t | S_t = s_t, S_{t-1} = s_{t-1}, \mathbf{Y}_{t-1} = \mathbf{y}_{t-1}) \\ &\quad = \tfrac{1}{2\pi|\Sigma^{(s_t)}|} exp(\tfrac{-1}{2}(\mathbf{Y}_t - \mu_t)' {\Sigma^{(s_t)}}^{-2} (\mathbf{Y}_t - \mu_t)) \end{aligned} \tag{D.5}$$

where,

$$\mu_t = \begin{bmatrix} \alpha_E^{(s_t)} \\ \alpha_G^{(s_t)} \end{bmatrix} + \begin{bmatrix} \phi_E^{(s_t)} & 0 \\ 0 & \phi_G^{(s_t)} \end{bmatrix} \left(\mathbf{Y}_{t-1} - \begin{bmatrix} \alpha_E^{(s_{t-1})} \\ \alpha_G^{(s_{t-1})} \end{bmatrix} \right) \tag{D.6}$$

and $\Sigma^{(S_t)}$ is defined in Equation D.2.

Lemma 1 Using graph theory, we show that S_t is independent of $\{\mathbf{Y}_{t-1}, \ldots, \mathbf{Y}_0\}$ given S_{t-1}, i.e., $S_t \perp \{\mathbf{Y}_{t-1}, \ldots, \mathbf{Y}_0\} | S_{t-1}$.

To make it easy, assume that $t = 2$; the result will be extended for each $t > 2$. The directed acyclic graph (DAG) of this relationship is represented as:

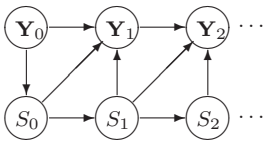

To determine the accuracy of $S_2 \perp \{\mathbf{Y}_1, \mathbf{Y}_0\} | S_1$, after dropping all nodes that are neither included in $(S_1, S_2, \mathbf{Y}_0, \mathbf{Y}_1)$ nor ancestors[1] of nodes in $(S_1, S_2, \mathbf{Y}_0, \mathbf{Y}_1)$, we convert the remaining DAG to a conditional independence graph:

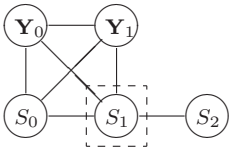

Using the global Markov property, since S_1 blocks all paths between S_2 and $\{\mathbf{Y}_1, \mathbf{Y}_0\}$, we can claim that $S_2 \perp \{\mathbf{Y}_1, \mathbf{Y}_0\} | S_1$.

[1] Ancestors of a node are all the upstream nodes (i.e., we can get from ancestors to the node by following the arrows).

We must now calculate the conditional log likelihood function, $l(\Theta)$, and then maximise it with respect to the unknown parameters, Θ.

$$l(\Theta) = log(f(\mathbf{Y}_T, \ldots, \mathbf{Y}_1 | \mathbf{Y}_0, \Theta)), \tag{D.7}$$

where $\Theta = \{p, q, \alpha_E^{(0)}, \alpha_E^{(1)}, \alpha_G^{(0)}, \alpha_G^{(1)}, \phi_E^{(0)}, \phi_E^{(1)}, \phi_G^{(0)}, \phi_G^{(1)}, \sigma_E^{(0)}, \sigma_E^{(1)}, \sigma_G^{(0)}, \sigma_G^{(1)}, \rho\}$.

Although calculating the maximum likelihood estimates of these large numbers of unknown parameters is analytically impossible, we may find them numerically. We can rewrite the conditional log likelihood function $l(\Theta)$ as

$$\begin{aligned} l(\Theta) &= log(f(\mathbf{Y}_T, \ldots, \mathbf{Y}_1 | \mathbf{Y}_0, \Theta)) = \textstyle\sum_{t=1}^{T} log(f(\mathbf{Y}_t | \mathbf{Y}_{t-1}, \ldots, \mathbf{Y}_0)) \\ &= \textstyle\sum_{t=1}^{T} log \sum_{s_t=0}^{1} \sum_{s_{t-1}=0}^{1} f(\mathbf{Y}_t, S_t = s_t, S_{t-1} = s_{t-1} | \mathbf{Y}_{t-1}, \ldots, \mathbf{Y}_0) \\ &= \textstyle\sum_{t=1}^{T} log \sum_{s_t=0}^{1} \sum_{s_{t-1}=0}^{1} f(\mathbf{Y}_t | S_t = s_t, S_{t-1} = s_{t-1}, \mathbf{Y}_{t-1}, \ldots, \mathbf{Y}_0) \\ &\quad \times Prob[S_t = s_t, S_{t-1} = s_{t-1} | \mathbf{Y}_{t-1}, \ldots, \mathbf{Y}_0] \end{aligned} \tag{D.8}$$

where,

$$\begin{aligned} &Prob[S_t = s_t, S_{t-1} = s_{t-1} | \mathbf{Y}_{t-1}, \ldots, \mathbf{Y}_0] \\ &= Prob[S_t = s_t | S_{t-1} = s_{t-1}, \mathbf{Y}_{t-1}, \ldots, \mathbf{Y}_0] \times Prob[S_{t-1} = s_{t-1} | \mathbf{Y}_{t-1}, \ldots, \mathbf{Y}_0] \\ &= Prob[S_t = s_t | S_{t-1} = s_{t-1}] \quad \text{(Using Lemma 1)} \\ &\quad \times \textstyle\sum_{s_{t-2}=0}^{1} Prob[S_{t-1} = s_{t-1}, S_{t-2} = s_{t-2} | \mathbf{Y}_{t-1}, \ldots, \mathbf{Y}_0] \end{aligned} \tag{D.9}$$

is a recursive equation, which can be calculated for all t (from 2 to T), with the initial values of $Prob[S_1 = s_1, S_0 = s_0 | \mathbf{Y}_0]$ (for $s_1, s_2 = 0, 1$), which is simply computable via the following equations together with the initial assumption of

$\Pi_0 = Prob[S_0 = 1|\mathbf{Y}_0]$.

$$\begin{aligned} Prob[S_t = 0, S_{t-1} = 0] &= p(1 - \Pi_0), \\ Prob[S_t = 1, S_{t-1} = 0] &= (1 - p)(1 - \Pi_0), \\ Prob[S_t = 1, S_{t-1} = 1] &= q\Pi_0, \\ Prob[S_t = 0, S_{t-1} = 1] &= (1 - q)\Pi_0. \end{aligned} \tag{D.10}$$

Substituting Equations D.5 and D.9 into Equation D.8, we are able to calculate the likelihood function, $l(\Theta)$, numerically.

Appendix E

Fitting the Variogram

In order to estimate the unknown parameters in Equation 2.33, we need to minimize the square error function $S(\Theta)$ with regard to the unknown parameters $\Theta = \{c, \kappa_e, \sigma_e\}$, where

$$S(\Theta) = \sum_{j=1}^{k} (\gamma_j^E(\Theta) - V_j^E)^2 \tag{E.1}$$

where, k[1] is the total number of empirical variograms which are considered in the fit. In theory, it would be possible to find these least-square error estimates; however, the presence of the local minimum makes it difficult to find the global minimum. Thus, we first need to guess the most appropriate initial parameters and then find the least-square error estimates.

As described so far (see Equation 2.31), the normalised increments of the data, L_n^E, can be written as

$$L_n^E = Z_n^E + \log(\gamma_E) + \log|\epsilon_n^E| \tag{E.2}$$

[1]The choice of k is an important practical consideration, which is suggested by Journel & Huijbregts (1978) as follows: assume that $J = max\{j : N_j > 0\}$ denote the largest possible lag to be considered in the fit; then fit only up to lags j for which $N_j > 30$ and $0 < k \leq J/2$.

where the stochastic variable Z_n^E is a mean-reverting process as follows

$$Z_n^E = (1 - \kappa_e \Delta t) Z_{n-1}^E + \sigma_e \Delta W_n^e \tag{E.3}$$

Combining these two equations, we get

$$L_n^E = \phi_e L_{n-1}^E + \alpha_e + \eta_n^e \tag{E.4}$$

where

$$\phi_e = 1 - \kappa_e \Delta t, \tag{E.5}$$

$$\alpha_e = (1 - \phi_e)(\log(\gamma_E) - 0.63), \tag{E.6}$$

and

$$\eta_n^e = 0.63(1 - \phi_e) - \phi_e \log|\epsilon_{n-1}^E| + \log|\epsilon_n^E| + \sigma_e \Delta W_n^e \tag{E.7}$$

is a random variable with approximate mean and variance of 0 and $0.23(1+\phi^2)+\sigma^2\Delta t$, respectively.[2]

Rewriting Equation E.4 in its expectation form, we have

$$\mathbb{E}(L_n^E | L_{n-1}^E) = \phi_e L_{n-1}^E + \alpha_e \tag{E.8}$$

which is a linear function and can be estimated using the least-square error method. These parameters estimaties are then used as the initial parameters in minimising Equation E.1.

[2]Using simulating, the approximately calculated mean and variance of $\log|\epsilon_n^E|$ are -0.63 and 0.23, respectively.

Appendix F

Cross-Variogram: Derivation of Equation (2.40)

We proceed by first rewriting Equations 2.36 and 2.37 as follows:

$$Z_t^E = e^{-\kappa_e t} z_0^E + \int_0^t e^{-\kappa_e (t-s)} \sigma_e dW_s^e \tag{F.1}$$

$$Z_t^G = e^{-\kappa_g t} z_0^G + \int_0^t e^{-\kappa_g (t-s)} \sigma_g dW_s^g \tag{F.2}$$

Then we find:

$$\begin{aligned} &\mathbb{E}(Z_t^E Z_t^G) \\ &\quad = e^{-(\kappa_e+\kappa_g)t} z_0^E z_0^G + \textstyle\int_0^t e^{-(\kappa_e+\kappa_g)(t-s)} \sigma_e \sigma_g \rho_{eg} ds \\ &\quad = e^{-(\kappa_e+\kappa_g)t} z_0^E z_0^G + \tfrac{\sigma_e \sigma_g \rho_{eg}}{\kappa_e+\kappa_g} (1 - e^{-(\kappa_e+\kappa_g)t}) \\ &\quad \to \tfrac{\sigma_e \sigma_g \rho_{eg}}{\kappa_e+\kappa_g} \quad as\ t \to \infty, \end{aligned} \tag{F.3}$$

$$
\begin{aligned}
&\mathbb{E}(Z^E_{t+t'} Z^G_t) \\
&\quad = E(Z^E_t e^{-\kappa_e t'} + \textstyle\int_t^{t+t'} e^{-\kappa_e (t+t'-s)} \sigma_e dW^e_s) Z^G_t \\
&\quad = e^{-\kappa_e t'} E(Z^E_t Z^G_t) \\
&\quad \to e^{-\kappa_e t'} \tfrac{\sigma_e \sigma_g \rho_{eg}}{\kappa_e + \kappa_g} \quad as\ t \to \infty
\end{aligned}
\tag{F.4}
$$

Similarly,

$$
\mathbb{E}(Z^E_t Z^G_{t+t'}) \to e^{-\kappa_g t'} \frac{\sigma_e \sigma_g \rho_{eg}}{\kappa_e + \kappa_g} \quad as\ t \to \infty. \tag{F.5}
$$

We can now calculate the following:

$$
\begin{aligned}
&\mathbb{E}\{(L^E_{n+j} - L^E_n)(L^G_{n+j} - L^G_n)\} \\
&= \mathbb{E}\{(\log(\sigma(Z^E_{n+j})) + \log|\epsilon^E_{n+j}| - \log(\sigma(Z^E_n)) - \log|\epsilon^E_n|) \\
&\ \times(\log(\sigma(Z^G_{n+j})) + \log|\epsilon^G_{n+j}| - \log(\sigma(Z^G_n)) - \log|\epsilon^G_n|)\} \\
&= \mathbb{E}\{(\log(\sigma(Z^E_{n+j})) - \log(\sigma(Z^E_n)))(\log(\sigma(Z^G_{n+j})) - \log(\sigma(Z^G_n)))\} \\
&\ +\mathbb{E}\{(\log|\epsilon^E_{n+j}| - \log|\epsilon^E_n|)(\log|\epsilon^G_{n+j}| - \log|\epsilon^G_n|)\}\ \text{(by independence[1])} \\
&= 2\mathbb{E}(\log(\sigma(Z^E))\log(\sigma(Z^G))) - \mathbb{E}(\log(\sigma(Z^E_{n+j})))\mathbb{E}(\log(\sigma(Z^G_n))) \\
&\ -\mathbb{E}(\log(\sigma(Z^E_n)))\mathbb{E}(\log(\sigma(Z^G_{n+j})))\ \text{(by stationarity)} \\
&\ +2\mathbb{E}(\log|\epsilon^E|\log|\epsilon^G|) - 2\mathbb{E}(\log|\epsilon^E|)E(|\log|\epsilon^G|) \\
&= 2\mathbb{E}(Z^E Z^G) - \mathbb{E}(Z^E_{n+j} Z^G_n) - \mathbb{E}(Z^E_n Z^G_{n+j}) + 2cov(\log|\epsilon^E|, \log|\epsilon^G|) \\
&= \tfrac{\sigma_e \sigma_g \rho_{eg}}{\kappa_e + \kappa_g}(2 - e^{-\kappa_e j \Delta t} - e^{-\kappa_g j \Delta t}) + 2cov(\log|\epsilon^E|, \log|\epsilon^G|)
\end{aligned}
\tag{F.6}
$$

[1] We assumed that random variables $\{Z^E_j, Z^G_j\}$ and $\{\epsilon^E_j, \epsilon^G_j\}$ for all possible values of j are independent.

Appendix G

Argument on the Uniqueness of the Solutions Obtained

The method of Adkins & Paxson (2010) used to obtain a solution for the real option value appears successful but does not itself prove that the obtained solution is unique. To prove uniqueness, standard techniques for such elliptic PDEs usually rely on proof by contradiction (see Mattheij *et al.* (2005) for more details). Taking the individual investment option problem solved in Section 3.2.3.2, if we assume that the solution found W for the real option value is *not* unique and that a second solution $\widetilde{W}$ exists, then the difference $\phi = W - \widetilde{W}$ also satisfies the Bellman equation (3.11). For illustration, we take a simpler form of the governing equation

$$\left(F^2\phi_F\right)_F + \left(C^2\phi_C\right)_C - \mu\phi = 0 \tag{G.1}$$

and assume that the free boundary for W is at $F = F^*(C)$ and the free boundary for $\widetilde{W}$ is at $F = \widetilde{F}(C)$. Then, multiplying the governing equation by

ϕ and integrating over the domain $\mathcal{D}$, which is the region $C > 0$ and $F > \max\left(F^*(C), \widetilde{F}(C)\right)$ in which both W and $\widetilde{W}$ are well defined, leads to

$$\begin{aligned}&\int_{max(F^*,\widetilde{F})} C^2\phi\phi_C \mathrm{d}F + \int_{\max(F^*,\widetilde{F})} F^2\phi\phi_F \mathrm{d}C \\ &= \iint_{\mathcal{D}} \mu\phi^2 + C^2(\phi_C)^2 + F^2(\phi_F)^2 \mathrm{d}C\mathrm{d}F \end{aligned} \tag{G.2}$$

where the right-hand side obviously must be greater than or equal to zero and the left-hand side is dependent only on the values at the free boundary; here, the boundary conditions at $F \to \infty$ and $C = 0$ are already accounted for in the integration by parts by assuming $\phi \to 0$ is a suitable manner. The proof of uniqueness then focuses on showing that this left-hand side cannot be strictly positive leading to $\phi = 0$ and, thus, $W = \widetilde{W}$ everywhere. Adopting this approach, it is trivial to show that two distinct solutions $W \neq \widetilde{W}$ cannot have the same free boundary, $F^*(C) = \widetilde{F}(C)$, as in that case ϕ and its first derivatives are zero on the free boundary, and, hence, the right-hand side of (G.2) is also zero. Indeed, for the case where say $\widetilde{F}(C) \leqslant F^*(C)$ everywhere and for a solution domain of finite extent, a reasonable argument for uniqueness can also be constructed. However, proving uniqueness via this approach for arbitrary $F^*(C) \neq \widetilde{F}(C)$ over a solution domain of infinite extent is more difficult, and an adequate proof remains currently under investigation.

Appendix H

Characteristics of the Roots of Equation (3.24)

For simplicity, we rewrite exponents a, b, and c in Equations (3.25-3.27) as follows:

$$a = (\frac{1}{2}\sigma_F^2 + \frac{1}{2}\sigma_C^2 - \rho\sigma_F\sigma_C)K_1 + (\sigma_C^2 - \rho\sigma_F\sigma_C)K_2 + \frac{1}{2}\sigma_C^2 K_3$$

$$b = a + (\alpha_F - \alpha_C)K_1 + (-\frac{1}{2}\sigma_F^2 + \alpha_F - 2\alpha_C)K_2 - \alpha_C K_3$$

$$c = (\mu - \alpha_F)K_1 - (\alpha_F - \frac{1}{2}\sigma_F^2 - 2\mu)K_2 + \mu K_3$$

where

$$K_1 = ((\epsilon_F - \epsilon_F^{(j)})QF)^2 \ > 0$$

$$K_2 = -(\mu - \alpha_F)(\epsilon_F - \epsilon_F^{(j)})QI^{(j)}F \ > 0$$

$$K_3 = (\mu - \alpha_F)^2 (I^{(j)})^2 \ > 0$$

Next, it can be shown that $c > a - b$:

$$\begin{aligned} c - a + b = \ & (\alpha_F - \alpha_C)K_1 + (-\tfrac{1}{2}\sigma_F^2 + \alpha_F - 2\alpha_C)K_2 - \alpha_C K_3 \\ & +(\mu - \alpha_F)K_1 - (\alpha_F - \tfrac{1}{2}\sigma_F^2 - 2\mu)K_2 + \mu K_3 \\ = \ & (\mu - \alpha_C)(K_1 + 2K_2 + K_3) \ > 0 \end{aligned} \tag{H.1}$$

We may now finalise the proof as follows:

$$c > a - b \ \Rightarrow \ b^2 + 4ac > 4a^2 - 4ab + b^2 = (2a - b)^2 \tag{H.2}$$

Thus,

$$-\sqrt{b^2 + 4ac} < (2a - b) < \sqrt{b^2 + 4ac} \ \Rightarrow \tag{H.3}$$

$$b - \sqrt{b^2 + 4ac} < 2a < b + \sqrt{b^2 + 4ac} \tag{H.4}$$

Therefore, $\eta_1^{(j)} > 1$ and $\eta_2^{(j)} < 1$. On the other hand, $\eta_2^{(j)}$ is not only less than 1, but also less than 0 because $b < \sqrt{b^2 + 4ac}$.

Appendix I

Parameters of Equation (3.17)

Table I.1 provides the calculated parameters of Equation 3.17, $\{\eta^{(pccs)}, \beta^{(pccs)}, C^{*(pccs)}(F), A^{(pccs)}\}$, for some values of F.

F	$\eta^{(pccs)}$	$\beta^{(pccs)}$	$C^{*(pccs)}(F)$	$A^{(pccs)}$	F	$\eta^{(pccs)}$	$\beta^{(pccs)}$	$C^{*(pccs)}(F)$	$A^{(pccs)}$
1	1.2919	-0.0091	48.15	7.4100E+10	26	1.3214	-0.1463	79.52	4.2098E+10
1.5	1.2929	-0.0135	48.77	7.2170E+10	26.5	1.3218	-0.1479	80.15	4.1879E+10
2	1.2938	-0.0177	49.40	7.0435E+10	27	1.3221	-0.1496	80.78	4.1665E+10
2.5	1.2947	-0.0219	50.02	6.8853E+10	27.5	1.3224	-0.1512	81.41	4.1456E+10
3	1.2956	-0.0260	50.65	6.7397E+10	28	1.3228	-0.1528	82.04	4.1253E+10
3.5	1.2964	-0.0300	51.27	6.6048E+10	28.5	1.3231	-0.1544	82.67	4.1055E+10
4	1.2973	-0.0338	51.90	6.4790E+10	29	1.3235	-0.1560	83.29	4.0861E+10
4.5	1.2981	-0.0376	52.53	6.3614E+10	29.5	1.3238	-0.1575	83.92	4.0673E+10
5	1.2989	-0.0414	53.15	6.2510E+10	30	1.3241	-0.1590	84.55	4.0488E+10
5.5	1.2997	-0.0450	53.78	6.1470E+10	30.5	1.3244	-0.1605	85.18	4.0309E+10
6	1.3005	-0.0486	54.41	6.0489E+10	31	1.3247	-0.1620	85.81	4.0133E+10
6.5	1.3012	-0.0520	55.03	5.9561E+10	31.5	1.3250	-0.1635	86.44	3.9961E+10
7	1.3020	-0.0554	55.66	5.8681E+10	32	1.3253	-0.1649	87.07	3.9794E+10
7.5	1.3027	-0.0588	56.29	5.7846E+10	32.5	1.3256	-0.1663	87.70	3.9630E+10
8	1.3034	-0.0620	56.91	5.7052E+10	33	1.3259	-0.1677	88.33	3.9470E+10
8.5	1.3041	-0.0652	57.54	5.6296E+10	33.5	1.3262	-0.1691	88.96	3.9313E+10
9	1.3048	-0.0683	58.17	5.5574E+10	34	1.3265	-0.1704	89.59	3.9160E+10
9.5	1.3054	-0.0714	58.79	5.4885E+10	34.5	1.3268	-0.1718	90.21	3.9010E+10
10	1.3061	-0.0744	59.42	5.4227E+10	35	1.3271	-0.1731	90.84	3.8864E+10
10.5	1.3067	-0.0774	60.05	5.3596E+10	35.5	1.3273	-0.1744	91.47	3.8720E+10
11	1.3073	-0.0802	60.68	5.2992E+10	36	1.3276	-0.1757	92.10	3.8580E+10
11.5	1.3079	-0.0831	61.30	5.2413E+10	36.5	1.3279	-0.1769	92.73	3.8442E+10
12	1.3085	-0.0858	61.93	5.1858E+10	37	1.3281	-0.1782	93.36	3.8308E+10
12.5	1.3091	-0.0886	62.56	5.1324E+10	37.5	1.3284	-0.1794	93.99	3.8176E+10
13	1.3097	-0.0912	63.19	5.0810E+10	38	1.3286	-0.1806	94.62	3.8047E+10
13.5	1.3102	-0.0938	63.81	5.0316E+10	38.5	1.3289	-0.1818	95.25	3.7920E+10
14	1.3108	-0.0964	64.44	4.9841E+10	39	1.3291	-0.1830	95.88	3.7797E+10
14.5	1.3113	-0.0989	65.07	4.9382E+10	39.5	1.3294	-0.1842	96.51	3.7675E+10
15	1.3119	-0.1014	65.70	4.8940E+10	40	1.3296	-0.1854	97.14	3.7556E+10
15.5	1.3124	-0.1038	66.33	4.8514E+10	40.5	1.3299	-0.1865	97.77	3.7439E+10
16	1.3129	-0.1062	66.95	4.8102E+10	41	1.3301	-0.1876	98.39	3.7325E+10
16.5	1.3134	-0.1086	67.58	4.7705E+10	41.5	1.3303	-0.1887	99.02	3.7213E+10
17	1.3139	-0.1109	68.21	4.7320E+10	42	1.3306	-0.1898	99.65	3.7103E+10
17.5	1.3144	-0.1131	68.84	4.6949E+10	42.5	1.3308	-0.1909	100.28	3.6995E+10
18	1.3148	-0.1153	69.47	4.6589E+10	43	1.3310	-0.1920	100.91	3.6889E+10
18.5	1.3153	-0.1175	70.09	4.6241E+10	43.5	1.3312	-0.1931	101.54	3.6785E+10
19	1.3158	-0.1197	70.72	4.5904E+10	44	1.3315	-0.1941	102.17	3.6683E+10
19.5	1.3162	-0.1218	71.35	4.5577E+10	44.5	1.3317	-0.1952	102.80	3.6582E+10
20	1.3166	-0.1239	71.98	4.5260E+10	45	1.3319	-0.1962	103.43	3.6484E+10
20.5	1.3171	-0.1259	72.61	4.4953E+10	45.5	1.3321	-0.1972	104.06	3.6387E+10
21	1.3175	-0.1279	73.24	4.4654E+10	46	1.3323	-0.1982	104.69	3.6293E+10
21.5	1.3179	-0.1299	73.86	4.4365E+10	46.5	1.3325	-0.1992	105.32	3.6199E+10
22	1.3183	-0.1318	74.49	4.4084E+10	47	1.3327	-0.2002	105.95	3.6108E+10
22.5	1.3187	-0.1337	75.12	4.3811E+10	47.5	1.3329	-0.2011	106.58	3.6018E+10
23	1.3191	-0.1356	75.75	4.3545E+10	48	1.3331	-0.2021	107.21	3.5930E+10
23.5	1.3195	-0.1374	76.38	4.3287E+10	48.5	1.3333	-0.2030	107.84	3.5843E+10
24	1.3199	-0.1393	77.01	4.3036E+10	49	1.3335	-0.2039	108.47	3.5758E+10
24.5	1.3203	-0.1411	77.64	4.2792E+10	49.5	1.3337	-0.2049	109.10	3.5674E+10
25	1.3207	-0.1428	78.26	4.2555E+10	50	1.3339	-0.2058	109.73	3.5591E+10
25.5	1.3210	-0.1446	78.89	4.2323E+10					

Table I.1: Parameters of Equation (3.17) for some PCCS

Appendix J

The Second-Order Sufficiency Condition for the Optimal Threshold, P^*

Proposition. Let $\psi(P) = \left(\frac{P_0}{P}\right)^{\beta}\{aP - bC - I\}$. Then, the second derivative of $\psi(P)$ at its critical point, $P = P^*$ (Equation (4.8)), is negative, i.e., $\psi''(P^*) < 0$.

Proof. The first and the second derivatives of $\psi(P)$ are calculated, respectively, as follows:

$$\psi'(P) = \left(\frac{P_0}{P}\right)^{\beta}\left(\frac{\beta(bC+I)}{P} - (\beta-1)a\right) \tag{J.1}$$

$$\begin{aligned}\Rightarrow \psi''(P) &= \frac{-\beta}{P}\left(\frac{P_0}{P}\right)^{\beta}\left(\frac{\beta(bC+I)}{P} - (\beta-1)a\right) + \left(\frac{P_0}{P}\right)^{\beta}\left(\frac{-\beta(bC+I)}{P^2}\right) \\ &= \frac{-\beta}{P^2}\left(\frac{P_0}{P}\right)^{\beta}[(\beta+1)(bC+I) - (\beta-1)aP] \end{aligned} \tag{J.2}$$

After plugging $P^* = \left(\frac{\beta}{\beta-1}\right)\frac{(I+bC)}{a}$ into the second derivative, we have:

$$\begin{aligned}
\psi''(P^*) &= \frac{-\beta}{P^{*2}}\left(\frac{P_0}{P^*}\right)^{\beta}[(\beta+1)(bC+I)-(\beta-1)aP^*] \\
&= \frac{-\beta}{P^{*2}}\left(\frac{P_0}{P^*}\right)^{\beta}\left[(\beta+1)(bC+I)-(\beta-1)a\left(\frac{\beta}{\beta-1}\right)\frac{(I+bC)}{a}\right] \\
&= \frac{-\beta}{P^{*2}}\left(\frac{P_0}{P^*}\right)^{\beta}(bC+I) < 0 \qquad \text{(J.3)}
\end{aligned}$$

Since β and b are positive, $\psi''(P^*)$ is negative.

Appendix K

Sensitivity of a Single-Exercise IL Contract Valuation to Volatility, σ

Here, we show, analytically, that the optimal threshold and the optimal value of a single-exercise IL contract are increasing functions of volatility, σ.

K.0.1 Optimal Threshold

Proposition. The optimal threshold of a single-exercise IL contract is an increasing function of the volatility.

Proof. We first calculate the derivative of the optimal threshold, Equation (4.8), with respect to σ, as follows:

$$\frac{\partial P^*}{\partial \sigma} = \frac{\beta'(\beta-1) - \beta'\beta}{(\beta-1)^2}\frac{I+bC}{a} = \frac{-\beta'}{(\beta-1)^2}\frac{I+bC}{a} \tag{K.1}$$

where $\beta' = \frac{\partial \beta}{\partial \sigma}$. Since β is the positive root of the characteristic quadratic equation $\frac{1}{2}\sigma^2\beta(\beta-1) + \alpha\beta - \rho = 0$, then, by taking the derivatives of the both sides of this equation with respect to σ, we have:

$$\begin{aligned} & \sigma\beta(\beta-1) + \frac{1}{2}\sigma^2\beta'(\beta-1) + \frac{1}{2}\sigma^2\beta\beta' + \alpha\beta' = 0 \\ \Rightarrow \quad & \beta' = \frac{-\sigma\beta(\beta-1)}{\frac{1}{2}\sigma^2(\beta-1) + \frac{1}{2}\sigma^2\beta + \alpha} < 0 \end{aligned} \tag{K.2}$$

Since β is greater than one, β' is negative for any $\sigma > 0$. On the other hand, $\frac{\partial P^*}{\partial \sigma}$, Equation (K.1), is always positive, which proves that the optimal threshold is an increasing function of σ.

K.0.2 Optimal Value

Proposition. The optimal value of the contract at the current electricity price, $F(P_0)$, when $P_0 < P^*$, is an increasing function of the volatility, σ.

Proof. We define function W as follows:

$$\begin{aligned} W &= \ln\left(F(P_0)\right) \\ &= \ln\left(\left(\frac{P_0}{P^*}\right)^{\beta}\left\{V(P^*) - I\right\}\right) = \beta\ln\left(\frac{P_0}{P^*}\right) + \ln\left(aP^* - bC - I\right) \end{aligned} \tag{K.3}$$

We now let $W' = \frac{\partial W}{\partial \sigma}$ and $F' = \frac{\partial F}{\partial \sigma}$:

$$\begin{aligned} W' = \frac{F'}{F} &= \beta'\ln\left(\frac{P_0}{P^*}\right) + \beta\left(-\frac{\frac{\partial P^*}{\partial \sigma}}{P^*}\right) + \frac{a\frac{\partial P^*}{\partial \sigma}}{aP^* - bC - I} \\ &= \beta'\ln\left(\frac{P_0}{P^*}\right) + \beta\left(-\frac{\frac{-\beta'}{(\beta-1)^2}}{\frac{\beta}{\beta-1}}\right) + \frac{a\frac{-\beta'}{(\beta-1)^2}\frac{I+bC}{a}}{a\frac{\beta}{\beta-1}\left(\frac{bC+I}{a}\right) - (bC+I)} \end{aligned}$$

$$
\begin{aligned}
&= \beta' \ln\left(\frac{P_0}{P^*}\right) + \frac{\beta'}{\beta - 1} + \frac{-\beta'(I + bC)/(\beta - 1)^2}{(bC + I)/(\frac{\beta}{\beta - 1} - 1)} \\
&= \beta' \ln\left(\frac{P_0}{P^*}\right) \qquad \text{(K.4)} \\
\Rightarrow F' &= \beta' \ln\left(\frac{P_0}{P^*}\right) F > 0 \qquad \text{(K.5)}
\end{aligned}
$$

Since $\beta' < 0$, $\ln\left(\frac{P_0}{P^*}\right) < 0$, and $F > 0$, F' is positive for any $\sigma > 0$, i.e., the optimal value of the contract given the current price of electricity is less than the optimal threshold is an increasing function of the volatility.

Appendix L

The $(N-1)$st Optimal Value

After inserting Equation (4.20) into the optimisation problem in Equation (4.16), we have:

$$
\begin{aligned}
F_{N-1}^{(N)}(P_{\tau_{N-2}+T_{N-2}+h}) = \max_{P_{\tau_{N-1}}^{*(N)} > P_{\tau_{N-2}+T_{N-2}+h}} & \left(\frac{P_{\tau_{N-2}+T_{N-2}+h}}{P_{\tau_{N-1}}^{*(N)}}\right)^{\beta} \Big\{ a_{N-1} P_{\tau_{N-1}}^{*(N)} \\
& - b_{N-1}C - I_{N-1} + e^{-\rho(T_{N-1}+h)} \Big[\Big(a_N P_{\tau_{N-1}}^{*(N)} e^{\alpha(T_{N-1}+h)} - b_N C - I_N \Big) \\
& \times \Phi\left(R(T_{n-1}+h, P_{\tau_N}^{*(N)}, P_{\tau_{N-1}}^{*(N)}) \right) + \left(\frac{P_{\tau_{N-1}}^{*(N)}}{P_{\tau_N}^{*(N)}} \right)^{\beta} \left(a_N P_{\tau_N}^{*(N)} - b_N C - I_N \right) \\
& \times e^{\gamma(T_{N-1}+h)} \left(1 - \Phi\left(R\left(T_{N-1}+h, P_{\tau_N}^{*(N)}, P_{\tau_{N-1}}^{*(N)} \right) \right) \right) \Big] \Big\}
\end{aligned} \tag{L.1}
$$

Taking the first-order necessary condition yields:

$$
\begin{aligned}
& \frac{\beta}{P_{\tau_{N-1}}^{*(N)}} \Big\{ a_{N-1} P_{\tau_{N-1}}^{*(N)} - b_{N-1}C - I_{N-1} + e^{-\rho(T_{N-1}+h)} \\
& \times \Big[\Phi\left(R(T_{N-1}+h, P_{\tau_N}^{*(N)}, P_{\tau_{N-1}}^{*(N)}) \right) \left(a_N P_{\tau_{N-1}}^{*(N)} e^{\alpha(T_{N-1}+h)} - b_N C - I_N \right)
\end{aligned}
$$

$$
\begin{aligned}
&+\left(1-\Phi\left(R(T_{N-1}+h,P^{*(N)}_{\tau_N},P^{*(N)}_{\tau_{N-1}})\right)\right)\left(\frac{P^{*(N)}_{\tau_{N-1}}}{P^{*(N)}_{\tau_N}}\right)^{\beta}\\
&\times\left[a_N P^{*(N)}_{\tau_N}-b_N C-I_N\right]e^{\gamma(T_{N-1}+h)}\Big]\Big\}\\
&=\Big\{a_{N-1}+e^{-\rho(T_{N-1}+h)}\left[\Phi\left(R(T_{N-1}+h,P^{*(N)}_{\tau_N},P^{*(N)}_{\tau_{N-1}})\right)a_N e^{\alpha(T_{N-1}+h)}\right.\\
&+\frac{\phi\left(R(T_{N-1}+h,P^{*(N)}_{\tau_N},P^{*(N)}_{\tau_{N-1}})\right)}{P^{*(N)}_{\tau_{N-1}}\sigma\sqrt{T_{N-1}+h}}\left[a_N P^{*(N)}_{\tau_{N-1}}e^{\alpha(T_{N-1}+h)}-b_N C-I_N\right]+e^{\gamma(T_{N-1}+h)}\\
&\times\left(a_N P^{*(N)}_{\tau_N}-b_N C-I_N\right)\left(\left(\frac{P^{*(N)}_{\tau_{N-1}}}{P^{*(N)}_{\tau_N}}\right)^{\beta}\frac{-\phi\left(R(T_{N-1}+h,P^{*(N)}_{\tau_N},P^{*(N)}_{\tau_{N-1}})\right)}{P^{*(N)}_{\tau_{N-1}}\sigma\sqrt{T_{N-1}+h}}\right.\\
&\left.\left.+\left(1-\Phi\left(R(T_{N-1}+h,P^{*(N)}_{\tau_N},P^{*(N)}_{\tau_{N-1}})\right)\right)\frac{\beta}{P^{*(N)}_{\tau_N}}\left(\frac{P^{*(N)}_{\tau_{N-1}}}{P^{*(N)}_{\tau_N}}\right)^{\beta-1}\right)\right]\Big\}
\end{aligned}
\tag{L.2}
$$

It should be noted that $\phi(x)\equiv\Phi'(x)$. Finally, simplifying Equation (L.2), we obtain the following:

$$
\begin{aligned}
&P^{*(N)}_{\tau_{N-1}}(\beta-1)\left(a_{N-1}+e^{-\rho(T_{N-1}+h)}a_N e^{\alpha(T_{N-1}+h)}\Phi\left(R(T_{N-1}+h,P^{*(N)}_{\tau_N},P^{*(N)}_{\tau_{N-1}})\right)\right)\\
&-\left[a_N P^{*(N)}_{\tau_{N-1}}e^{\alpha(T_{N-1}+h)}-b_N C-I_N\right]\phi\left(R(T_{N-1}+h,P^{*(N)}_{\tau_N},P^{*(N)}_{\tau_{N-1}})\right)\\
&\times\frac{e^{-\rho(T_{N-1}+h)}}{\sigma\sqrt{T_{N-1}+h}}+\left(\frac{P^{*(N)}_{\tau_{N-1}}}{P^{*(N)}_{\tau_N}}\right)^{\beta}\left[a_N P^{*(N)}_{\tau_N}-b_N C-I_N\right]\frac{e^{-(\rho-\gamma)(T_{N-1}+h)}}{\sigma\sqrt{T_{N-1}+h}}\\
&\times\phi\left(R(T_{N-1}+h,P^{*(N)}_{\tau_N},P^{*(N)}_{\tau_{N-1}})\right)\\
&=\beta\left[I_{N-1}+b_{N-1}C+e^{-\rho(T_{N-1}+h)}(I_N+b_N C)\Phi\left(R(T_{N-1}+h,P^{*(N)}_{\tau_N},P^{*(N)}_{\tau_{N-1}})\right)\right]
\end{aligned}
\tag{L.3}
$$

Re-writing Equation (L.3), we have:

$$
P^{*(N)}_{\tau_{N-1}}(\beta-1)\left[a_{N-1}+a_N e^{-(\rho-\alpha)(T_{N-1}+h)}\left(\Phi\left(R(T_{N-1}+h,P^{*(N)}_{\tau_N},P^{*(N)}_{\tau_{N-1}})\right)\right.\right.
$$

$$
\begin{aligned}
&-\frac{\phi\left(R(T_{N-1}+h, P^{*(N)}_{\tau_N}, P^{*(N)}_{\tau_{N-1}})\right)}{(\beta-1)\sigma\sqrt{T_{N-1}+h}}\left(1-\left(\frac{P^{*(N)}_{\tau_{N-1}}}{P^{*(N)}_{\tau_N}}\right)^{\beta-1} e^{\gamma(T_{N-1}+h)}\right)\Bigg)\Bigg] \\
&= \beta\Bigg[I_{N-1}+b_{N-1}C+(I_N+b_NC)e^{-\rho(T_{N-1}+h)}\left(\Phi\left(R(T_{N-1}+h, P^{*(N)}_{\tau_N}, P^{*(N)}_{\tau_{N-1}})\right)\right. \\
&\left.-\frac{\phi\left(R(T_{N-1}+h, P^{*(N)}_{\tau_N}, P^{*(N)}_{\tau_{N-1}})\right)}{\beta\sigma\sqrt{T_{N-1}+h}}\left(1-\left(\frac{P^{*(N)}_{\tau_{N-1}}}{P^{*(N)}_{\tau_N}}\right)^{\beta} e^{\gamma(T_{N-1}+h)}\right)\right)\Bigg] \qquad \text{(L.4)}
\end{aligned}
$$

Appendix M

Conditional Expectation of the $(n+1)$st Interruption's Option Given Information at Time τ_n

The $(n+1)$st interruption's option value, depending on the electricity spot price at time $\tau_n + T_n + h$, can take the form:

$$F_{n+1}^{(N)}(P_{\tau_n+T_n+h}) = \begin{cases} a_{n+1}P_{\tau_n+T_n+h} - b_{n+1}C - I_{n+1} + e^{-\rho(T_{n+1}+h)} \\ \times\mathbb{E}\left[F_{n+2}^{(N)}(P_{\tau_n+T_n+h+T_{n+1}+h})|P_{\tau_n+T_n+h}\right] & \text{if } P_{\tau_n+T_n+h} \geq P_{\tau_{n+1}}^{*(N)} \\ \\ \left(\frac{P_{\tau_n+T_n+h}}{P_{\tau_{n+1}}^{*(N)}}\right)^{\beta}\left(a_{n+1}P_{\tau_{n+1}}^{*(N)} - b_{n+1}C - I_{n+1} + e^{-\rho(T_{n+1}+h)}\right. \\ \left.\times\mathbb{E}\left[F_{n+2}^{(N)}(P_{\tau_{n+1}+T_{n+1}+h})|P_{\tau_{n+1}} = P_{\tau_{n+1}}^{*(N)}\right]\right) & \text{otherwise} \end{cases} \tag{M.1}$$

Therefore, the conditional expectation given information at time τ_n can be calculated as follows:

$$\begin{aligned}
\mathbb{E}\left[F_{n+1}^{(N)}(P_{\tau_n+T_n+h})|P_{\tau_n}=P_{\tau_n}^{*(N)}\right] &= (a_{n+1}e^{\alpha(T_n+h)}P_{\tau_n}^{*(N)}-b_{n+1}C-I_{n+1}\\
&+e^{-\rho(T_{n+1}+h)}\mathbb{E}\left[\mathbb{E}\left[F_{n+2}^{(N)}(P_{\tau_n+T_n+h+T_{n+1}+h})|P_{\tau_n+T_n+h}\right]|P_{\tau_n}=P_{\tau_n}^{*(N)}\right])\\
&\times\mathbb{P}\left(P_{\tau_n+T_n+h}\geq P_{\tau_{n+1}}^{*(N)}|P_{\tau_n}=P_{\tau_n}^{*(N)}\right)+(a_{n+1}P_{\tau_{n+1}}^{*(N)}-b_{n+1}C-I_{n+1}\\
&+e^{-\rho(T_{n+1}+h)}\mathbb{E}\left[\mathbb{E}\left[F_{n+2}^{(N)}(P_{\tau_{n+1}+T_{n+1}+h})|P_{\tau_{n+1}}=P_{\tau_{n+1}}^{*(N)}\right]|P_{\tau_n}=P_{\tau_n}^{*(N)}\right])\\
&\times e^{\gamma(T_n+h)}\left(\frac{P_{\tau_n}^{*(N)}}{P_{\tau_{n+1}}^{*(N)}}\right)^{\beta}\left(1-\mathbb{P}\left(P_{\tau_n+T_n+h}\geq P_{\tau_{n+1}}^{*(N)}|P_{\tau_n}=P_{\tau_n}^{*(N)}\right)\right) \qquad \text{(M.2)}
\end{aligned}$$

We have:

$$\begin{aligned}
&\mathbb{E}\left[\mathbb{E}\left[F_{n+2}^{(N)}(P_{\tau_n+T_n+h+T_{n+1}+h})|P_{\tau_n+T_n+h}\right]|P_{\tau_n}=P_{\tau_n}^{*(N)}\right]\\
=\;&\mathbb{E}\left[F_{n+2}^{(N)}(P_{\tau_n+T_n+h+T_{n+1}+h})|P_{\tau_n}=P_{\tau_n}^{*(N)}\right] \qquad \text{(M.3)}
\end{aligned}$$

Moreover, since $\mathbb{E}\left[F_{n+2}^{(N)}(P_{\tau_{n+1}+T_{n+1}+h})|P_{\tau_{n+1}}=P_{\tau_{n+1}}^{*(N)}\right]$ is independent of P_{τ_n}, Equation (M.2) can, therefore, be re-written as follows:

$$\begin{aligned}
\mathbb{E}\left[F_{n+1}^{(N)}(P_{\tau_n+T_n+h})|P_{\tau_n}=P_{\tau_n}^{*(N)}\right] &= \left(a_{n+1}e^{\alpha(T_n+h)}P_{\tau_n}^{*(N)}-b_{n+1}C-I_{n+1}\right.\\
&\left.+e^{-\rho(T_{n+1}+h)}\mathbb{E}\left[F_{n+2}^{(N)}(P_{\tau_n+T_n+h+T_{n+1}+h})|P_{\tau_n}=P_{\tau_n}^{*(N)}\right]\right)\\
&\times\Phi\left(R(T_n+h,P_{\tau_n}^{*(N)},P_{\tau_{n+1}}^{*(N)})\right)+\left(a_{n+1}P_{\tau_{n+1}}^{*(N)}-b_{n+1}C-I_{n+1}+e^{-\rho(T_{n+1}+h)}\right.\\
&\left.\times\;\mathbb{E}\left[F_{n+2}^{(N)}(P_{\tau_{n+1}+T_{n+1}+h})|P_{\tau_{n+1}}=P_{\tau_{n+1}}^{*(N)}\right]\right)e^{\gamma(T_n+h)}\left(\frac{P_{\tau_n}^{*(N)}}{P_{\tau_{n+1}}^{*(N)}}\right)^{\beta}\\
&\times\left(1-\Phi\left(R(T_n+h,P_{\tau_n}^{*(N)},P_{\tau_{n+1}}^{*(N)})\right)\right) \qquad \text{(M.4)}
\end{aligned}$$

Appendix N

Approximate and Exact Value Functions

Proposition. $F_1^{(N)}(P_0) \geq J_1^{(N)}(P_0)$ for any $P_0 < P_{\tau_1'}^{*(N)}$.

Proof. Jensen's inequality in the context of probability theory states that if X is a random variable and g is a convex function, then $\mathbb{E}[g(X)] \geq g(\mathbb{E}[X])$. By letting $g(.) = F_N^{(N)}(.)$ together with the information that for the last interruption $F_N^{(N)}(.) = J_N^{(N)}(.)$, we have:

$$\begin{aligned} \mathbb{E}_{P_{\tau'_{N-1}}^{*(N)}}\left[F_N^{(N)}(P_{\tau'_{N-1}+T_{N-1}+h})\right] &\geq F_N^{(N)}\left(\mathbb{E}_{P_{\tau'_{N-1}}^{*(N)}}[P_{\tau'_{N-1}+T_{N-1}+h}]\right) \\ &\equiv J_N^{(N)}\left(\mathbb{E}_{P_{\tau'_{N-1}}^{*(N)}}[P_{\tau'_{N-1}+T_{N-1}+h}]\right) \end{aligned} \quad \text{(N.1)}$$

Since $F_{N-1}^{(N)}(P_0)$ is maximised at $P_{\tau_{N-1}}^{*(N)}$ (under the assumption $P_0 < P_{\tau_{N-1}}^{*(N)}$), for any $P_0 < P_{\tau'_{N-1}}^{*(N)}$, we have:

$$\begin{aligned}
F_{N-1}^{(N)}(P_0) &= \left(\frac{P_0}{P_{\tau_{N-1}}^{*(N)}}\right)^{\beta}\Big(a_{N-1}P_{\tau_{N-1}}^{*(N)} - b_{N-1}C - I_{N-1} \\
&\quad + e^{-\rho(T_{N-1}+h)}\mathbb{E}_{P_{\tau_{N-1}}^{*(N)}}\left[F_N^{(N)}(P_{\tau_{N-1}+T_{N-1}+h})\right]\Big) \\
&\geq \left(\frac{P_0}{P_{\tau'_{N-1}}^{*(N)}}\right)^{\beta}\Big(a_{N-1}P_{\tau'_{N-1}}^{*(N)} - b_{N-1}C - I_{N-1} \\
&\quad + e^{-\rho(T_{N-1}+h)}\mathbb{E}_{P_{\tau'_{N-1}}^{*(N)}}\left[F_N^{(N)}(P_{\tau'_{N-1}+T_{N-1}+h})\right]\Big) \\
&\geq \left(\frac{P_0}{P_{\tau'_{N-1}}^{*(N)}}\right)^{\beta}\Big(a_{N-1}P_{\tau'_{N-1}}^{*(N)} - b_{N-1}C - I_{N-1} \\
&\quad + e^{-\rho(T_{N-1}+h)}J_N^{(N)}(\mathbb{E}_{P_{\tau'_{N-1}}^{*(N)}}\left[P_{\tau'_{N-1}+T_{N-1}+h}\right])\Big) \\
&= J_{N-1}^{(N)}(P_0) \qquad \text{(N.2)}
\end{aligned}$$

The next-to-last inequality results from Jensen's inequality, Equation (N.1). Under the assumption $F_{N-1}^{(N)}(P_0) \geq J_{N-1}^{(N)}(P_0)$ for any $P_0 < P_{\tau'_{N-1}}^{*(N)}$, we can then prove that $F_{N-2}^{(N)}(P_0) \geq J_{N-2}^{(N)}(P_0)$ for any $P_0 < P_{\tau'_{N-2}}^{*(N)}$. Working backwards to the first interruption, it is proved that the optimal value of an N-exercise IL contract is greater than its approximation, i.e., $F_1^{(N)}(P_0) \geq J_1^{(N)}(P_0)$ for any $P_0 < P_{\tau'_1}^{*(N)}$.

Appendix O

Approximate Price Thresholds

We solve the problem when $N = 3$. Since the last optimal price threshold can be calculated from Equation (4.14), we have:

$$P_{\tau_3}^{*(3)} = \frac{\beta}{\beta - 1} \frac{b_3 C + I_3}{a_3} \tag{O.1}$$

Working backwards to the second interruption, which is available at time $\tau_1' + T_1 + h$, if $P_{\tau_2'}^{*(3)} \geq P_{\tau_1'+T_1+h}$, then the LSE's problem, Equation (4.26), can be re-written as follows:

$$\begin{aligned} J_2^{(3)}(P_{\tau_1'+T_1+h}) &= \max_{P_{\tau_2'}^{*(3)} \geq P_{\tau_1'+T_1+h}} \left(\frac{P_{\tau_1'+T_1+h}}{P_{\tau_2'}^{*(3)}} \right)^{\beta} \Big\{ a_2 P_{\tau_2'}^{*(3)} - b_2 C - I_2 \\ &\quad + e^{-\rho(T_2+h)} J_3^{(3)} \left(\mathbb{E}\left[P_{\tau_2'+T_2+h} | P_{\tau_2'} = P_{\tau_2'}^{*(3)} \right] \right) \Big\} \\ &= \max_{P_{\tau_2'}^{*(3)} \geq P_{\tau_1'+T_1+h}} \left(\frac{P_{\tau_1'+T_1+h}}{P_{\tau_2'}^{*(3)}} \right)^{\beta} \Big\{ a_2 P_{\tau_2'}^{*(3)} - b_2 C - I_2 \\ &\quad + e^{-\rho(T_2+h)} J_3^{(3)} \left(e^{\alpha(T_2+h)} P_{\tau_2'}^{*(3)} \right) \Big\} \end{aligned} \tag{O.2}$$

We now let $M_2 = e^{\alpha(T_2+h)}P^{*(3)}_{\tau_2'}$. Taking the first-order necessary condition and simplifying the result yields:

$$\begin{aligned} & P^{*(3)}_{\tau_2'}(\beta-1)\left(a_2 - \frac{e^{-\rho(T_2+h)}}{\beta-1}\left.\frac{\partial J_3^{(3)}(M_2)}{\partial P_{\tau_2'}}\right|_{P_{\tau_2'}=P^{*(3)}_{\tau_2'}}\right) \\ = \;& \beta(b_2C + I_2 - e^{-\rho(T_2+h)}J_3^{(3)}(M_2)) \end{aligned} \tag{O.3}$$

Here,

$$J_3^{(3)}(M_2) = \begin{cases} a_3M_2 - b_3C - I_3 & \text{if } M_2 \geq P_{\tau_3} \equiv P^{*(3)}_{\tau_3} \\ \left(\frac{M_2}{P^{*(3)}_{\tau_3}}\right)^{\beta}\left[V_3^{(3)}\left(P^{*(3)}_{\tau_3}\right) - I_3\right] & \text{otherwise} \end{cases} \tag{O.4}$$

Therefore, Equation (O.3) can be solved for $P^{*(3)}_{\tau_2'}$ using the two conditions in Equation (O.4):

- If $M_2 < P^{*(3)}_{\tau_3}$:

$$\begin{aligned} & P^{*(3)}_{\tau_2'}(\beta-1)\left(a_2 - \frac{e^{-\rho(T_2+h)}}{\beta-1}e^{\alpha\beta(T_2+h)}\frac{\beta}{P^{*(3)}_{\tau_2'}}\left(\frac{P^{*(3)}_{\tau_2'}}{P^{*(3)}_{\tau_3}}\right)^{\beta}\left[a_3P^{*(3)}_{\tau_3} - b_3C_3 - I_3\right]\right) \\ & = \beta(b_2C + I_2 - e^{-(\rho-\alpha\beta)(T_2+h)}\left(\frac{P^{*(3)}_{\tau_2'}}{P^{*(3)}_{\tau_3}}\right)^{\beta}\left[a_3P^{*(3)}_{\tau_3} - b_3C_3 - I_3\right]) \\ & \Rightarrow P^{*(3)}_{\tau_2'}(\beta-1)a_2 - e^{-(\rho-\alpha\beta)(T_2+h)}\beta\left(\frac{P^{*(3)}_{\tau_2'}}{P^{*(3)}_{\tau_3}}\right)^{\beta}\left[a_3P^{*(3)}_{\tau_3} - b_3C_3 - I_3\right] \\ & = \beta(b_2C + I_2) - \beta e^{-(\rho-\alpha\beta)(T_2+h)}\left(\frac{P^{*(3)}_{\tau_2'}}{P^{*(3)}_{\tau_3}}\right)^{\beta}\left[a_3P^{*(3)}_{\tau_3} - b_3C_3 - I_3\right] \\ & \Rightarrow P^{*(3)}_{\tau_2} = \frac{\beta}{\beta-1}\frac{b_2C + I_2}{a_2} \end{aligned} \tag{O.5}$$

- If $M_2 \geq P^{*(3)}_{\tau_3}$:

$$\begin{aligned}
& P^{*(3)}_{\tau_2'}(\beta-1)\left(a_2 - \frac{e^{-\rho(T_2+h)}}{\beta-1}a_3 e^{\alpha(T_2+h)}\right) \\
= \;& \beta\left(b_2 C + I_2 - e^{-\rho(T_2+h)}\left(a_3 M_2 - b_3 C - I_3\right)\right) \\
\Rightarrow \;& P^{*(3)}_{\tau_2'}\left[(\beta-1)a_2 - e^{-(\rho-\alpha)(T_2+h)}a_3 + \beta e^{-(\rho-\alpha)(T_2+h)}a_3\right] \\
= \;& \beta\left(b_2 C + I_2 + e^{-\rho(T_2+h)}\left(b_3 C + I_3\right)\right) \\
\Rightarrow \;& P^{*(3)}_{\tau_2'} = \frac{\beta}{\beta-1}\frac{(b_2 C + I_2) + e^{-\rho(T_2+h)}(b_3 C + I_3)}{a_2 + e^{-(\rho-\alpha)(T_2+h)}a_3}
\end{aligned} \tag{O.6}$$

Finally, for the first interruption, which is available at time 0, if it is still optimal to wait, i.e., $P^{*(3)}_{\tau_1'} \geq P_0$, then the following equation must be solved for $P^{*(3)}_{\tau_1'}$:

$$\begin{aligned}
& P^{*(3)}_{\tau_1'}(\beta-1)\left(a_1 - \frac{e^{-\rho(T_1+h)}}{\beta-1}\left.\frac{\partial J^{(3)}_2(M_1)}{\partial P_{\tau_1'}}\right|_{P_{\tau_1'}=P^{*(3)}_{\tau_1'}}\right) \\
= \;& \beta(b_1 C + I_1 - e^{-\rho(T_1+h)}J^{(3)}_2(M_1))
\end{aligned} \tag{O.7}$$

where $M_1 = e^{\alpha(T_1+h)}P^{*(3)}_{\tau_1'}$.

- If $M_1 < P^{*(3)}_{\tau_2'}$ (it is optimal to wait at time $\tau_1' + T_1 + h$):

$$\begin{aligned}
J^{(3)}_2(M_1) \;=\; & \left(\frac{M_1}{P^{*(3)}_{\tau_2}}\right)^{\beta}\Big[V^{(3)}_2\left(P^{*(3)}_{\tau_2}\right) - I_2 \\
& + e^{-\rho(T_2+h)}J^{(3)}_3\left(\mathbb{E}_{P^{*(3)}_{\tau_2'}}\left(P_{\tau_2+T_2+h}\right)\right)\Big]
\end{aligned} \tag{O.8}$$

Substituting Equation (O.8) into Equation (O.7), we have:

$$\begin{aligned}
& P^{*(3)}_{\tau_1'}(\beta-1)\left(a_1-\frac{e^{-(\rho-\alpha\beta)(T_1+h)}}{\beta-1}\frac{\beta}{P^{(3)}_{\tau_1'}}\left(\frac{P^{*(3)}_{\tau_1'}}{P^{*(3)}_{\tau_2}}\right)^{\beta}\left[V_2^{(3)}\left(P^{*(3)}_{\tau_2}\right)-I_2\right.\right. \\
& \left.\left.+e^{-\rho(T_2+h)}J_3^{(3)}\left(\mathbb{E}_{P^{*(3)}_{\tau_2'}}\left(P_{\tau_2+T_2+h}\right)\right)\right]\right) \\
= \;& \beta(b_1C+I_1-e^{-(\rho-\alpha\beta)(T_1+h)}\left(\frac{P^{*(3)}_{\tau_1'}}{P^{*(3)}_{\tau_2}}\right)^{\beta}\left[V_2^{(3)}\left(P^{*(3)}_{\tau_2}\right)-I_2\right. \\
& \left.+e^{-\rho(T_2+h)}J_3^{(3)}\left(\mathbb{E}_{P^{*(3)}_{\tau_2'}}\left(P_{\tau_2+T_2+h}\right)\right)\right]) \\
\Rightarrow \;& P^{*(3)}_{\tau_1'}=\frac{\beta}{\beta-1}\frac{b_1C+I_1}{a_1} \qquad \text{(O.9)}
\end{aligned}$$

- If $M_1 \geq P^{*(3)}_{\tau_2'}$ and $e^{\alpha(T_1+T_2+2h)}P^{*(3)}_{\tau_1'} < P^{*(3)}_{\tau_3'}$ (it is optimal to invest immediately at time $\tau_1'+T_1+h$, but to wait at time $\tau_1'+T_1+h+T_2+h$):

$$P^{*(3)}_{\tau_1'}=\frac{\beta}{\beta-1}\frac{(b_1C+I_1)+e^{-\rho(T_1+h)}(b_2C+I_2)}{a_1+e^{-(\rho-\alpha)(T_1+h)}a_2} \qquad \text{(O.10)}$$

- If $M_1 \geq P^{*(3)}_{\tau_2'}$ and $e^{\alpha(T_1+T_2+2h)}P^{*(3)}_{\tau_1'} \geq P^{*(3)}_{\tau_3'}$ (it is optimal to invest immediately both at times $\tau_1'+T_1+h$ and $\tau_1'+T_1+h+T_2+h$)

$$P^{*(3)}_{\tau_1'}=\frac{\beta}{\beta-1}\frac{(b_1C+I_1)+e^{-\rho(T_1+h)}(b_2C+I_2)+e^{-\rho(T_1+T_2+2h)}(b_3C+I_3)}{a_1+e^{-(\rho-\alpha)(T_1+h)}a_2+e^{-(\rho-\alpha)(T_1+T_2+2h)}a_3} \qquad \text{(O.11)}$$

References

Abadie, L.M. & Chamarro, J.M. (2008a). European CO_2 prices and carbon capture investments. *Energy Economics*, **30**, 2992–3015. 23, 24, 80, 82, 123

Abadie, L.M. & Chamarro, J.M. (2008b). Valuing flexibility: The case of an Integrated Gasification Combined Cycle power plant. *Energy Economics*, **30**, 1850–1881. 23, 80

Adkins, R. & Paxson, D. (2010). Renewing assets with uncertain revenues and operating costs. *Journal of Financial and Quantitative Analysis, forthcoming*. 23, 24, 71, 73, 139

Aiube, F.A.L., Baidya, T.K.N. & Tito, E.A.H. (2008). Analysis of commodity prices with the particle filter. *Energy Economics*, **30**, 597–605. 33

Azadeh, A., Ghaderi, S.F. & Sohrabkhani, S. (2008). A simulated-based neural network algorithm for forecasting electrical energy consumption in Iran. *Energy Policy*, **36**, 2637–2644. 20

Baldick, R., Kolos, S. & Tompaidis, S. (2006). Interruptible electricity contracts from an electricity retailers point of view: valuation and optimal interruption. *Operations Research*, **54**, 627–642. 26, 96

Baldwin, C.Y. (1982). Optimal sequential investment when capital is not readily reversible. *Journal of Finance*, **37**, 763–782. 25

Bar-Ilan, A. & Strange, W.C. (1998). A model of sequential investments. *Journal of Economic Dynamics and Control*, **22**, 437–463. 26

BBC (2006a). Ukraine gas row hits EU supplies. http://news.bbc.co.uk/1/hi/world/europe/4573572.stm. 31

BBC (2006b). Ukraine takes extra Russian gas. http://news.bbc.co.uk/1/hi/world/europe/4642684.stm. 31

Bernard, J.T., Khalaf, L., Kichian, M. & McMahon, S. (2008). Forecasting commodity prices: GARCH, jumps, and mean reversion. *Journal of Forecasting*, **27**, 279–291. 33

Bolle, F. (1992). Supply function equilibria and the danger of tacit collusion: the case of spot markets for electricity. *Energy Economics*, **14**, 94–102. 30

Cartea, A. & Figueroa, M.G. (2005). Pricing in electricity markets: A mean reverting jump diffusion model with seasonality. *Applied Mathematical Finance*, **12**, 313–335. 51

Cartea, A. & Williams, T. (2008). UK gas markets: the market price of risk and applications to multiple interruptible supply contracts. *Energy Economics*, **30**, 829–846. 33

Celebi, M. & Graves, F. (2009). Co_2 price volatility: consequences and cures. http://www.brattle.com/_documents/uploadlibrary/upload736.pdf. 75

Chib, S., Nardari, F. & Shephard, N. (2002). Markov chain Monte Carlo methods for stochastic volatility models. *Journal of Econometrics*, **108**, 281–316. 45

Chilés, J.P. & Delfiner, P. (1999). *Geostatistics: Modeling Spatial Uncertainty*. Wiley, New York. 47

Clewlow, L., Strickland, C. & Kaminski, V. (2005). *Extending mean-reversion jump diffusion*. Energy Power Risk Management, Risk Waters Group, February. 51

Connor, J.T. (1996). A robust neural network filter for electricity demand prediction. *Journal of Forecasting*, **15**, 437–458. 20

Cortazar, G. & Schwartz, E.S. (1994). The evaluation of commodity contingent claims. *Journal of Derivatives*, **1**, 27–39. 19, 61

Cox, J.C. & Ross, S.A. (1976). The valuation of options for alternative stochastic processes. *Journal of Financial Economics*, **3**, 145–166. 52

Décamps, J.P., Mariotti, T. & Villeneuve, S. (2006). Irreversible investment in alternative projects. *Economic Theory*, **28**, 425–448. 22, 24, 85

Deng, S.J. (2000). *Stochastic models of energy commodity prices and their applications: mean reversion with jumps and spikes*. Working Paper, University of California, Berkely. 51

Deng, S.J. & Xia, Z. (2006). A real options approach for pricing electricity tolling agreements. *International Journal of Information Technology & Decision Making*, **5**, 421–436. 27

Deng, S.J., Johnson, B. & Sogomonian, A. (2001). Exotic electricity options and the valuation of electricity generation and transmission assets. *Decision Support Systems*, **30**, 383–392. 53

Dickey, D.A. & Fuller, W.A. (1979). Distribution of the estimators for autoregressive time series with a unit root. *Journal of the American Statistical Association*, **74**, 427–431. 38

Dixit, A.K. (1993). Choosing among alternative discrete investment projects under uncertainty. *Economic Letters*, **41**, 265–268. 22

Dixit, A.K. & Pindyck, R.S. (1994). *Investment under Uncertainty*. Princeton University Press, Princeton, New Jersey. 21, 22, 25, 69, 70, 99

EIA-861 (2008). Annual electric power industry report. http://www.eia.doe.gov/cneaf/electricity/page/eia861.html. 106

Etheridge, A. (2002). *A Course in Financial Calculus*. Cambridge University Press, Cambridge, UK. 102

Fleten, S.E. & Lemming, J. (2003). Constructing forward price curves in electricity markets. *Energy Economics*, **25**, 409–424. 20

Fleten, S.E., Maribu, K. & Wangensteen, I. (2007). Optimal investment strategies in decentralized renewable power generation under uncertainty. *Energy*, **32**, 803–815. 105

Fouque, J.P., Papanicolau, G. & Sircar, R.K. (2000). *Derivatives in Financial Markets with Stochastic Volatility*. Cambridge University Press. 45, 46, 47

Gollier, C., Proult, D., Thais, F. & Walgenwitz, G. (2005). Choice of nuclear power investments under price uncertainty: valuing modularity. *Energy Economics*, **27**, 667–685. 26, 27

Green, R. (1996). Increasing competition in the British electricity spot markets. *The Journal of Industrial Economics*, **44**, 205–216. 30

Green, R.J. & Newbery, D.M. (1992). Competition in the British electricity spot market. *The Journal of Political Economy*, **100**, 929–953. 30

Guthrie, G. & Videbeck (2007). Electricity spot price dynamics: beyond financial models. *Energy Policy*, **35**, 5614–5621. 36

Hamilton, J.D. (1989). A new approach to the economic analysis of non-stationary time series and the business cycle. *Probability in the Engineering and Informational Sciences*, **57**, 357–384. 19, 39

Hamilton, J.D. (1994). *Time Series Analysis*. Princeton University Press, Princeton, N. J. 38

Harvey, A.C. (1989). *Forecasting Structural Time Series Models and the Kalman Filter*. Cambridge University Press, Cambridge, UK. 34

Henney, A., Bower, J. & Newbery, D. (2002). An independent review of NETA. Tech. rep. 30

Herbelot, O. (1992). *Option valuation of flexible investments: the case of environmental investments in the electric power industry*. Ph.D. thesis, Department of Nuclear Engineering, Massachusetts Institute of Technology, Cambridge, MA, USA. 23

Hesmondhalgh, S. (2003). Is NETA the blueprint for wholesale electricity trading arrangements of the future? *IEEE Transactions on Power Systems*, **18**, 548–554. 30

Hildebrand, A.N. & Herzog, H.J. (2008). Optimization of carbon capture percentage for technical and economic impact of near-term CCS implementation at coal-fired power plants. In *9th International Conference on Green House Gas Control Technologies*, Washington, DC, USA. 22, 66, 80

IPCC (2005). *IPCC Special Report on Carbon Dioxide Capture and Storage*. Cambridge University Press, Cambridge, UK. 21, 22, 66

IPCC (2007). *Climate Change 2007: Synthesis Report*. IPCC, Geneva, Switzerland. 21

Jaillet, P., Ronn, E.I. & Tompaidis, S. (2004). Valuation of commodity-based swing options. *Management Science*, **50**, 909–921. 27

Journel, A. & Huijbregts, C. (1978). *Mining Geostatistics*. Academic Press 600p, London. 135

Kamat, R. & Oren, S.S. (2001). Exotic options for interruptible electricity supply contracts. *Operations Research*, **50**, 835–850. 26, 124

Karakatsani, N.V. & Bunn, D.W. (2008). Intra-day and regime-switching dynamics in electricity price formation. *Energy Economics*, **30**, 1776–1797. 20, 40, 64, 122

Klemperer, P. & Meyer, M.A. (1989). Supply function equilibria in oligopoly under uncertainty. *Econometrica*, **57**, 1243–1277. 30

Kosater, P. & Mosler, K. (2006). Can Markov regime-switching models improve power-price forecasts? Evidence from German daily power prices. *Applied Energy*, **83**, 943–958. 19, 20, 39, 54, 64

Kumbaroğlu, G. & Madlener, R. (2003). Energy and climate policy analysis with the hybrid bottom-up computable general equilibrium model SCREEN: the case of the Swiss CO_2 act. *Energy Economics*, **25**, 409–424. 20

Laughton, D.G. & Jacoby, H.D. (1993). Reversion, timing options, and long-term decision-making. *Financial Management*, **22**, 225–240. 19, 61

Laurikka, H. & Koljonen, T. (2006). Emissions trading and investment decisions in the power sector: a case study in Finland. *Energy Policy*, **34**, 1063–1074.

Majd, S. & Pindyck, R. (1987). Time to build, option value and investment decisions. *Journal of Financial Economics*, **18**, 7–27. 25, 67

Maribu, K.M., Galli, A. & Armstrong, M. (2007). Valuation of spark-spread options with mean reversion and stochastic volatility. *International Journal of Electronic Business Management*, **5**, 173–181. 20, 34, 44

Martinsen, D., Linssen, J., Markewits, P. & Vögele, S. (2003). CCS: a future CO_2 mitigation option for Germany?-A bottom-up approach. *Energy Economics*, **25**, 409–424. 20

Mattheij, R.M.M., Rienstra, S.W. & ten Thije Boonkkamp, J.H.M. (2005). *Partial Differential Equations: Modelling, Analysis, Computation*. Society for Industrial and Applied Mathematics, Philadelphia, PA, USA. 139

Mount, T.D., Ning, Y. & Cai, X. (2005). Predicting price spikes in electricity markets using a regime-switching model with time-varying parameters. *Energy Economics*, **28**, 62–88. 122

Näsäkkälä, E. & Fleten, S.E. (2005). Flexibility and technology choice in gas fired power plant investments. *Review of Financial Economics*, **18**, 371–393. 19, 32

NERC (2008). Wholesale market data. http://www.eia.doe.gov/cneaf/electricity/wholesale/wholesalet2.xls. 106

Nesterov, A. (2009). Russia-Ukraine gas war damages both economies. http://www.worldpress.org/Europe/3307.cfm. 31

Oren, S.S. (2001). Integrating real and financial options in demand-side electricity contracts. *Decision Support Systems*, **30**, 279–288. 26

ORNL (2009). America's 10 Energy Challenges. *ORNL Review*, **42**, available from: www.ornl.gov/info/ornlreview/v42_2_09/v42_no2_09review.pdf. 80

Paxson, D. & Pinto, H. (2005). Rivalry under price and quantity uncertainty. *Review of Financial Economics*, **14**, 209–224. 123

PG&E (2008a). 2008 corporate responsibility report. http://www.pgecorp.com/corp_responsibility/reports/2008/img/pge_crr_2008.pdf. 25

PG&E (2008b). PeakChoice. http://www.pge.com/tariffs/tm2/pdf/ELEC_SCHEDS_E-PEAKCHOICE.pdf. 97, 106

PG&E (2009). Base Interruptible Program (BIP). http://www.pge.com/tariffs/tm2/pdf/ELEC_SCHEDS_E-BIP.pdf. 97, 106

Pindyck, R.S. (1999). The long-run evolution of energy prices. *The Energy Journal*, **20**. 19, 67, 123

Pindyck, R.S. (2002). Optimal timing problems in environmental economics. *Journal of Economic Dynamics & Control*, **26**, 1677–1697. 23

Reinaud, J. (2003). *Emissions Trading and its Possible Impacts on Investment Decisions in the Power Sector*. IEA Information Paper, International Energy Agency, Paris, France.

Rodriguez, C.P. & Anders, G.J. (2004). Energy price forecasting in the Ontario competitive power system market. *IEEE Transactions on Power Systems*, **19**, 366–374. 20

Schwartz, E. & Smith, J.E. (2000). Short-term variations and long-term dynamics in commodity prices. *Management Science*, **46**, 893–911. 19, 32, 33

Smith, J.E. & McCardle, K.F. (1998). Valuing oil properties: integrating option pricing and decision analysis approaches. *Operations Research*, **46**, 198–217. 19, 61

Swedish Government Budget Bill (2008). Higher carbon dioxide tax for reduced traffic emissions. http://www.regeringen.se/content/1/c6/08/86/13/5e9ed088.pdf. 87

Szkuta, B.R., Sanabria, L.A. & Dillon, T.S. (1999). Electricity price short-term forecasting using artificial neural networks. *IEEE Transactions on Power Systems*, **14**, 851–857. 20

Treasury, H. (2005). Explanatory memorandum to the financial services and markets act 2000. http://www.opsi.gov.uk/si/em2005/uksiem_20050592_en.pdf. 32

Wickart, M. & Madlener, R. (2007). Optimal technology choice and investment timing: A stochastic model of industrial cogeneration vs. heat-only production. *Energy Economics*, **29**, 934–952. 23

Wilson, R. (2002). Architecture of power markets. *Econometrica*, **70**, 1299–1340. 18

Wolak, F.A. (1999). Market design and price behavior in restructured electricity markets: an international comparison. In T. Ito & A. Krueger, eds., *Competition Policy in the Asia Pacific Region, EASE Volume 8*, 79–134, University of Chicago Press. 18, 30